

# **SPATIO-TEMPORAL ANALYSIS OF COVID-19 PANDEMIC IN BANGLADESH**

by

Sadia Afroj

**MASTER OF URBAN AND REGIONAL PLANNING**



Department of Urban and Regional Planning




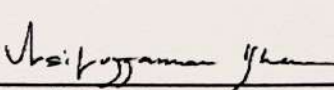

**BANGLADESH UNIVERSITY OF ENGINEERING AND TECHNOLOGY**

**June, 2022**

## THESIS ACCEPTANCE FORM

The thesis titled "SPATIO-TEMPORAL ANALYSIS OF COVID-19 PANDEMIC IN BANGLADESH", submitted by Sadia Afroj, Student No. 1018152009, Session: October, 2018, has been accepted as satisfactory in partial fulfillment of the requirement for the degree of MASTER OF URBAN AND REGIONAL PLANNING by Course work and Thesis on 29/06/2022.

### BOARD OF EXAMINERS

1.   
\_\_\_\_\_  
Dr. Afsana Haque  
Professor  
Department of Urban and Regional Planning,  
BUET, Dhaka, Bangladesh. Chairman  
(Supervisor)
2.   
\_\_\_\_\_  
Dr. Afsana Haque  
Professor and Head  
Department of Urban and Regional Planning,  
BUET, Dhaka, Bangladesh. Member  
(Ex-officio)
3.   
\_\_\_\_\_  
Dr. Md. Musleh Uddin Hasan  
Professor  
Department of Urban and Regional Planning,  
BUET, Dhaka, Bangladesh. Member
4.   
\_\_\_\_\_  
Dr. Asif-Uz-Zaman Khan  
Associate Professor  
Department of Urban and Regional Planning,  
BUET, Dhaka, Bangladesh. Member
5.   
\_\_\_\_\_  
Dr. Julio D Davila  
Professor  
Development Planning Unit (DPU), University  
College London (UCL) The Bartlett, UK. Member  
(External)

## **CANDIDATE'S DECLARATION**

It is hereby declared that this thesis or any part of it has not been submitted elsewhere for the award of any degree or diploma.

*Sadia Afroj*

---

Sadia Afroj

*Dedicated to my beloved father who still inspires me even in his absence  
and all the frontline workers who sacrificed their lives due to COVID- 19*

## ACKNOWLEDGEMENT

All praises belong to the Almighty Allah who bestowed upon me the ability to conduct this research successfully.

I will be ever-grateful to my supervisor Dr. Afsana Haque, Professor and Head, Department of Urban and Regional Planning, BUET for her invaluable support, continuous guidance, imperative suggestions, and encouragement at all the stages of the research work. As a person, I've learned a lot of new things and life hacks from her throughout the journey which motivates me a much to go forwards. I think I am the luckiest one to have her as my supervisor. It would have been really impossible to conduct the study without her consistent support and guideline.

I wish to express my gratitude to my husband Mr. Towshik-ur-Rahman for supporting me at the most crucial moment of this research as well as my life. Without his help, probably I could fail to find my balance point among family, study, and career. I would also like to express my gratitude to My Mother Mahmuda Khanam for fueling my strength throughout my life. Without her support, I could not be able to reach here. It would be impossible for me to articulate how much I owe her. I would like to thank my beloved junior Rifah Mashiat Jane for her tremendous support during the data collection phase. I would like to thank my friend Ms. Mamata Jafrin Mouli for encouraging me throughout the research. I would also like to thank my colleagues, especially Mr. Niaz Mahmud Zafri and Ms. Paromita Shome for their encouragement in doing this research.

Finally, I would like to express my appreciation to my family for their constant support, inspiration, and patience during the pursuit of my Master's degree. All these have helped me a lot to complete this dissertation successfully.

## ABSTRACT

The world has been experiencing the shock of Novel Coronavirus (COVID-19) with multiple waves. Bangladesh, like other countries, is witnessing pandemic waves as of March 8, 2020. Within three successive waves in Bangladesh, approximately two million cases of COVID-19 infection and thirty thousand deaths have been reported. Various demographic, climatic, and hospital factors have already been proven as linked to the infection scenario in the literature. Implemented aspatial countermeasures, according to some studies, could also have an impact on the pandemic situation. The regional and temporal growth of pandemic waves could be regulated based on these features. Although many studies have been conducted around the world, the majority of them have focused on the initial COVID-19 outbreak, projections of spatial diffusion and temporal trends during this time, mapping of infected cases related to public movement, and public perception of the pandemic, and advancements in healthcare technology. To the best author's knowledge, there are still few studies comparing the spatio-temporal dynamics of waves and emphasizing both the temporal and spatial aspects. In this context, this study aims to look at how spatial factors affect the COVID-19 pandemic's temporal variation in Bangladesh. Under this aim, the temporal patterns of the three successive waves of COVID-19 are compared from both spatial and aspatial perspectives. The effects of spatial features on waves are investigated later.

In this research, the incident rate is considered to represent the spread. Sixty-four districts of Bangladesh comprise the study area for this research. The data on district-wise confirmed cases and the daily number of tests of three waves have been collected from the Directorate General of Health Services (DGHS). Additionally, information on demographic characteristics, healthcare facilities, infrastructure facilities, geographic features, meteorological attributes, and economic attributes have been obtained from other secondary sources. Sen's slope estimation, the Pettit test, and the Mann-Kendall (M-K) test have been used to examine the temporal pattern. Global and local spatial autocorrelation methods (Moran's I) have been used to figure out the spatial pattern. Scan statistics have been employed in conjunction with a discrete Poisson probability approach to comprehend the spatiotemporal growth of the outbreak. Finally, the Ordinary Least Squares (OLS) model and spatial regression models have been used to identify the effects of spatial components.

Bangladesh as a whole exhibited no statistically significant trend throughout the first and second waves, but the deployment of long-term spatial containment measures caused an abrupt drop in infection during the first wave in almost all districts. The Bangladesh government implemented many of these non-pharmaceutical measures during the initial wave, including the closure of educational institutions and social gathering places, lockdown, social distancing measures, case isolation, demarcating of the most infected regions, and movement restrictions. The third wave had a noticeable decline in incident rates and lasted for a shorter period. In all waves, Dhaka and the neighboring areas were the first hit and were infected more heavily. Due to the arrival of new virus strains in the surrounding nations, the Western area of the country suffered a cluster of greater COVID-19 occurrences during the second and third waves. In terms of infection, the Eastern portion, including the districts of Sylhet and Mymensingh division, were always in a better state due to their local geographic features.

The country's testing facilities were unevenly distributed, which had an impact on the number of confirmed cases in areas. May to July is identified as the period of time when the infection was most likely to spread. Urban population density, poverty rate, the number of ICU beds in each district, and the population over 65 are all identified as contributing spatial features during the first wave. On the other hand, factors that are determined to be significant in the second wave include rainfall, the number of bus stops, and the distance from the most affected area. The third wave highlights important contributions of urban population density, hospitals per thousand people, temperature, and rainfall. To conclude, it is anticipated that the findings of this study could help to formulate an appropriate pandemic management framework that takes into account seasonal and regional factors to combat future outbreaks.

# TABLE OF CONTENTS

	Page No
ACKNOWLEDGEMENT	i
ABSTRACT	ii
TABLE OF CONTENTS	iv
LIST OF TABLES	vii
LIST OF FIGURES	viii
LIST OF ABBREVIATIONS	ix
<b>Chapter 1 : Introduction .....</b>	<b>1</b>
1.1. Background of the Study	1
1.3. Scopes and Limitations of the Study	5
1.4. Organization of the Report	7
<b>Chapter 2 : Literature Review .....</b>	<b>8</b>
2.1. History of Pandemics	8
2.2. Theoretical Framework behind Spatio-temporal Analysis	10
2.3. Applications and Techniques of Spatio-temporal Analyses in Public Health Planning	11
2.3.1. Applications of Spatial Analyses	12
2.3.2. Application of Temporal Analyses	14
2.3.3. Application of Spatio-temporal Analyses	14
2.4. Factors Influencing Pandemic Patterns	15
2.5. COVID-19 as a Matter of Concern	16
2.5.1. Researches on COVID-19	17
2.5.2. COVID-19 in Bangladesh context	17
2.6. Motivation of this Research	18
<b>Chapter 3 : Methodology .....</b>	<b>20</b>
3.1. Study Area	20
3.2. Data Collection	22
3.2.1. Data on COVID-19 related attributes	22
3.3. Data Processing	26
3.4. Data Analysis	27
3.4.1. Detecting temporal pattern	27
3.4.2. Determining spatial pattern	30
3.4.3. Identifying the spatial influential factors behind the spread	33
3.5. Findings and Recommendation	35



## **Chapter 4 : Temporal Pattern of COVID-19 at Three Subsequent Waves in Bangladesh.....36**

4.1. Temporal Pattern of the COVID-19 at National Level	36
4.2. Temporal Pattern of the COVID-19 at District Level	41
4.2.1. During the first wave	41
4.2.2. During the second wave	45
4.2.3. During the third wave	47

## **Chapter 5 : Spatio-temporal Pattern of COVID-19 in Three Waves 50**

5.1. Spatio-temporal Pattern during First Wave	50
5.1.2. Spatial distribution of clusters and outliers	52
5.1.3. Space-time cluster of COVID-19 during the first wave	54
5.2. Spatio-temporal Pattern during the Second Wave	57
5.2.1. Spatial pattern at national context	57
5.2.2. Spatial distribution of clusters and outliers	58
5.2.3. Space-time cluster of COVID-19 during the second wave	59
5.3. Spatio-temporal Pattern during Third Wave	61
5.3.1. Spatial pattern at national context	61
5.3.2. Spatial distribution of clusters and outliers	62
5.3.3. Space-time cluster of COVID-19 during the third wave	63

## **Chapter 6 : Influence of Spatial Attributes on COVID-19 Outbreak in Bangladesh.....65**

6.1. Variables Considered	65
6.2. Contribution of Spatial Attributes on the First Wave	68
6.2.1. Results of the Ordinary Least Squares (OLS) and spatial regression models	68
6.2.2. Findings from the developed models	69
6.3. Contribution of Spatial Attributes on the Second Wave	73
6.3.1. Results of the OLS, SLM and SEM models	73
6.3.2. Findings from the developed models	74
6.4. Contribution of Spatial Attributes on the Third Wave	77
6.4.1. Results of the OLS, SLM and SEM models	77
6.4.2. Findings from the developed models	78

## **Chapter 7 : Major Findings and Recommendations.....82**

7.1. Spatio-temporal Analyses of Three COVID-19 Waves	82
7.2. Contribution of Spatial Characteristics on Incident Rate	85
7.3. Recommendations	87

<b>Chapter 8 : Conclusion.....</b>	<b>91</b>
References	94
Appendix A	103
Appendix B	104

## LIST OF TABLES

	Page No
Table 2.1: Spatial analysis techniques in epidemiology .....	12
Table 2.2: Temporal analysis techniques in epidemiology.....	14
Table 2.3: Spatio-temporal analysis techniques in epidemiology .....	15
Table 2.4: COVID-19 in literature.....	17
Table 3.1: Considered spatial attributes for analysis .....	25
Table 4.1: Nation-wide temporal pattern of COVID-19 confirmed cases and incident rate in three subsequent waves.....	37
Table 5.1: Spatial pattern of COVID-19 at each incubation period of first wave .....	51
Table 5.2: Features of the detected space-time clusters of cases during the first wave .....	56
Table 5.3: Spatial pattern of COVID-19 at each incubation period of the second wave .....	57
Table 5.4: Features of the detected space-time clusters of cases during the second wave .....	61
Table 5.5: Spatial pattern of COVID-19 at each incubation period of the third wave .....	62
Table 5.6: Features of the detected space-time clusters of cases during the third wave .....	64
Table 6.1: Summary statistics of the considered variables .....	65
Table 6.2: Results of the OLS and spatial regression models for the first wave .....	70
Table 6.3: Results of the OLS and spatial regression models for the second wave .....	76
Table 6.4: Results of the OLS and spatial regression models for the third wave .....	80

## LIST OF FIGURES

	Page No
Figure 3.1: The study area in the (a) global context (ArcGIS hub, 2020); and (b) Asian context (ArcGIS hub, 2020). (c) Map of Bangladesh.....	20
Figure 3.2: Distribution of cumulative COVID-19 incidences till 9 March 2022 in Bangladesh.....	21
Figure 4.1: COVID-19 infection in three subsequent COVID-19 waves in Bangladesh .....	38
Figure 4.2: Timeline of COVID-19 related events in Bangladesh .....	40
Figure 4.3: Temporal pattern of COVID-19 for different districts during three subsequent waves.....	42
Figure 4.4: Trend of confirmed cases in districts showing ITAC pattern in the first wave .....	43
Figure 4.5: Trend of incident rate of districts showing DTAC pattern in first wave...44	
Figure 4.6: Trend of incident rate for districts showing ITAC pattern in the second wave .....	46
Figure 4.7: Trend of incident rate for districts showing DTAC pattern in the third wave .....	48
Figure 5.1: Location of clusters and outliers of incident rate during the first wave ....	53
Figure 5.2: Space-time clusters of COVID-19 cases and tests in the first wave at the district level.....	55
Figure 5.3: Location of clusters and outliers of incident rate during the second wave	58
Figure 5.4: Space-time clusters of COVID-19 cases and test in the second wave .....	60
Figure 5.5: Location of clusters and outliers of incident rate during the third wave ...	62
Figure 5.6:Space-time clusters of COVID-19 cases and test in the third wave.....	63
Figure 6.1: Spatial distribution of COVID-19 incident rate in three subsequent waves .....	67

## LIST OF ABBREVIATIONS

DGHS	Directorate General of Health Services
OLS	Ordinary Least Squares
ICU	Intensive Care Unit
ITAC	Increasing Trend and Abrupt Change
ITNO	Increasing Trend and No Abrupt Change
DTAC	Decreasing Trend and Abrupt Change
DTNO	Decreasing Trend and No Abrupt Change
NTAC	No Trend and Abrupt Change
NTNO	No Trend and No Abrupt Change
SLM	Spatial Lag Model
SEM	Spatial Error Model
WHO	World Health Organization
IEDCR	Institute of Epidemiology, Disease Control, and Research
LISA	Local Indicator of Spatial Association
UNICEF	United Nations Children's Fund
HIES	Household Income and Expenditure Survey
VIF	Variance Inflation Factor
RR	Relative Risk

# **Chapter 1 : Introduction**

## **1.1. Background of the Study**

In the last century, the world experienced more than twenty pandemic events and more than a hundred epidemics (WHO, 2020). When any epidemic spreads over multiple countries and continents, it is declared a pandemic. Climate change, alteration in biodiversity as well as demographic pattern, and changes in living standards are expediting the induction of new epidemics frequently. Again sometimes the situation is turning into a pandemic (Curseu et al., 2010; Lafferty, 2009). Such pandemics do not finish readily once they come, rather return with subsequent waves to various places at different times. The severity of these pandemics also varied across the waves. From the history of previous pandemics, it has been found that Influenza flu occurred in four different times at different parts of the world and the outbreak and temporal length of waves were not identical in all events (Viasus et al., 2012). The world also experienced seven Cholera pandemics in the past two centuries, where the duration of each wave and infected areas were not analogous (Mandal et al., 2011). Spanish Flu affected the population of Spain, France, Great Britain, and Italy with two spikes (Martini et al., 2019). Based on the severity of their waves over space and time, both short run and long run impacts of pandemics changed; consequently, preventive and precautionary measures to tackle any pandemic were also transformed. Similar circumstances may repeat during the existing or future pandemic events.

It has already been evident from the previous epidemiological experiences that local demographic, meteorological, and hospital features are differently associated with one pandemic wave to another (Bandaranayake et al., 2011; Mamelund, 2018). The first wave of Spanish flu caused more infection among elder groups; alternatively, younger groups were infected more during its second wave (Martini et al., 2019). Marco and his colleagues (2011) found that Influenza showed up in three subsequent waves in Mexico where the reasons behind each wave were different. Regional movement patterns influenced the first wave, whereas the less effective measure of social distancing and opening of educational institutions were responsible for the second and third waves. Population density, urbanization rate, demographic structure, and climatic conditions contributed differently to the first and second waves of Influenza Flu pandemic

(Chowell et al., 2014). Therefore, exploring the spatio-temporal characteristics of such outbreaks is necessary to avoid the unforeseeable subversive effects of pandemics. Similar exploration is also necessary to understand the benefits or detriments of varying policy interventions, and control strategies on virus transmission (Ahmed et al., 2011; Zheng et al., 2019).

The world has been experiencing the shock of Novel Coronavirus (COVID-19) since December, 2019. Right now, it is going through the third wave (somewhere fourth wave) of COVID-19 with an exponential increase of confirmed cases (Engelbrecht et al., 2021; Graichen, 2021; Middleton et al., 2020). The effects of this pandemic are not only bound to the health sector but also encompassed other sectors like education, transportation, agriculture, economy, and so on. Researches showed that COVID-19 changed the travel behavior of people, the use of public transportation, and the public activity pattern worldwide (Bhaduri et al., 2020; Bucsky, 2020; Shamshiripour et al., 2020). According to World Bank (2020), the global economy experienced the deepest recession during the first wave of COVID-19. This pandemic has also disrupted traditional educational practices due to the adoption of social distancing measures and restrictive movement policies (Pokhrel et al., 2021). Food supply chain and security have been severely affected in the developing countries (Workie et al., 2020). COVID-19 has also emoted the urban lifestyle and living standard, particularly urban low-income groups suffered a lot due to their higher exposure to risks, socio-economic inequalities and limited access to basic services; even some of them migrated to other places due to the pandemic. In some cases, the environmental qualities of the cities got improvement due to the long-term application of lockdown measures (Sharifi et al., 2020). However, these researches could make it clear that the consequences of COVID-19 should not be overlooked, and consideration of COVID-19 impacts is necessary in developing future plans and policies sustainably.

Like other countries, Bangladesh confronted more than thirteen epidemic outbreaks in the last century (IEDCR, 2020) and it has experienced the third wave of corona virus outbreak very recently till March, 2022. Around two million people have been reported as COVID-19 positive within two years of the first detection and almost thirty thousand people have died due to this pandemic (IEDCR, 2020). As in other nations, Bangladesh has also experienced the dire consequences of this pandemic almost in all sectors of the economy like industry, housing, tourism, transportation, education, etc. The use of

transportation modes has changed drastically during the first wave (Zafri et al., 2021) as well as public mobility has also reduced due to the imposition of pandemic policies (Shaik et al., 2021). Readymade garments sector, foreign remittance, food and agricultures, local trade, national GDP, SDGs (Sustainable Development Goals), government revenue and employment have been identified as the most vulnerable sectors due to COVID-19 (Mottaleb et al., 2020). Therefore, the consideration of the COVID-19 issue is indispensable in formulating the development policies of the country to ensure a safe future. However, the intensity of viral spread is not same over the time based on what the impacts may change.

Different control measures like lockdown, closure of all activities, deployment of armed forces, restriction on movement, public transportation, and so on have been imposed at the early stage of the first wave to tackle the nationwide situation. The condition was under control over the country after ten months. Unfortunately, within a few months, the pandemic returned with the second wave, and the corresponding measures were tried to be implemented once again. At the end of the second wave, another wave took place. By this time, the measures employed to tackle the situation varied from wave to wave. Demographic and locational characteristics of the districts of Bangladesh might have also contributed in a different way while tackling the pandemic situation across these waves.

Research on Bangladesh showed that urban population, population density, number of health workers, and distance from the capital influenced the pandemic incidences during the first wave (Rahman et al., 2021). Foreign population entry and late implementation of non-pharmaceutical measures were responsible factors for early community transmission in Bangladesh (Masrur et al., 2020). Several meteorological attributes like temperature, relative humidity, and rainfall might also contribute to the situation in the first wave (Islam et al., 2021). Containment strategies towards pandemic (i.e. closure of educational institutions, deployment of armed forces, restriction on religious gathering, closure of commercial activities and garments factories) and local events like the presence of the month of the Ramadan (the holy month of fasting for the Muslims) influenced public movements cum pandemic situation to some extent (Zafri et al., 2021).



The test rate of COVID-19 and the occurrence of some socio-cultural events are not identical in all districts of Bangladesh even in consecutive waves. Such circumstances may govern the spatial diffusion of incidences over the waves. Disparities in the testing and healthcare facilities are very common in developing countries; consequently, these discrepancies may have impacted the area-wise incident rate that needs to be considered in spatio-temporal analysis of waves. Again, the vaccination program in Bangladesh has been started during the second wave which can more or less control the outbreak situation of the second and third waves. Time-specific local response towards pandemic and taken pharmaceutical (i.e., vaccination) and non-pharmaceutical measures (i.e., lockdown, etc.) could shape spatio-temporal dynamics of the pandemic during subsequent waves and the scenario may also differ from the first wave like previous pandemic events. Such comparative analysis among the subsequent waves is yet an unexplored premise in the pandemic-related research of Bangladesh and even for that of the world.

Several researches have been done worldwide considering the prediction of the virus outbreak, projection of spatial diffusion and temporal trends at the initial period, mapping of the infected cases relating to public movement, public perception towards pandemic, improvement of healthcare technologies, and effective strategies for prevention and control in the first wave (Gayawan et al., 2020; Giuliani et al., 2020; Mahmood et al., 2020; Patrinley et al., 2020). Some studies again emphasized on the periodic impact of COVID-19 in different sectors like economic, social, environmental, transportation, and healthcare (Iyengar et al., 2020; Ozili, 2020; Xu et al., 2020; Zafri, Afroj, Ali, et al., 2021). However, studies are still limited in the context of the developing countries where spatio-temporal dynamics of pandemic waves are compared. But there is no denying of the fact that these investigations are necessary to design the time-specific preparedness actions for future epidemics and to control the unusual spikes of pandemic waves.

In this context, the present study attempts to contribute to formulating apposite spatial and temporal policies for Bangladesh by envisaging COVID-19 incident rates in subsequent waves. Hopefully, the findings will help to understand the spatio-temporal characteristics for interpreting the pandemic phenomenon of Bangladesh and provide an insight to formulate spatial policies considering public health issues.

## **1.2. Objectives of the Study**

In view of the above discussion, the current research aims at investigating the influence of locational characteristics on temporal variation of the COVID-19 pandemic in Bangladesh. To satisfy this aim the following two objectives have been considered:

- i. To compare the temporal pattern of the subsequent waves of COVID-19 in Bangladesh from both spatial and aspatial perspectives.
- ii. To explore the influence of spatial attributes on the subsequent waves of COVID-19 in Bangladesh.

## **1.3. Scopes and Limitations of the Study**

This study intends to understand the effects of different aspatial and spatial characteristics on COVID-19 transmission in Bangladesh. Generally, the pattern of spread and the contributory factors behind it cannot be uniform from wave to wave of each pandemic. In developing countries, variations in pandemic control measures are quite common. Considering the context, this research identifies the temporal pattern of COVID-19 outbreak in each district of Bangladesh in three subsequent waves. Due to paucity of data, the weekly incident rate, that is weekly number of COVID-19 confirmed cases with respect to the weekly total number of COVID-19 tests, is considered for investigation. Daily data on confirmed cases and the number of tests for each district are not updated, which has ultimately generated some missing data in the time series. Moreover, data on number of deaths per day for each district is not available. That is why only incident rate has been considered to explore the spatio-temporal dynamics of the outbreak. If the death rate could have also been considered, the associated contributory demographic attributes for the outbreak could be different.

In this study, different socio-economic, demographic, and infrastructural variables have been considered to understand the effects of spatial characteristics. Most of the data on demographic variables (i.e. total population, gender-wise population, urban population) have been collected from the “District Statistics, 2011”, because no updated data are available after this period. The data of these variables have, therefore, been projected for the study period 2021. The updated data could have influenced the research findings

differently. The study has considered the distribution of public places (i.e. local markets, religious institutions) and transit stations (i.e. bus stations) over the districts as important determinants, which are subject to change with the dynamic activity pattern over space. Nevertheless, this study accounts for these variables as static ones specifically due to a lack of data that may affect the findings to some extent.

Data on poverty rate and consumption pattern have been accumulated from “Household Income and Expenditure Survey (HIES)-2016”, conducted by the Bangladesh Bureau of Statistics. Such attributes represent the economic condition of the districts. The areas with poorer communities may suffer from inequalities due to limited access to facilities and lower income. They need to go out of home daily to feed their families which may increase their exposure to the pandemic. On the other hand, people in the areas of higher consumption could go to the market places more to satisfy their demands during pandemic which could increase their risk of infection. But the updated data of these attributes are not available for the study period which may affect the research findings to some extent. This research hypothesized that where the number of hospitals is higher, a higher incident rate may occur. Because the increase in the number of a hospital raises the chance of more interactions with infected people or exposure to the virus, consequently more infections may occur over the population. Therefore, accessibility to healthcare facilities, management systems within such facilities, public behavior in hospitals, and their awareness also could affect the pandemic scenario. These issues could be envisaged in detail in future research. Moreover, some meteorological attributes (i.e. wind speed, seasonal temperature) could not be integrated into this study due to data unavailability. But these variables may also influence the incident rate more or less and could provide a better understanding about the impacts of meteorological characteristics on the viral spread. This research finds the correlation between the number of ICU beds and the incident rate during the first wave. If the death rate could be considered, the findings may be different which could be investigated in future studies. Therefore these issues are some of the major limitations of this research.

During the first wave of COVID-19, many people migrated from cities to own villages in Bangladesh which might possibly influence the COVID-19 scenario. Some of these migrated populations lost their income-generating activities in cities, some could shift due to the rapid spread of COVID-19 in urban areas. Either this shift could be temporary or permanent. In the long run, the permanent shift could change the urban and rural

population and economic distribution of the country. But this issue could not be possible to address in this study due to a lack of reliable data. Further studies could consider this fact in analyzing the spatio-temporal dynamics of the pandemic.

With national-level policy interventions, sometimes community-level measures have been carried out by different organizations, which could influence the local scenario. By integrating information from such a micro level, the influence of local intervention on transmission could have been comprehended more precisely. However, the inclusion of such information has not been made possible as the study has been carried out at the district level.

#### **1.4. Organization of the Report**

This report contains eight chapters. Among them, the first chapter highlights the background of this research including the objectives to be attained. The history of pandemic, concept of spatio-temporal analysis, theoretical framework of the study, a brief outline of the studies carried out in previous times, various techniques available for spatio-temporal analysis, and the motivation of this research have been discussed in the second chapter. The following chapter represents the methodological framework of this research including its working procedure. The fourth chapter covers the temporal pattern of COVID-19 in three subsequent waves at each district. The fifth chapter describes the spatial pattern at different points of time along with spatio-temporal changes of the pandemic scenario. Spatial factors responsible for the outbreak are highlighted in the sixth chapter. Major findings from this study including suggestions based on that have been discussed in the later chapter (Chapter 7). And the final chapter includes concluding remarks.

## **Chapter 2 : Literature Review**

This chapter begins with a brief history of pandemics experienced by the world. Later it outlines the necessity of exploring spatial and temporal dimensions of any pandemic along with the concept of spatio-temporal analyses. Applications and techniques of different spatio-temporal analyses in public health planning are discussed briefly in the next sections. Factors shaping the spatial and temporal situation of pandemic outbreaks highlighted in previous works are alluded later. Relevant literature on COVID-19 including the research gap is discussed after that. Finally, the motivation behind this study is revealed in the last section.

### **2.1. History of Pandemics**

Due to the change in meteorological features, human behavior, and biodiversity, many new diseases are being incited from time to time (Curseu et al., 2010). Based on their prediction rates and geographical spread, these are defined as endemic, outbreak, epidemic, or pandemic. When any disease shows a predictable increase, it is termed as endemic; if it spreads into an unpredictable growth among population, it becomes an outbreak. Epidemic occurs when this outbreak spreads over a larger geographical area and at the final stage, it can be announced as a pandemic when the disease prevails globally (Grennan, 2019). In human history, numerous pandemic outbreaks had remarkable impacts on almost each and every sector. Till now this world experienced many significant pandemics like Spanish Flu, H1N1 Influenza, Cholera, SARS, Malaria, H7N9, Ebola, Yellow Fever, Plague, Zika, Hong Kong Flu, Diphtheria, Swine Flu, and so on (Qiu et al., 2017).

By investigating the history of pandemics, it has been found that Plague was the very first pandemic that convulsed the world in 541s and repeated three times as the Plague of Justinian, Black Death, and Third Plague (Zietz et al., 2004). These three pandemics of the Plague occurred with subsequent waves, though the infection periods and areal spread were not same. The underlying reasons, surveillance and control programs were also different across the waves (Prentice et al., 2007). Like Plague, the Cholera pandemic occurred seven times in different regions of the world. The severity of the outbreak and prevention strategies varied from early outbreak to late due to changes in

virus strain, technological revolution, globalization and settlement pattern (Chowdhury et al., 2017). Similarly in the context of Influenza pandemics, the severity of viral outbreaks depended on the transmissibility of strain and the susceptibility of the population (Simonsen et al., 1998). Different parts of the world responded in a diversified way against this pandemic following several containment strategies like the closure of schools and religious places, restrictions on public gatherings, maintaining social distances, etc. However, such strategies were not unique at all waves in all areas; these were changed with instantaneous incident rates, social patterns and virus strains (Henderson et al., 2009).

In the case of SARS-CoV, low infectivity and long incubation period elongated the implementation period of preventive measures. Case identification and isolation of the detected cases were found as effective against this pandemic, consequently discarding the effect of subsequent waves (Ge et al., 2013). Zhang et al. (2020) showed the success of non-pharmaceutical measures over clinical treatment in the context of the MERS-CoV epidemic. Appropriate hospital hygiene practices and implementation of contact and droplet precautions helped to limit the progression of the case as well as reduce the risk of future waves.

During the very recent SARS-CoV-2 pandemic, all nations around the world are going through its waves despite the characteristics of waves are not identical. Both pharmaceutical and non-pharmaceutical interventions have been performing from the initial stage for flattening the epidemic infection curve. Some of these have responded successfully to changing the spatial and temporal pattern of the outbreak (Ganyani et al., 2020). However, the outbreak is still persisting.

By exploring the history of various pandemics, it is clear that geographic as well as temporal pattern of outbreak and their associated policy interventions are not identical across the waves. These situations are controlled by several factors like demographic, social, economic, and environmental factors, which have to be investigated in depth for preventing further waves and future epidemics.

## **2.2. Theoretical Framework behind Spatio-temporal Analysis**

The data which are geographically referenced and related to space, are named as spatial data. Such data can be used to generate demanded output through spatial statistics by exploring spatial causality, association, aggregation, or disaggregation. The underlying assumption behind such analyses follows Waldo Tobler's (1970) First Law of geography where it has been stated that "Everything is related to everything else. But near things are more related than distant things" (Miller, 2004). These analyses generally reveal the impact of neighboring areas on the area of interest in a particular issue as well as its condition. And these characteristics make them unique from other statistical analyses. Different forms of spatial analysis techniques are available and commonly classified into two categories: global and local. Global measures show the overall scenario considering data as a whole; whereas local measures identify the location of any spatial interest in detail and local impacts from the surroundings. However, in most cases, the output of local techniques tends to be proportional to their corresponding global techniques (Fotheringham et al., 1999). The infliction of spatial analysis techniques can be fruitful to know the effects of neighboring areas on the local outbreak and locate the clusters of high or low infected areas of pandemics. Besides using local mapping of an outbreak, it is also possible to ascertain the contribution of various spatial attributes in pandemic situations which can be conducive to tackling the pandemic waves (Rezaeian et al., 2007). Due to their worth, the applications of such analyses are not limited to a few sectors and often apply in detecting spatial patterns of any event and defining their underlying reasons (Auchincloss et al., 2012; Graham et al., 2004).

On the other hand, temporal data refers to the data related to time. When same incidences are examined for different time periods, it is termed as temporal analysis (Turner, 1990). By using temporal statistics, temporal correlation, trend of pandemic outbreak, point of any drastic change, etc. can be comprehended (Meliker & Sloan, 2011; Ward & Carpenter, 2000). However, neither temporal nor spatial analyses alone can provide completeness in exploring any event (Meliker & Sloan, 2011). To bring a trade-off and understand the overall scenario, spatio-temporal analyses are becoming popular day by day in researches where incidences can be checked out both in space and time windows. Space-time scan statistics are commonly used in this regard.

If an event occurs in a specific location, it may have a geographical spread and a temporal period of occurrence. The event's impact fluctuates according to its spatiotemporal span. The event's locational extension is generally regulated by a number of local conditions, which can cause the event's intensity to alter or the event to be repeated in the future. Based on such factors, somewhere the occurrence rate may be larger, while somewhere, it may be minimal. Any seasonal or diurnal change is possible. A particular intervention can also influence such departure. Such concerns may be revealed by a spatiotemporal examination of the event. To alleviate the negative effects of the event and develop effective policies, it is crucial to investigate its spatiotemporal dimension. Spatio-temporal analysis can help to understand the effects of aspatial attributes (i.e. seasonal impact, effectiveness of containment strategies, preventive measures) on pandemic situations and compare the subsequent wave scenarios. Space-time scan statistics can be performed in this regard. The space-time scan statistics are employed either for retrospective analysis (where historic data are used to detect viral propagation), or for prospective surveillance analysis (where the analysis is repeated for every day, week, month or year to determine future risk). These analyses mainly show space-time clustering of diseases in which geographical locations with faster and slower transference considering time are displayed. Such investigations have already been done on fever, Zika, Influenza, COVID-19 and other epidemics around the world (Chen et al., 2016; Lian et al., 2007; Maggi et al., 2017; Métras et al., 2012; Siljander et al., 2022). However, to understand the emerging COVID-19 pandemic in the context of developing countries, both space-time dimensions of spread need to be investigated so that responses of spatial and aspatial policy interventions can be deployed more objectively.

### **2.3. Applications and Techniques of Spatio-temporal Analyses in Public Health Planning**

The techniques available for spatio-temporal studies can be divided into three categories: i) solely spatial, ii) purely temporal, and iii) spatio-temporal. Although these techniques are used in all sectors such as urban planning, transportation, environmental planning, disaster management, accident analysis, and geographical analysis, their use



in public health planning is robust and commendable in defining contributory factors behind different circumstances.

**2.3.1. Applications of Spatial Analyses**

One of the most notable characteristics of epidemics is their spatial spread, which is governed by the nature of the epidemic, human mobility, and control tactics (Gross et al., 2020). Spatial statistical techniques enable scientifically informed decision-making when it comes to limiting the geographic spread of epidemics. Since the functions of all techniques are different, they must be chosen based on the study requirements. Table 2.1 displays some of the often-used spatial analysis methods in public health planning, their roles, and previous research applications.

Table 2.1: Spatial analysis techniques in epidemiology

<b>Spatial Analysis Techniques</b>	<b>Functions</b>	<b>Applications</b>
Spatial autocorrelation (SAC) with Moran’s I	This is used to identify whether the epidemic cases follow any pattern as clustered, dispersed, or spatially random at a macroscopic level.	It has been applied to identify the pattern of COVID-19 cases in developed countries (Siljander et al., 2022) at the recent time and also in the context of other epidemics previously (Auchincloss et al., 2012; Lian et al., 2007; Meliker et al., 2011).
Local Indicator of Spatial Association (LISA)	It reveals both the spatial clustering of incidences with similar values and divergent values. The result is also shown by mapping and works at a microscopic level.	This has been used to know the location of clusters of Influenza, Plague and COVID-19 cases (Curseu et al., 2010; Fotheringham et al., 1999; Gross et al., 2020).
Hotspot analysis and Getis–Ord $G_i^*$ statistic	This technique measures the level of spatial autocorrelation using a global index. The findings are displayed on maps as hotspots and coldspots of incidences.	To relate and explain the findings from spatial autocorrelation, this technique has been employed in the spatial analysis of COVID-19, Fever and West Nile epidemic (Graham et al., 2004; Lian et al., 2007; Siljander et al., 2022).

<b>Spatial Analysis Techniques</b>	<b>Functions</b>	<b>Applications</b>
Kernel Density Estimation (KDE)	It is used when data show non-parametric behavior and is mostly applied to detect high-density areas of incidences.	To understand the effect of preventive measures on the spatial spread of COVID-19, it has been employed in a few researches (Kato, 2021; Shi et al., 2021).
Ordinary Least Squares (OLS) regression	This simply defines the significant relationships between dependent and independent variables without considering spatial issues. If any spatial autocorrelation exists on the residuals of the OLS model, then it proceeds with any of the spatial regression methods for detecting spatial risk factors behind the spread of epidemics.	It has been extensively used in identifying the influential factors behind pandemics (Siljander et al., 2022), defining the effect of the built environment on viral spread (Yip et al., 2021) and finding the relation between pandemic and other socio-economic determinants (Agrahari et al., 2021; Murray et al., 2006; Rababah et al., 2020).
Spatial Lag Model (SLM)	This facilitates to define how events at a location are influenced by the events of their surrounding locations.	It has been employed to know the effects of ecological factors on Influenza, pneumonia and COVID-19 (Crighton et al., 2007; Maliszewski et al., 2011; M. H. Rahman et al., 2021).
Spatial Error Model (SEM)	This technique is used to determine the spatial autocorrelations of the residuals as an advanced tool of OLS. Generally, it is applied with SLM in combination.	This spatial regression model has been used with SLM to understand the effects of residuals in the context of pandemics (Crighton et al., 2007; M. H. Rahman et al., 2021).
Geographically Weighted Regression (GWR)	This technique calculates the indicators for all points considering the spatial variation in the relationships. Different factors can be considered here and their spatial relationship with the patterns under study can be identified by applying GWR.	To explore the local effects of meteorological factors on Influenza (Lopez et al., 2014), to analyze the spatial relationships between cholera cases and household water supply (Carrel et al., 2011), and to identify the influence of socio-economic factors on COVID-19 (Giuliani et al., 2020).

### **2.3.2. Application of Temporal Analyses**

Unlike geographical analysis, the applications of temporal analysis methods only are relatively uncommon in case of pandemic issues. However, these are mostly employed to comprehend the consequences of policy initiatives, the influence of local events, or changes in pandemic dynamics. And most of the time, these are applied along with spatial analysis. Table 2.2 lists some of the methods that can be used to explore the temporal characteristics of pandemics.

Table 2.2: Temporal analysis techniques in epidemiology

<b>Temporal Analysis Techniques</b>	<b>Functions</b>	<b>Applications</b>
Poisson model	This technique is used to forecast the evolving cases with containment strategies of epidemics.	During the COVID-19 pandemic, it has been employed to know the time-varying reproduction number of cases (Hong et al., 2020).
Mann Kendal (M-K) test	It is applied to understand the trend of epidemics by time-series analysis.	To analyze the effects of lockdown on environmental particles, this test has been employed (Pal et al., 2022)
Sen's slope estimator	It defines the magnitude of an identified trend from M-K test.	Meteorological effects on COVID-19 have been explored using this technique (Goswami et al., 2020).
Pettit test	This test is applied to detect any abrupt changes in time-series data of epidemics.	To identify the changes in dengue trend at Brazil, it has been employed (de Oliveira-Júnior et al., 2019).

### **2.3.3. Application of Spatio-temporal Analyses**

Spatio-temporal analysis enables the detection of epidemic clusters based on a time window. It aids in locating areas where diseases spread quickly and slowly. The most often used techniques for spatio-temporal analysis of any event are space-time scan statistics. Though all techniques perform similarly to some extent, they have to be chosen depending on available data while keeping their limitations in application in mind. Table 2.3 summarizes the most commonly used space-time scan statistical analysis techniques and their applications in pandemic planning.

Table 2.3: Spatio-temporal analysis techniques in epidemiology

<b>Spatio-temporal Analysis Techniques</b>	<b>Functions</b>	<b>Applications</b>
Bernoulli model	It analyses the epidemic cases based on their existence or non-existence in a geographic territory.	To estimate the transmissibility of Influenza this technique has been applied (Chong et al., 2017).
Discrete Poisson model	In this analysis, clusters are specified considering the population size of the study area.	To detect Cholera hotspots based on historic data, this model has been employed (Mwaba et al., 2020).
Space-Time permutation model	This model deals only with case and geographic data. Population at risk is not considered here.	For understanding the nature of Anthrax outbreak, it has been used considering constant population (Wilson et al., 2016).
Multinomial model	It is used as an advanced tool of Bernoulli model when the control status of pandemics could be categorized.	Parimala and Lopez (2016) applied this to connect the epidemic cases with human mobility patterns.
Exponential model	It is used when the analysis needs to be done on a case-by-case basis and epidemic cases have some associated covariates like death cases, survival period of each case, etc.	To forecast pandemic cases by considering surrounding environments and associated information, this has been used (Nieto-Chaupis, 2021).

## **2.4. Factors Influencing Pandemic Patterns**

Throughout history, a variety of causes have influenced different waves of pandemics. Both geographical and aspatial factors have been stated to have played a role in determining the scenario. In pandemic research, demographic variables like population density, percentage of urban population, poverty level, and population distribution according to age are frequently identified as contributory causes of a spatial outbreak (Chowell et al., 2014; Lenzi et al., 2011; Martini et al., 2019; Sannigrahi et al., 2020). Again, the association between epidemic cases and socioeconomic characteristics may shift from early to late in the outbreak (Dinh et al., 2018). To some extent, the spatial spread is also influenced by the distribution and availability of healthcare facilities

(Dureab et al., 2018). Investigating the correlation of geographical patterns with demographic and hospital-related variables in different wave scenarios is therefore critical. Meteorological factors such as average maximum temperatures and total rainfall have been proven to be significant in the context of dengue fever, malaria, and cholera (Baharom et al., 2021; Goto et al., 2013). Sarkodie et al. (2020) showed that temperature, wind speed and humidity are important to mold the condition during the first wave of COVID-19. The same scenario may occur in later waves, which has to be investigated.

To address the pandemic crisis, numerous pharmacological and non-pharmaceutical strategies are being implemented. Generally, pharmaceutical measures like medicine, vaccine, installation or development of testing facilities, etc. serve to slow down the spread of the outbreak (Ibuka et al., 2010). Non-pharmaceutical measures include the closure of educational institutions and social meeting places, lockdown, social distancing measures, case isolation, demarcating the most infected regions, and movement restrictions (Duerr et al., 2007). To some extent, these measures control the magnitude of pandemic waves, although they cannot be the same for all waves even for the same pandemic. Responses to such measures must be assessed by examining the time-series and spatio-temporal characteristics of incident rates. Policy solutions addressing public health issues can be established based on the outcomes of these assessments in the future.

## **2.5. COVID-19 as a Matter of Concern**

From December 2019 to the present, almost the entire world has been affected by the COVID-19 ripple. At this point, the instances in many countries have shown a fluctuating trend. Even though various containment methods have been implemented early on, all nations have been affected within a year. Around 0.5 billion people have been infected and six million have died, both of which are unprecedented in pandemic history (worldometer, 2022). Activities have come to a standstill, affecting many sectors including health, economy, transportation, and the environment. As a result, everyone's attention has been attracted to this pandemic. In the beginning, nonpharmaceutical measures have been used to regulate the situation, while pharmaceutical measures (such as medication and vaccination) have been in the

experimental stage (Zafri et al., 2021). However, both interventions could affect the subsequent waves altering the situation to some extent, which needs to be investigated.

**2.5.1. Researches on COVID-19**

Since the outbreak of the COVID-19 pandemic, several studies have been carried out. The researches range from the virus's genetic state to its impact on development sectors. Table 2.4 outlines the literature on COVID-19 to the best of the author's knowledge.

Table 2.4: COVID-19 in literature

<b>Focus of the research</b>	<b>Findings</b>
Mapping of spatial pattern of incidences	Spatial clustering of COVID-19 cases in local provinces during the initial stage of the first wave has been shown by Li et al. (2020), Huang et al. (2020), and Tang et al. (2020). Spatial autocorrelation technique was adopted in these studies to understand the existence of clusters.
Predicting future spread of cases	By defining the reproduction number of cases and using numeric or prospective spatio-temporal analysis, a potential outbreak situation has been predicted (Andrade et al., 2020; Hong et al., 2020).
Defining the relationship of COVID-19 cases with different influential factors	Relationship of COVID-19 incidences with built environment, meteorological factors and socio-economic attributes has been investigated in the studies of Yip et al. (2021), Scarpone et al. (2020) and Giuliani et al. (2020) respectively using different regression models.
Change of COVID-19 scenario according to control strategies	The effect of various control strategies to tackle the pandemic situation at different phases has been examined by employing space-time scan statistics in the context of China and South Korea (Kim et al., 2020; Liao et al., 2020).
Developing pandemic management strategies for future	By analyzing the scenarios at different waves, different control measures and pandemic management frameworks have been proposed to confine the future spread of pandemics (Baveja et al., 2020; Zafri, Afroj, Nafi, et al., 2021).

**2.5.2. COVID-19 in the Bangladesh context**

The first coronavirus case in Bangladesh was detected on March 8, 2020, ten weeks after the world's first reported case in Wuhan, China. To control the outbreak, the

Government of Bangladesh (GoB) implemented several containment measures such as general leave, lockdown, closure of educational institutions, social distancing, restrictions on social gatherings, and so on. However, such initiatives did not perform effectively during the onset of their implementation. Literature acknowledged that a wide-scale community transmission occurred during the first wave due to a lack of a notable legal structure for pandemic planning and limited public acceptance of health standards (Shammi et al., 2020). In the first wave, around two million cases were confirmed, with approximately 20,000 deaths (WHO dashboard for coronavirus, 2021). According to the literature, urban population, population density, number of health personnel involved in the service, distance from the capital, entry of immigrant population, and lack of action synchronization- all played a role in the initial outbreak (Masrur et al., 2020; M. H. Rahman et al., 2021). However, the role of these risk factors may have changed in later waves, which are currently unknown. To create an effective pandemic prevention framework, risk factors must be identified and compared across all scenarios, including their time-specific contribution to the pandemic outbreak.

## **2.6. Motivation of this Research**

Bangladesh has recently experienced the third wave of the COVID-19 pandemic. From the initial wave to the present, pandemic dynamics have shown a manageable condition at large. Few researches demonstrate the spatial expansions of the disease and their associated determinants in the initial wave. Meanwhile, vaccination programs and other specialized interventions have also been implemented, which may have contributed to keep the situation under control.

Again, most of the testing facilities in the country were initially concentrated in the capital city, Dhaka. Later, testing laboratories could be made available in divisional districts along with Dhaka. Among the COVID-19 testing laboratories, around 61% were located in Dhaka and its adjacent districts (DGHS, 2022). However, the number of the testing laboratories has been increased by this time and till the third wave, all districts of the country have at least a COVID-19 testing laboratory. Therefore, such inequities in the distribution of testing facilities and healthcare facilities over the waves should be considered when defining the incident rate and spatial pattern of outbreaks.

To the best of the author's knowledge, no research focusing on Bangladesh has taken this issue into account.

Time-specific local events or measures can also change the waves, causing variation in spatio-temporal patterns. The characteristics of the succeeding waves may differ; one may display a prolonged spike, while another may cease in a brief rise due to various management tactics. Therefore, temporal dynamics must be highlighted alongside spatial patterns. Furthermore, comparing the following waves can aid in developing appropriate spatial and aspatial policies for dealing with pandemic situations that have not yet been investigated. This research has been carried out to comprehend the spatio-temporal patterns through one lens for distinct pandemic times so that spatial and aspatial policies addressing public health issues can be formulated.



## Chapter 3 : Methodology

The present research intends to explore the spatial and aspatial context of COVID-19 waves in Bangladesh including the intensity of spread, the direction of transmissibility, and contributory causes of diffusion or suppression. The research methodology is demonstrated in this chapter.

### 3.1. Study Area

Bangladesh, a South-Asian developing country experienced the stress of COVID-19 since March 2020. Geographically this country shares its boundaries with India, Myanmar and the Bay of Bengal (Figure 3.1).

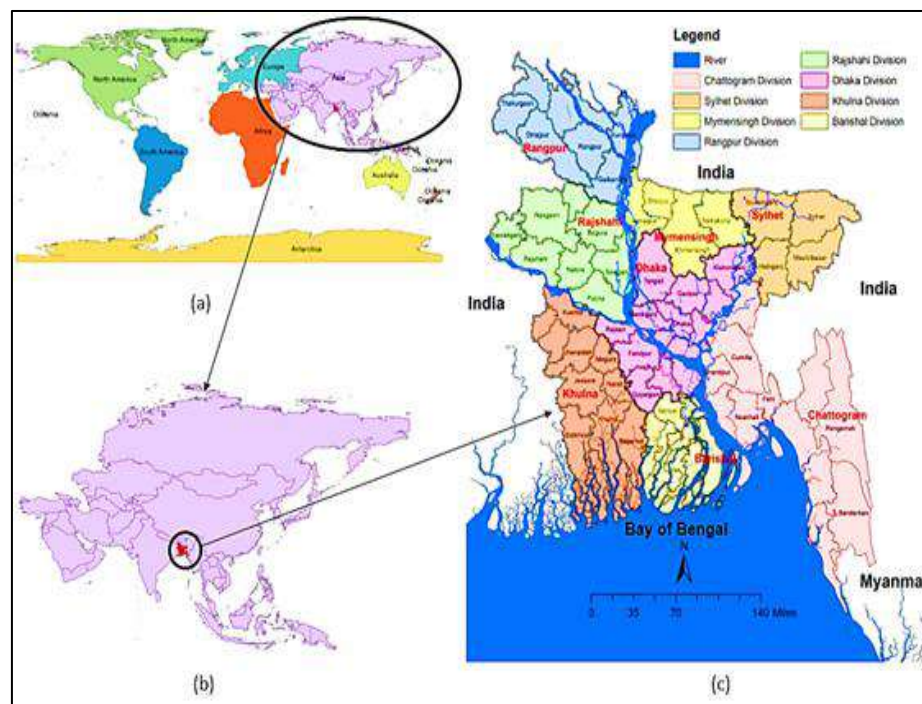


Figure 3.1: The study area in the (a) global context (ArcGIS hub, 2020); and (b) Asian context (ArcGIS hub, 2020). (c) Map of Bangladesh

Almost 163.7 million people (as estimated for 2018) live on 147, 570 sq. km. area of the country (MoF, 2020). Around 22% people live below the poverty line (MoF, 2020). As of 2018, the ratio of persons to registered physicians is 1:1,724 (MoF, 2020). The central area of the country, including the capital city Dhaka though experienced the

early detection of COVID-19, the infections transfused in all of the eight divisions within a month. Till 9 March 2022, around two million people got infected by the outgrowth of the virus in three subsequent waves. Figure 3.2 shows the distribution of cumulative COVID-19 incidences till 9 March 2022 in Bangladesh.

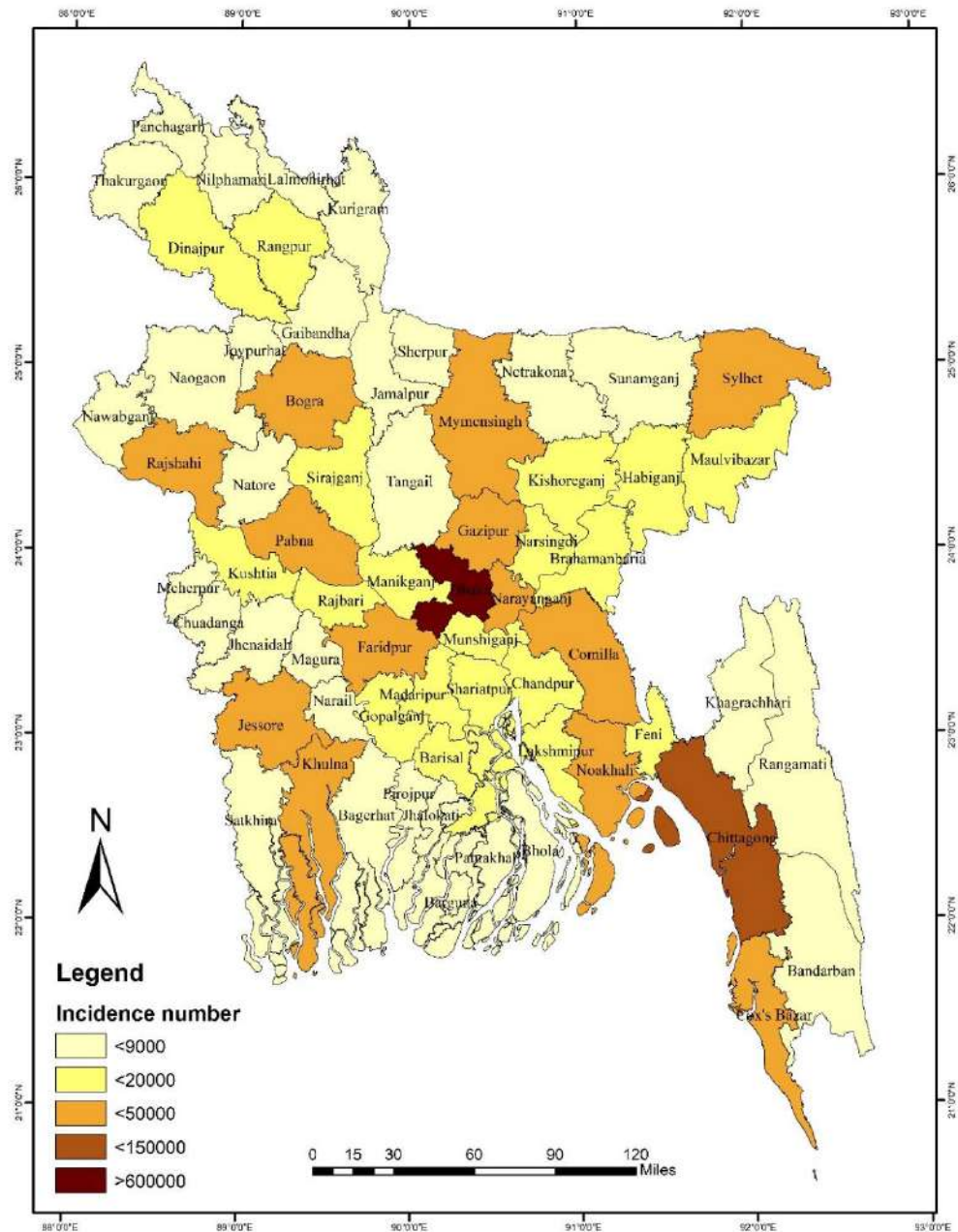


Figure 3.2: Distribution of cumulative COVID-19 incidences till 9 March 2022 in Bangladesh. The figure clearly reveals the spatial variation of COVID-19 infection across the country. Figure 3.2 demonstrates the capital of the country (Dhaka) grossly experienced more than 0.6 million infections in three waves. The confirmed cases were higher in the divisional districts of Bangladesh. Among all districts, 13 districts contained around

fifty thousand infected populations individually. Therefore it can be stated that dynamics of spread were not spatially identical over 64 districts. In order to explore the spatio-temporal dynamics COVID-19 pandemic in Bangladesh, the present study eventually selects all 64 districts of the country as its study area.

## **3.2. Data Collection**

### **3.2.1. Data on COVID-19 related attributes**

In the absence of a precise definition, the current study relies on expert opinion (Appendix A) while defining the waves of COVID-19. Accordingly, the pandemic can be considered under control if the incident rate continues to diminish and stays below 5% for two consecutive weeks in a row. Following this description, three COVID-19 waves have been discovered in Bangladesh till 9 March 2022. The data on district-wise confirmed cases and daily number of tests from 8 March 2020 to 23 January 2021 (first wave including the day of the first reporting), 10 March 2021 to 28 September 2021 (second wave), and from 6 January 2022 to 9 March 2022 (third wave) have been collected from COVID-19 dashboard of Directorate General of Health Services (DGHS). On 7 February 2021, immediately after the end of the first wave, a nationwide vaccination program was initiated in Bangladesh. To interpret the status in the second and third waves, district-level vaccination data have been obtained from the same Dashboard.

Government interventions to tackle COVID-19 have been noted from the weekly situation reports of Bangladesh, published by the World Health Organization (WHO) and Bangladesh National Preparedness and Response Plan for COVID-19, published by the Directorate General of Health Services (DGHS), Bangladesh. The data on various non-pharmaceutical countermeasures have been gathered from National Stringency Indices prepared by the University of Oxford. The index was developed using nine response matrices: school closure, workplace closure, public event cancellation, restrictions on public gatherings, public transportation closures, stay-at-home requirements, public awareness campaigns, internal movement restrictions, and international travel controls (Hale et al., 2021).

### **3.2.2. Data on Spatial Attributes**

It is assumed that COVID-19 transmission is the greatest in the areas surrounding the most infected places. Consequently, the data on district administrative boundary and travel distance of each district in terms of distance from the most infected district within its division have been collected from the GIS portals of Bangladesh's Local Government Engineering Department (LGED) and Roads and Highways Department (RHD), respectively.

As humans are the primary host for COVID-19 transmission and the presence of greater physical infrastructure with more population activities can raise the likelihood of the disease outbreak. Therefore, this study hypothesizes that the incidence of COVID-19 is proportional to the total population, population density, urban population, and young population group. Therefore, data on demographic characteristics such as district-wise total population, population density, urban population, male and female population, population under 14 years of age, population over 65 years of age, and number of slum population have been accumulated from Bangladesh Bureau of Statistics' publication "District Statistics, 2011" of each district and "Census of Slum and Floating Population 2014". These data have been projected for 2021 (study period) using the geometric growth population projection technique. The growth of the slum population may increase the risk of infection due to their unhygienic living condition and failure of maintaining self-distancing (Sharifi et al., 2020; Workie et al., 2020). Public awareness about the health issues can also affect the local level infection. Considering this issue, district-wise literacy rate has been included as a proxy variable to represent local awareness level. It is assumed that the higher the literacy rate, the higher the awareness among the public is, hence, the lower the incident rate is. Because when people are aware of the pandemic situation, they are supposed to know about their response to the pandemic and follow the basic hygiene rules to prevent the spread. Though human behavior is the manifestation of numerous cultural, and socio-political factors; some basic education may affect the scenario.

Local markets, bus terminals, railway stations, and religious institutions are the potential hubs of public gatherings and human activities in Bangladesh; so, these variables may have an impact on the spatial transmission of disease. Therefore, the district-wise number of these social gathering places has been acquired from District

Statistics, 2011. Here it is notable that, the most updated data on these variables were available for the year 2011; so the study relied on this database.

During the onset of every pandemic, healthcare institutions play a crucial role. This research hypothesizes that the distribution of healthcare centers and designated COVID-19 hospitals have a significant influence on the spatial pattern of COVID-19 incidences too. In addition, the service capacities of these variables can also be a matter of concern. The data on district-wise number of healthcare centers, designated COVID-19 hospitals, number of COVID-19 testing laboratories, number of doctors, number of hospital beds and number of Intensive Care Unit (ICU) beds have been accumulated from the Directorate of General Health Services (DGHS) database, 2016. The increase in the number of hospitals including the relevant services in an area increases the chance of interaction with the infected population. Consequently, it can increase the transmission of COVID-19 virus. District-wise data on the percentage of population having proper hand wash facilities have been gathered from the dashboard of the United Nations Children's Fund (UNICEF) to understand local awareness levels relating to health issues. If people maintain hygiene practices properly, the risk of viral transmission reduces.

Literature has shown that local meteorological characteristics can affect the transmission of a pandemic (Chapter 2, Section 2.4). This can also be true for the COVID-19 pandemic. Therefore, the data on maximum and minimum temperature, rainfall, and humidity of each district have been collected from the Bangladesh Meteorological Department.

District-wise poverty rate and monthly consumption are considered here as proxy variables to represent local economic conditions. Higher consumption refers to the increased chance of going out from the home to fulfill the basic consumption demand, consequently increasing the risk of viral transmission. Again, the poorer section of the community has to go out of home for their basic need, so the increased rate of poverty may also affect the COVID-19 spread scenario. These data have been collected from Household Income and Expenditure Survey (HIES)-2016 respectively. Table 3.1 shows the aforementioned spatial attributes of this study including their data source and the underlying hypotheses to be considered.

Table 3.1: Considered spatial attributes for analysis

Category	Variables	Hypothesis	Data Source
Geographical information	District administrative boundary	The shared boundary with the most infected district exists, the higher is the infection	LGED GIS Portal
Demographic characteristics	Population	The higher the population, the higher is the infection	District Statistics, 2011
	Population density	The higher population density, the higher is the infection	
	Urban population density	The higher urban population density, the higher is the infection	
	Male population	The higher the male population, the higher is the infection	
	Female population	*The higher the female population, the lower is the infection	
	Population under 14 years of age	* The higher the population under the age of 14 years, the lower is the infection	
	Population over 65 years	* The higher the population over the age of 65 years, the lower is the infection	
	District-wise number of slum population	The higher the slum population, the higher is the infection	Census of Slum and Floating Population, 2014
	Literacy rate	*The higher the literacy rate, the lower is the infection	District Statistics, 2011
Infrastructural facilities	Number of local markets	The higher the number of social gathering places (local markets, railway stations, bus stations, religious institutions), the higher is the infection	District Statistics, 2011
	Number of railway stations		
	Number of bus stations		
	Number of religious institutions		
	Travel distance from the most infected district	*The longer the travel distance from the most infected district, the lower is the infection	Roads and Highways Department
Healthcare facilities	Number of healthcare centers	*The higher the number of healthcare facilities (healthcare centers, COVID-19 hospitals, COVID-19 testing facilities, doctors, hospital beds, ICU beds), the higher is the infection	Directorate General of Health Services database, 2016
	Number of designated COVID-19 hospitals		
	Number of COVID-19 testing laboratories		
	Number of doctors		
	Number of hospital beds		

Category	Variables	Hypothesis	Data Source
	Number of Intensive Care Unit (ICU) bed		
	Percentage of population having proper handwash facilities	*The higher the percentage of population having proper handwash facilities, the lower is the infection	Dashboard of UNICEF
Meteorological characteristics	Maximum temperature	The higher the temperature, the higher is the infection	Bangladesh Meteorological Department, 2021
	Minimum temperature		
	Average rainfall	*The higher the average rainfall, the lower is the infection	
	Humidity	The higher the humidity, the higher is the infection	
Economic characteristics	Poverty rate	The higher the poverty rate, the higher is the infection	Household Income and Expenditure Survey (HIES)-2016
	Monthly consumption	The higher the monthly consumption is, the higher is the infection	Household Income and Expenditure Survey (HIES)-2016

### 3.3. Data Processing

During the initial phase of the first wave, some abnormal peaks in the daily data of confirmed cases have been observed, which are not expected to be present. While investigating the causes of such surges, it has been learned that the confirmed case counts are not reported in some districts for multiple days. When the counts are reported after 3 to 6 days, they exhibit some abrupt levels in comparison to the earlier successive counts. In order to handle these anomalies, the weekly count of confirmed COVID-19 cases and the weekly count of the number of tests are used to trace temporal patterns. It is important to note that the quantity of testing and healthcare facilities are not uniform throughout the districts of Bangladesh, which may influence the counts of COVID-19 confirmed cases and skew the results of the study. According to the researcher's knowledge, no Bangladeshi study has examined this perspective. A previous study focusing on the first wave highlighted the incident rate in terms of per thousand population (Rahman et al., 2021), where the issue of the testing inequality was not revealed. But it may also happen that the areas with higher testing facilities

reported more cases than others. Using the actual number of cases or case number with respect to population may not address such inequalities. Considering such fact in mind, this research has used incident rate in terms of the number of tests. Finally, this study focuses on the district-level incident rate of COVID-19 rather than the absolute incidence number. The incident rate is defined as the number of COVID-19 confirmed cases relative to the number of COVID-19 tests. Using the following formula, the district-level incident rate is determined.

$$\text{Weekly COVID-19 incident rate of a district} = \frac{\text{Total number of Covid-19 confirmed cases in a week}}{\text{Total number of Covid-19 tests in a week}} \times 100\%$$

### **3.4. Data Analysis**

The nonparametric tests have been used to identify the temporal pattern of COVID-19 in all waves across 64 districts of Bangladesh. The discovered patterns have been examined in the light of the policy interventions imposed to tackle the outbreak. Spatial pattern, on the other hand, has been determined following spatial autocorrelation approaches. The spatio-temporal progression has been checked by space-time scan statistics. Finally, using spatial statistics, the contributions of several spatial factors to the revealed patterns have been identified. The following subsections provide a summary of the analysis techniques.

#### **3.4.1. Detecting temporal pattern**

The Mann-Kendall (M-K) test, Sen's slope estimation, and Pettit test have been employed to identify the temporal pattern of COVID-19 in Bangladesh.

##### **Mann-Kendall (M-K) test and Sen's slope estimation**

The Mann-Kendall (M-K) test is a widely used nonparametric method in time series analysis (Ahmad et al., 2015; Mann, 1945; Oliveira Júnior et al., 2018). It has been employed in this study to determine the temporal patterns of the COVID-19 incident rate at three waves. This test is useful because it is unaffected by irregular measurement of time points, missing values, or the length of the time series (Mann, 1945). Furthermore, no specific statistical distribution of data, such as normal or linear distribution, is required in this test. This test can even be done when outliers exist in the time series data.



The null hypothesis ( $H_0$ ) behind this test is, there is no trend in the time series, and the alternative hypothesis ( $H_a$ ) is that there is a trend in the data series. If a time series is constructed with  $(X_1, X_2, \dots, X_n)$ , while  $X_i$  and  $X_j$  refer to the sample recorded at the time  $i$  and  $j$  respectively, the M–K statistic,  $S$  is represented as,

$$S = \sum_{i=2}^n \sum_{j=1}^{i-1} \text{Sign}(X_j - X_i) \tag{1}$$

Where,

$$\text{Sign} = \begin{cases} 1 & X_j - X_i > 0 \\ 0 & X_j - X_i = 0 \\ -1 & X_j - X_i < 0 \end{cases} \tag{2}$$

If no monotonic trend or not much tied values exist in the data series with more than 10 elements (the null hypothesis), then the statistic  $S$  approximately follows the normal distribution. A normal Z statistic test can then be used for the dataset by standardizing the statistic,  $S$  using the following equation (3).

$$Z = \begin{cases} \frac{S - 1}{\sqrt{\text{Var}(S)}} & S > 0 \\ 0 & S = 0 \\ \frac{S + 1}{\sqrt{\text{Var}(S)}} & S < 0 \end{cases} \tag{3}$$

Here  $\text{Var}(S)$  refers to the variance of  $S$ , defined as,

$$\text{Var}(s) = \frac{1}{18} \left[ n(n-1)(2n+5) - \sum_k^m t_k(t_k-1)(2t_k+5) \right] \tag{4}$$

Where  $n$ ,  $m$ , and  $t_k$  are the number of data in the time series, number of tied groups (a set of data having the same value), and the number of data in the  $k$ th tied group respectively. A positive value of  $Z$  denotes an increasing trend and a negative value expresses a decreasing trend. In this research, the significant trend has been tested at a

95% confidence level. Mann-Kendall (M-K) test traces only the existence and direction of the trend, but cannot identify any possible magnitude of the slope of the trend. Therefore, Sen's slope is further calculated to capture the magnitude of the detected trends. It is the median of all linear slopes persisting in the time series and is calculated using the following equation (5).

$$\text{Sen's Slope} = \text{Median} \left\{ \frac{X_j - X_i}{j - i} : i < j \right\} \quad (5)$$

Where  $X_j$  and  $X_i$  refer to the sample recorded at time  $j$  and  $i$  respectively. By computing Sen's slope of the identified trend, the intensity of propagation or decrement has been comprehended.

#### Pettit test

Soon after the first report of COVID-19 case in Bangladesh, the government implemented a number of counter-measures, including a countrywide lockdown, closing of commercial areas, movement restrictions, closure of all educational institutions, and so on. These interventions have been carried out at various scales throughout the study period, which may have affected the incident rate with a sudden spike or fall. As a result, the Pettit test has been used to understand the effect of such interventions by detecting the change point within the time series.

This method has already been applied in many researches to determine the sudden change in data series (de Oliveira-Júnior et al., 2019; Hay et al., 2020; Yang et al., 2020). For a data series  $(X_1, X_2, \dots, X_n)$  with a change point at the date  $\tau$ , the distribution for  $X_t (t = 1, 2, \dots, \tau)$  is different from that of  $X_t (t = \tau + 1, \tau + 2, \dots, n)$ . The null hypothesis ( $H_0$ ) is, there is no abrupt change in the time series and the alternative hypothesis ( $H_a$ ) is, abrupt change exists which is checked using the  $K_n$  statistic and can be described as,

$$K_n = \text{Max} |U_{t,n}|, 1 \leq \tau \leq n \quad (6)$$

Where,

$$U_{t,n} = \sum_{i=1}^t \sum_{j=t+1}^n \text{Sign}(X_i - X_j) \quad (7)$$

The probability ( $P$ ) denotes the presence of an abrupt change point and represents the significance of the  $K_n$  statistic, which can be defined as,

$$P \cong 2 \exp\left(\frac{-6k^2}{n^3 + n^2}\right) \quad (8)$$

Here, Mann-Kendall (M-K) test, Sen's slope estimation and Pettit test, all have been done using the "trend" package in R studio, version 1.1.4.

Based on the level of significance of the trends and sudden shifts, six types of temporal patterns are possible: ITAC, ITNO, DTAC, DTNO, NTAC, and NTNO. The ITAC pattern denotes Increasing Trend and Abrupt Change, whereas the ITNO pattern indicates Increasing Trend but no Abrupt Change. Again, DTAC stands for Decreasing Trend and Abrupt Change, and DTNO refers to Decreasing Trend Only. The NTAC implies just Abrupt Change, while NTNO shows that neither of the two traits exists. Such temporal trends have been estimated for all districts of Bangladesh, taking into account all three COVID-19 waves. The temporal pattern findings have been interpreted in conjunction with the adopted countermeasures for understanding the impact of policy initiatives.

### **3.4.2. Determining spatial pattern**

Moran's I indices have been adopted for this study to assess the spatial autocorrelation or dependency of the COVID-19 incident rate. Later, the Discrete Poisson Probability Model has been utilized to describe the temporal growth of the spatial pattern.

#### **Spatial Autocorrelation**

Global Moran's I index has been calculated formerly to identify the nature of spatial pattern (dispersed, random or cluster) of COVID-19 incident rate across the country. Then Local Moran's I indices have been applied to reveal spatial dependency locally by detecting the cluster of similar rates or outliers. To define the adjacency of districts, it has been assumed that while any district shares a common boundary with another

districts, they are considered neighbors. Global Moran's I indices have been calculated using the following equation (9),

$$I = \frac{n \sum_{i,j} W_{ij} (X_i - \bar{X})(X_j - \bar{X})}{\sum_{i \neq j} W_{ij} \sum_i (X_i - \bar{X})^2} \quad (9)$$

Where  $i$  and  $j$  express the district indices and  $W_{ij}$  denotes the adjacency between district  $i$  and district  $j$ .  $X_i$  and  $X_j$  refers to the COVID-19 incident rate over any particular wave in districts  $i$  and  $j$  respectively.  $\bar{X}$  represents the average incident rate in the whole area for the wave.

The Moran's I value can be varied from -1 to +1. A Global Moran's I value of 0 implies that there is no spatial autocorrelation. A positive value represents similar values inside the cluster, whereas a negative value represents different values. The geographic autocorrelation is stronger when the absolute value of Global Moran's I increases. Thus, spatial patterns for all waves of Bangladesh have been determined.

Local Moran's I statistics have been employed to ascertain each district's contribution to the overall geographical pattern during the study periods and where distinct forms of cluster exist. The Local Moran's I index at district  $i$  can be represented as,

$$I_L = \frac{X_i - \bar{X}}{S_i^2} \sum_{j=1, j \neq i}^n W_{ij} (X_j - \bar{X}) \quad (10)$$

Where,  $\bar{X}$  represents the average incident rate,  $W_{ij}$  denotes the adjacency between district  $i$  and district  $j$  and  $S_i^2$  can be calculated by,

$$S_i^2 = \frac{\sum_{j=1, j \neq i}^n (X_j - \bar{X})^2}{n - 1} - \bar{X}^2 \quad (11)$$

Based on the Local Moran's I index ( $I_L$ ), a normal Z statistic value has been derived to ascertain whether spatial clusters or outliers exist. Overall, four types of spatial patterns are found: High-High (HH) cluster, High-Low (HL) outlier, Low-Low (LL) cluster, and Low-High (LH) outlier. When the Z statistic value is higher than 1.64 (confidence level of 95%), districts with higher incident rates form the HH cluster and districts with lower incident rates mold LL cluster. In contrast, when the Z statistic is smaller than -

1.64, a district with a high incident rate is surrounded by lower rates as HL outlier and a district with fewer rate is surrounded by higher rates as LH outlier.

The spatial autocorrelation patterns have been identified using ArcGIS 10.3.1. For both spatial autocorrelation techniques, inverse distance has been selected as the conceptualization method assuming that a nearby feature has a larger influence on the computation of a target feature than the feature that locates far away.

#### *Discrete Poisson Probability Model*

In this study, the retrospective space-time scan has been undertaken, considering the temporal spans of Bangladesh's three pandemic waves. To investigate the space-time clusters of incidences and tests, each district of Bangladesh has been regarded as a spatial unit, each week within a wave as a temporal unit, and weekly COVID-19 incidence as well as COVID-19 tests data has been used to know the clusters. A cylindrical scanning window has been utilized to identify the risk zone, with the circular base representing geographical space and the cylinder's height representing the study time. The base of the scanning cylinder has been centered on the district's centroid. At the moment of scanning, the cylindrical window has navigated around space and time and produced cylinders of various heights and diameters. Each cylinder represents a potential cluster. Later, a probability model has been performed to determine the likelihood of getting cases within the window relative to that of obtaining cases outside the window.

The discrete Poisson probability model is adopted in this regard. This model assumes that the predicted number of cases in each area is proportional to its population size, which is its primary advantage and what sets it apart from other scan statistics methods. As humans are the primary carriers of COVID-19, the spatial and temporal dynamics need to be analyzed according to population size. Consequently, a discrete Poisson probability model has been applied, with the case and population counts of each district, as well as their geographic coordinates, serving as inputs. For scanning, 50% of the population at risk and 50% of the study period have been defined as spatial and temporal windows, respectively. The null hypothesis for the scanning window is that there is no elevated risk within the window compared to outside, whereas the alternative

hypothesis is that there is an elevated risk within the window. Using the following equation (12), the Likelihood Ratio (LR) has been computed for each area:

$$LR = \left( \frac{c}{E[c]} \right)^c \left( \frac{C - c}{C - E[c]} \right)^{C-c} I \quad (12)$$

Where  $C$  is the total number of cases in a particular wave,  $c$  is the observed number of cases within the window and  $E[c]$  is the expected number of cases within the window.  $I$  is an indicator function that denotes the existence of any cluster of high incidences. During scanning for clusters with high rates,  $I$  is equal to 1, that is, the window has more cases than expected, and otherwise  $I$  equals to 0. Monte Carlo simulation for 999 times has been used to calculate the  $p$ -value of LR. Clusters have been found if a significant ( $p$ -value < 0.05) number of cases is reported within a spatio-temporal window than the expected number of cases during the study period. No geographical overlap has been used as criteria for reporting secondary clusters. These spatio-temporal analyses have been conducted using SATScan software, version 10.0.2.

### **3.4.3. Identifying the spatial influential factors behind the spread**

To identify the influential factors behind the spread in three waves, both spatial and non-spatial regression modeling have been employed. Spatial autocorrelation and spatial heterogeneity, both have been checked before running the spatial regression models.

First, Ordinary Least Squares (OLS) models have been developed considering the incident rate for three COVID-19 waves to define the linear relationships among the incident rate and spatial attributes. This relationship can be characterized by:

$$y_i = b_o + bx_i + e_i \quad (13)$$

Here,  $y_i$  denotes the incident rate in district  $i$ ,  $b_o$  is the intercept,  $x_i$  represents the matrix of independent variables in district  $i$ ,  $e_i$  expresses the random error and  $b$  is the matrix of regression coefficients.

Before developing the model, the normality of the variables has been checked using Stem-and-Leaf plot, Kolmogorov–Smirnov test and the Shapiro–Wilk test. Based on the results of these tests, outliers of the dataset have been determined and treated

accordingly. Later Pearson's correlation coefficients have been estimated to know the correlation between dependent and independent variables. This correlation test has also been applied to check the relations among independent variables. However, the variables ( $r > 0.6$ ) which are strongly correlated have not been considered for the final model to eliminate the risk of multicollinearity. Final OLS models have been developed through a stepwise forward process. The existence of multicollinearity in the final model has been checked through the values of Tolerance (T) and Variance Inflation Factor (VIF). When the  $VIF > 5$  and  $T < 0.1$  have been found for any variable, the correlated variables have been entered into the model one by one and the results of the model have been checked. The variable which has represented a better result has been remained in the final model and the other has been eliminated. The independence of observations has been checked by the result of the Durbin-Watson statistic. To check the homoscedasticity, the predicted values and residuals have been plotted through scatter plots.

Once the OLS models for each wave are developed, spatial autocorrelation within the residuals has been identified using Moran's I statistic. When Moran's I has showed the existence of spatial autocorrelation ( $p\text{-value} < 0.05$ ), Spatial Lag Model (SLM) and Spatial Error Model (SEM) have been developed. SLM generally addresses the effect of independent variables over the dependent variable of other neighboring areas. And SEM considers the error terms (residuals) across different districts that are correlated. For SLM, the developed model can be represented as,

$$y_i = b_o + bx_i + \rho W_i + e_i \quad (14)$$

Where,  $y_i$  denotes the incident rate in district  $i$ ,  $x_i$  represents the matrix of independent variables in district  $i$ ,  $e_i$  expresses the random error,  $b$  is the matrix of regression coefficients,  $\rho$  is the spatial autoregressive parameter and  $W_i$  indicates spatial weight matrix. Here  $\rho W_i$  mainly shows spatial interdependency among dependent variable of an area with independent variables of adjacent areas.

The SEM can be expressed as,

$$y_i = b_o + bx_i + \lambda W_i \xi_i + e_i \quad (15)$$

Here,  $y_i$  denotes the incident rate in district  $i$ ,  $x_i$  represents the matrix of independent variables in district  $i$ ,  $b$  is the matrix of regression coefficients,  $e_i$  expresses the spatially

uncorrelated error term,  $\xi_i$  indicates the error's spatial component at district  $i$ ,  $\lambda$  shows the spatial error regression coefficient, and  $W_i$  indicates spatial weight matrix.  $W_i \xi_i$  represents the magnitude of spatial correlations among the residuals.

Besides spatial autocorrelation, spatial heterogeneity in the developed OLS models has also been checked using the Breusch-Pagan test. This test has shown whether the relationship between dependent and independent variables changes over space. If the result of the test has been found significant ( $p$ -value  $< 0.05$ ), Geographically Weighted Regression (GWR) has been developed. Otherwise, OLS results have explained the scenario as a whole. All of these regression modelings have been done in GeoDa platform (version 1.8.12).

### **3.5. Findings and Recommendations**

The major findings from the research have been highlighted incorporating the differences with literature. Finally, the recommendations have been given based on the research findings in order to help policy formulation.



## **Chapter 4 : Temporal Pattern of COVID-19 at Three Subsequent Waves in Bangladesh**

Since the first detection of COVID-19 case in Bangladesh, the outbreak of the disease was rapid from March to April 2020. After that, the spread kept going. Meanwhile, the virus strain transformed itself and the new variants showed their strength in subsequent waves. Consequently, the government of Bangladesh took different steps to fight against the pandemic.

In this chapter, temporal patterns are initially investigated considering the nation as a single entity, and then local contexts are observed by examining the pattern for each district. In addition, the patterns identified in three waves are examined in the light of various aspatial interventions.

### **4.1. Temporal Pattern of the COVID-19 at the National Level**

Bangladesh has experienced three waves of the COVID-19 pandemic, where the duration of the first, second and third waves are around 46, 29 and 10 weeks respectively. The temporal trends of these waves are statistically tested by Mann-Kendall (M-K) test, Sen's slope estimation and Pettit test to check their significance. Based on the results of these three tests, temporal patterns are detected. Here the temporal patterns are checked both for confirmed cases and incident rate. Because deficiencies in the testing facilities existed over the country as mentioned earlier. Only by detecting the pattern based on the confirmed cases cannot be able to trace this fact. Therefore the temporal pattern of incident rate is focused to explain the scenario. However, the temporal pattern of the confirmed cases is also identified so that any abrupt change in the absolute number of cases can be ascertained relating to aspatial interventions. The results of these nonparametric tests are presented in Table 4.1. These tests reveal that the first wave shows NTAC (No trend but abrupt change) pattern both for confirmed cases and incident rate. Whereas, the second wave shows NTNO (No trend, no abrupt change). The third wave contains DTNO (Decreasing trend, no abrupt change) pattern for confirmed cases and DTAC (Decreasing trend and abrupt change) for incident rate respectively (Table 4.1).

Despite the first wave followed no statistically significant trend, a significant abrupt change occurred in the time series in the case of confirmed cases ( $p\text{-value} < 0.05$ ). Figure 4.1 reveals that a notable rise in weekly confirmed cases happened after 10 May 2020, though the rise in incident rate was not so rapid at this time. Therefore, it can be stated that number of test was increased over the country at this time which has been reflected by the increment of confirmed cases but the actual incident scenario did not change that much. This could be the outcome of the increase of COVID-19 testing laboratories and the increase of testing facilities after 12 May 2020 (DGHS, 2022). Moreover, according to the COVID-19 dashboard of the Directorate General of Health Services (DGHS), all districts of the country experienced the infection since 08 May 2020. This fact could aware people of COVID-19 spread. Consequently, they could feel interested to go for COVID-19 testing if it might any symptoms appear.

Table 4.1: Nation-wide temporal pattern of COVID-19 confirmed cases and incident rate in three subsequent waves

Consideration	Tests and Patterns	1 <sup>st</sup> wave	2 <sup>nd</sup> wave	3 <sup>rd</sup> wave
Weekly confirmed cases	Mann-Kendall (M-K) test	$M\text{-}K\text{ statistic} = 0.03, p\text{-value} > 0.775$	$M\text{-}K\text{ statistic} = 0.108, p\text{-value} > 0.42$	$M\text{-}K\text{ statistic} = -0.555, p\text{-value} < 0.032$
	Sen's slope	---	---	-838.6
	Pettit test	$K=350, p\text{-value} < 0.001$	$K=118, p\text{-value} > 0.067$	$K=29, p\text{-value} > 0.058$
	Detected Pattern	NTAC	NTNO	DTNO
Weekly incident rate	Mann-Kendall (M-K) test	$M\text{-}K\text{ statistic} = -0.145, p\text{-value} > 0.158$	$M\text{-}K\text{ statistic} = 0.012, p\text{-value} > 0.94$	$M\text{-}K\text{ statistic} = -0.539, p\text{-value} < 0.039$
	Sen's slope	---	---	-0.316
	Pettit test	$K=283, p\text{-value} < 0.013$	$K=89, p\text{-value} > 0.382$	$K=22, p\text{-value} < 0.049$
	Detected Pattern	NTAC	NTNO	DTAC

When the incident rate is taken into account, the change point is discovered on 06 September 2020. After this point of time, the incident rate started to drop, and confirmed case followed the same pattern. It reflects that the situation began to stabilize after 06 September 2020, which could be the result of the long-term application of control measures (Figure 4.2). Countrywide lockdown, enforcement of armed force, closure of garments factories, market places, and educational institutions, restriction on public gathering, mandatory mask-wearing, restriction on public vehicles and

international traveling, delineation of risk zones, and imposition of social distancing measures were implemented during the first wave (Figure 4.2).

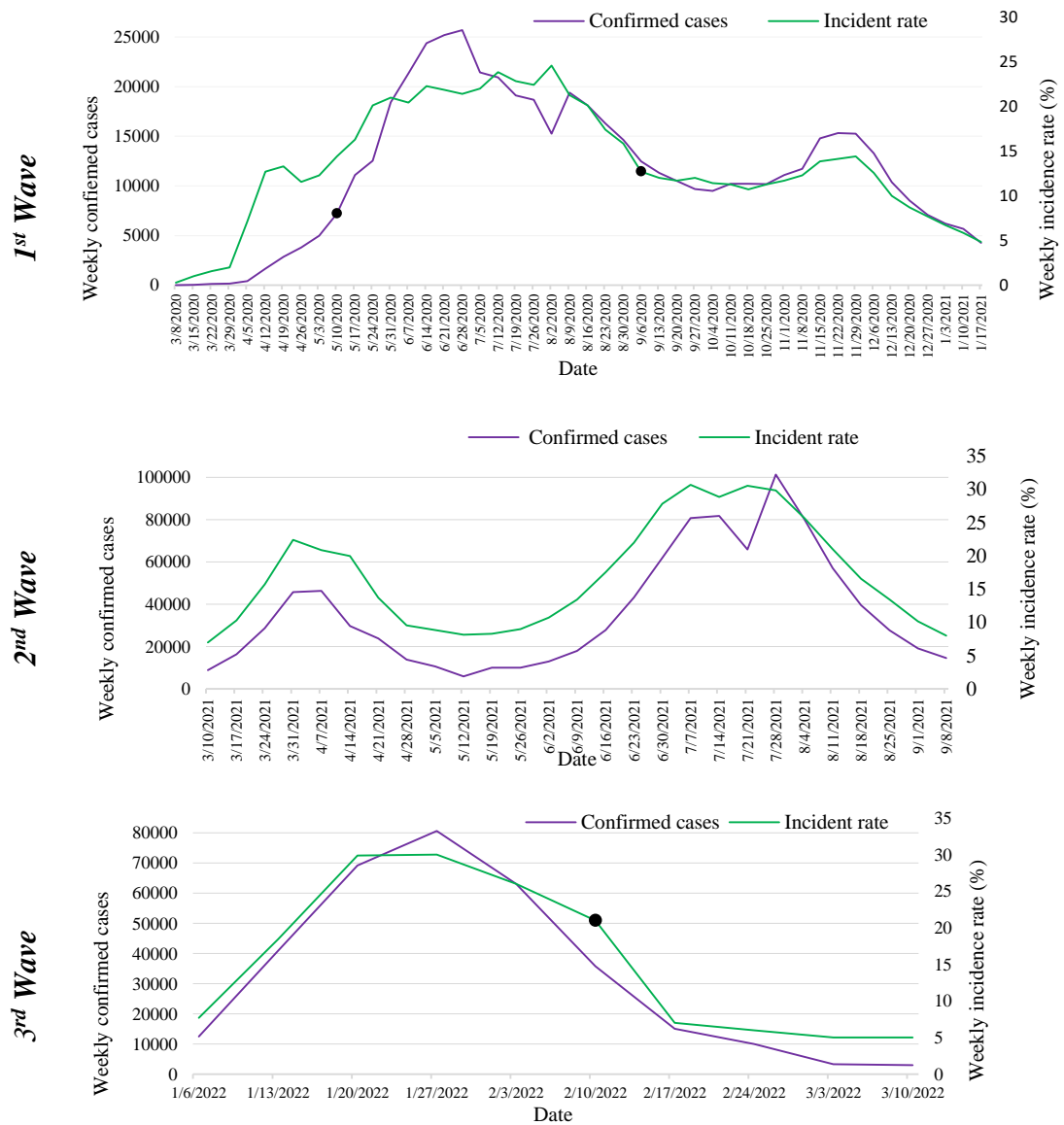


Figure 4.1: COVID-19 infection in three subsequent COVID-19 waves in Bangladesh (Source: DGHS, 2022)

On 26 April 2020 and 16 May 2020, the garments factories and shopping centers were reopened respectively. Immediately after that, a rising trend of confirmed cases was observed. More sharp increase of cases and incident rate have been observed from May 2020 to July 2020 in Bangladesh.

Moreover, it is probable that, due to lack of experience of such a pandemic, lack of knowing the effectiveness of measures, lack of people's awareness and shortage of pharmaceutical interventions, the first wave of COVID-19 in Bangladesh could elongate more than other waves. Over time many pharmaceutical interventions (i.e. medication, vaccination) came into action and people got to know how to respond- these may have contributed to shorten the length of the second and third waves.

In Bangladesh, the nationwide vaccination campaign was started on 07 February 2021, which could have an impact on the scenario during the second and third waves. Nevertheless, the number of confirmed cases and the incident rate were both higher in the second and third waves. These were most likely the result of the introduction of new variants with the changing strain and the relaxation of measures (Figure 4.2). The result of the second wave indicates that no statistically significant trend and no abrupt change occurred within this wave ( $p$ -value  $> 0.05$ ). There was a consistent trend throughout the duration, with no sudden spike or drop. From May to August 2021, the second wave had a higher number of cases and incident rate that were basically similar to the first wave (Figure 4.1). Though the nationwide lockdown was still in effect during these months, it could be possible that other contributing factor/s exacerbated the situation. This fact, however, can be further examined when the spatial concerns are studied thoroughly in the next chapters of this research.

According to Table 4.1, a statistically significant declining trend is seen in the third wave. When the incident rate is considered, an abrupt change point in the time series is also detected. The change point is detected on 10 February 2022. After 10 February 2022, the incident rate was decreasing (Sen's slope = -0.316) radically and the situation was improving. Though the measures were implemented in a somewhat restricted manner during this time period, they could help to quickly control the nationwide situation (Figure 4.2). This could be the result of the combined pharmaceutical and nonpharmaceutical interventions. However, when the number of confirmed cases is taken into account, no statistically significant change point is discovered. This result demonstrates that the number of tests conducted daily had an impact on the situation. Though the number of cases was largely steady, the number of tests greatly increased during the third wave. This ultimately reduced the incident rate.

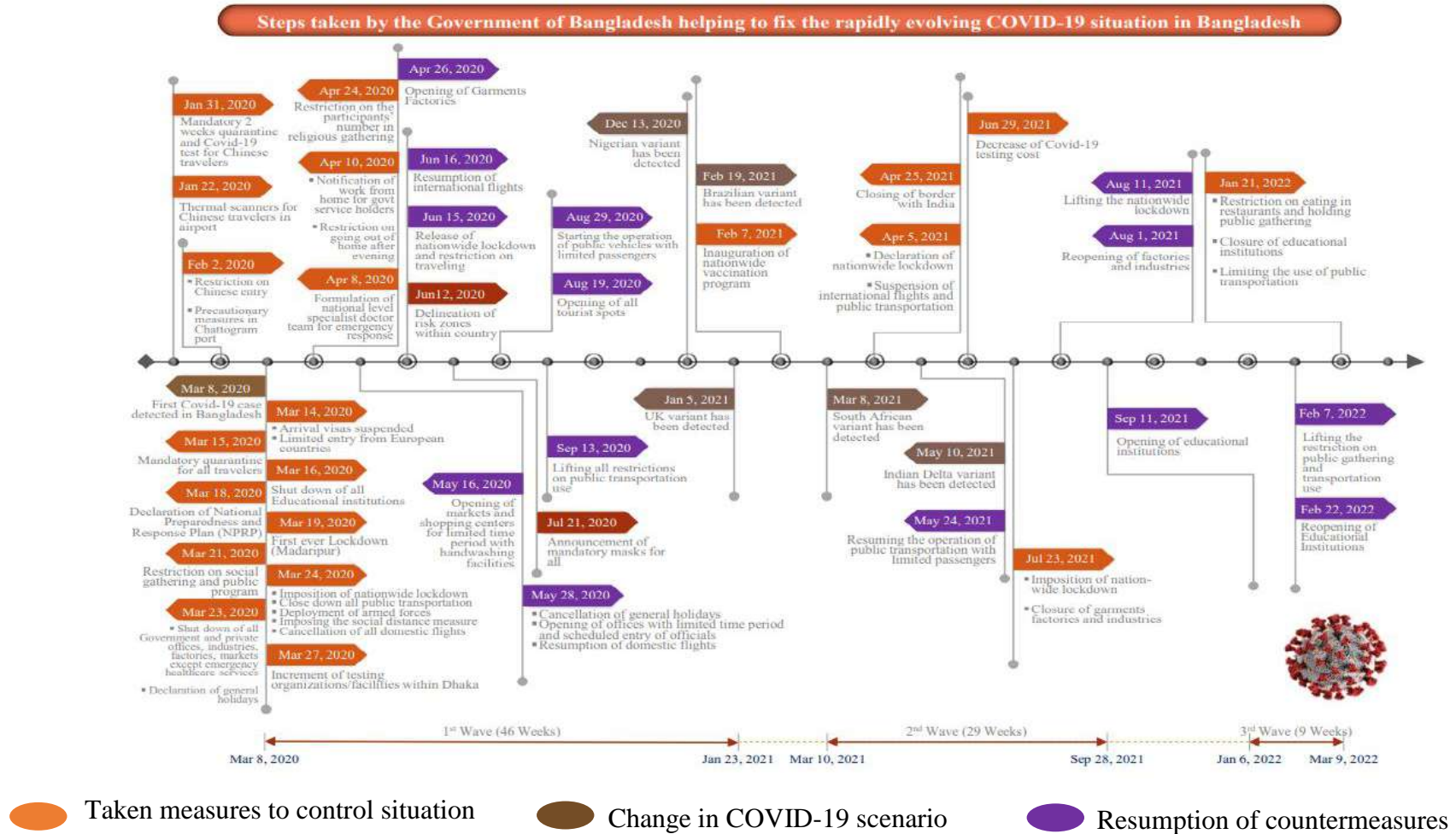


Figure 4.2: Timeline of COVID-19 related events in Bangladesh

Along with the aforementioned understandings, it is also necessary to comprehend how different regions contributed to the national situation. As a result, the next section describes the temporal dynamics at the district level to disclose the substantive picture and identify the greater risk zones during the waves.

## **4.2. Temporal Pattern of the COVID-19 at District Level**

Like the national level, the temporal pattern of COVID-19 infection in districts has been tested considering both weekly confirmed cases and incident rate. Figure 4.3 shows the results of the countrywide situation.

### **4.2.1. During the first wave**

When the weekly confirmed case is considered, four types of patterns (DTAC, ITAC, NTAC, and NTNO) are discovered. 51 of the 64 districts exhibit the NTAC (No trend and abrupt change) pattern, which could be contributory to the nationwide NTAC pattern in the first wave. Furthermore, some divisional districts (like Rajshahi, Rangpur, Chattogram, and Dhaka) and their neighboring districts show a significant increasing trend with an abrupt transition point in confirmed cases. The surge in cases of these locations occurred from the 11th to 18th week (17 May 2020 to 05 July 2020) of the first wave, and a bigger number of people were infected in Dhaka, Bangladesh's capital (Figure 4.4).

Figure 4.2 shows that as of May 16, 2020, all commercial establishments reopened; as of May 28, 2020, all government offices and domestic flights resumed, and general holidays were canceled; and as of June 20, 2020, the nationwide lockdown and restrictions on all types of travel were postponed. The release of the potential control measures during this time period was also reflected in the country's Stringency Indices score (Appendix A). Because most government offices, commercial centers, and transportation hubs are located in Dhaka and nearby divisional districts, relaxation of these measures might be responsible for a surge in cases in these areas. Furthermore, the majority of COVID-19 testing laboratories are centered in Dhaka and divisional towns (DGHS, 2022) which could influence the rise of cases in these areas. Therefore, the incident rate could more accurately reflect the spatial situation.

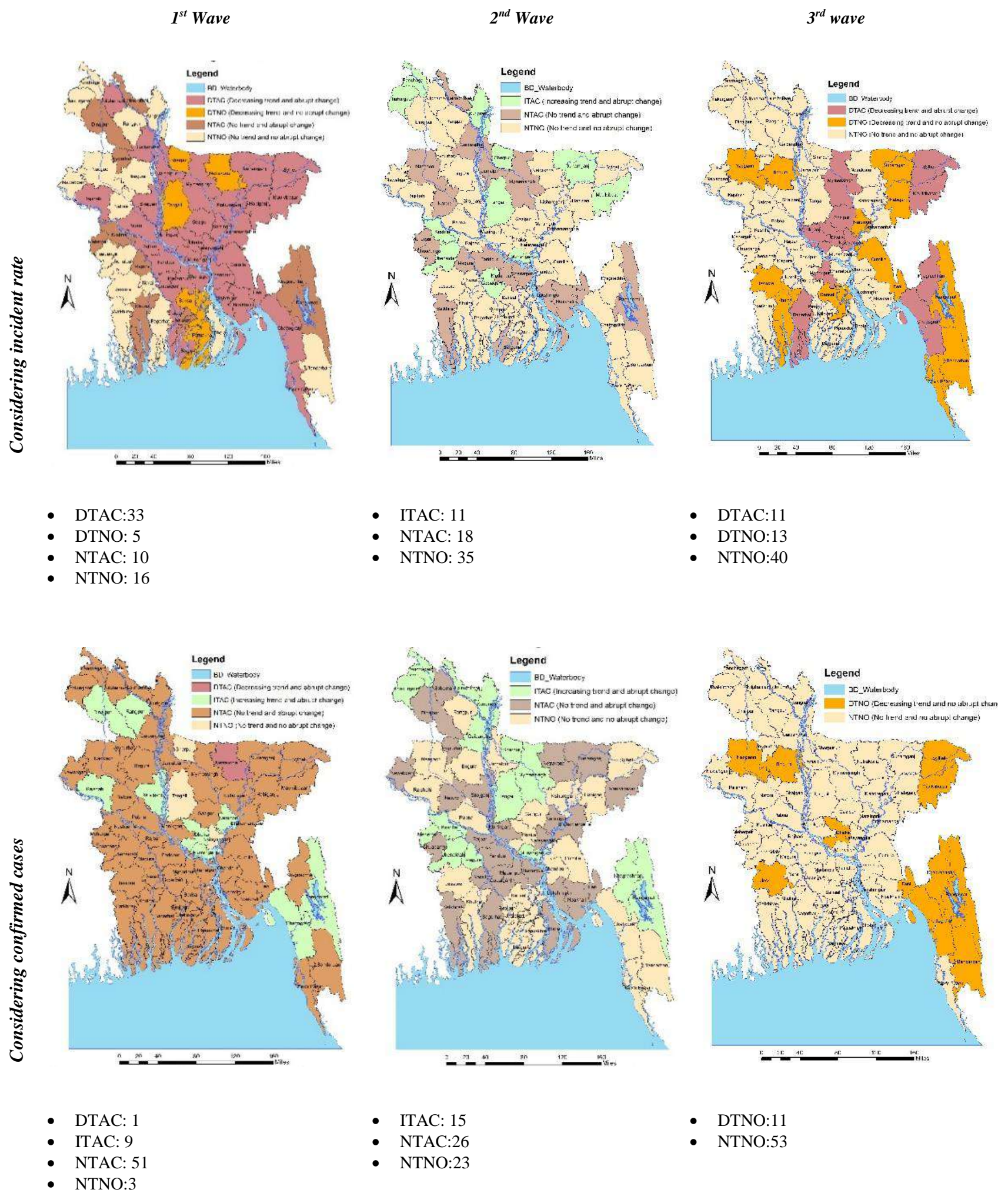


Figure 4.3: Temporal pattern of COVID-19 for different districts during three subsequent waves

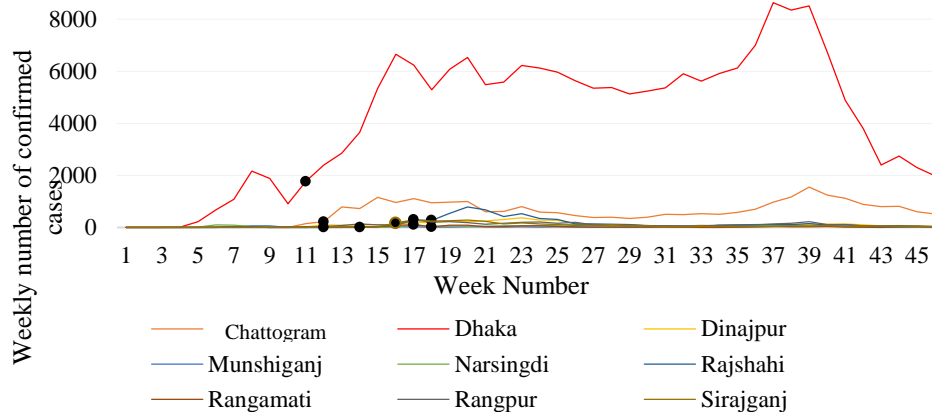
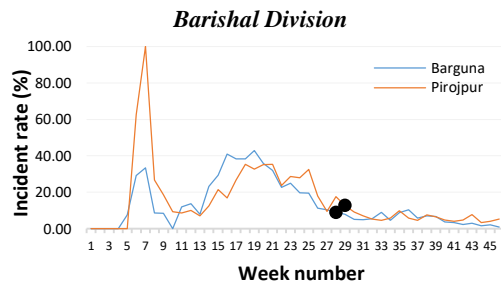


Figure 4.4: Trend of confirmed cases in districts showing ITAC pattern in the first wave  
(Source: DGHS, 2022)

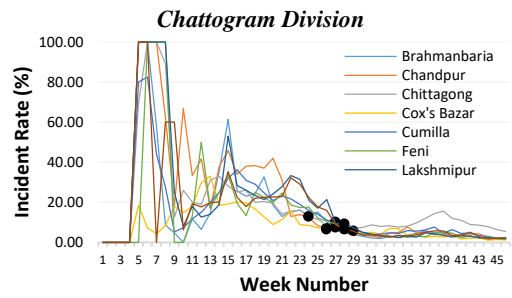
When incident rate is considered, four patterns (i.e. DTAC, DTNO, NTAC, NTNO) appear in the data series. Nearly all districts expressing the DTAC pattern are situated in close proximity to Bangladeshi rivers, and the majority of them are found in the country's eastern region. The expansion of testing facilities and restrictions on local and international transit could have an impact on these regions. In addition, the majority of the country's population resides in these regions. Due to long-term quarantine and restricted movement, the risk of community transmission of the outbreak decreased, which would help to minimize the incident rate in these locations later. Figure 4.5 illustrates a considerable decline in incident rate occurs from the 23rd to 29th week of the first wave (16 August 2020 to 26 September 2020). From the timeline of policy interventions (Figure 4.2), it is evident that some new measures, such as the delineation of risk zones within the community, the mandatory use of masks, and passenger limitation in transport modes were implemented just before this period, despite the postponement of the nationwide lockdown after three months. Together, these steps could bring about a controlled environment in these districts.

The estimation of Sen's slope refers to the magnitude of the declining trend. Figure 4.5 indicates that the districts of Chattogram and Dhaka divisions experienced a relatively steeper (Sen's slope  $>0.35$  for all districts) decrement in incident rate after the 24<sup>th</sup> to 29<sup>th</sup> week of the pandemic.

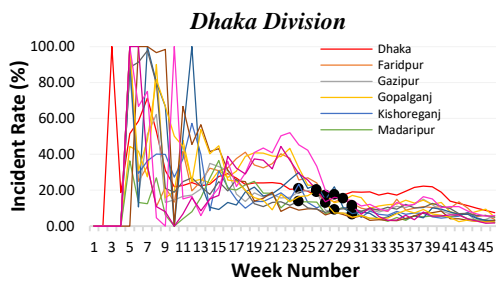




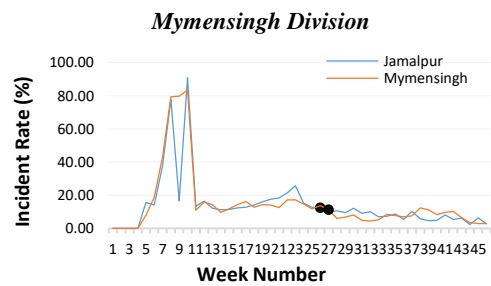
Sen's Slope: Barguna (-0.29), Pirojpur (-0.25)



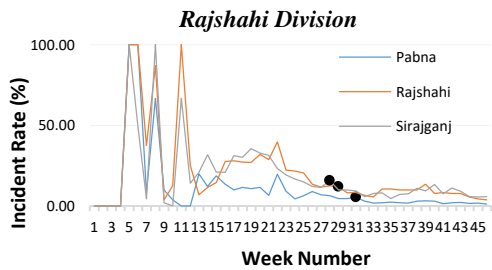
Sen's Slope: Brahmanbaria (-0.41), Chandpur (-0.77), Chittagong (-0.46), Cox's Bazar (-0.34), Cumilla (-0.56), Feni (-0.46), Lakshmipur (-0.57)



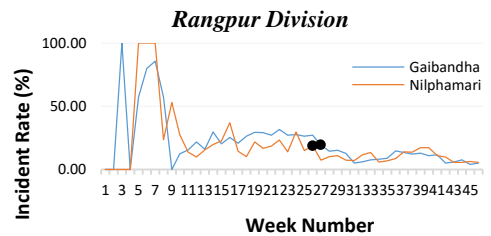
Sen's Slope: Dhaka(-0.44), Faridpur (-0.48), Gazipur (-0.35), Gopalganj (-0.58), Kishoreganj (-0.53), Madaripur (-0.38)



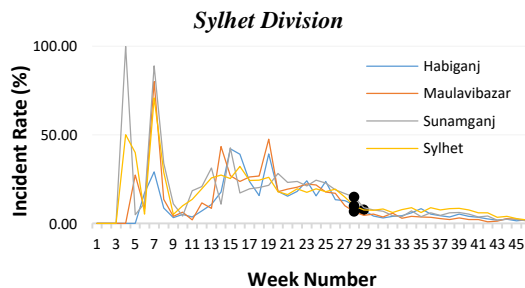
Sen's Slope: Jamalpur (-0.27), Mymensingh (-0.23)



Sen's Slope: Pabna (-0.26), Rajshahi (-0.48), Sirajganj (-0.43)



Sen's Slope: Gaibandha (-0.5), Nilphamari (-0.33)



Sen's Slope: Habiganj (-0.23), Maulavibazar(-0.29), Sunamganj (-0.41), Sylhet (-0.51)

Figure 4.5: Trend of incident rate of districts showing DTAC pattern in the first wave

(Source: DGHS, 2022)

This was because high incident rate in the immediate weeks in these areas. Dhaka and Chattogram are two major business hubs and densely populated cities of the country. In addition, Chattogram plays an immense role to maintain regional connectivity as a port city. After the imposition of a flexible lockdown approach and reopening of official activities with transport in early June of 2020, Chattogram city faced a massive increase of cases and death (Siam et al., 2021). And Dhaka went through a deadly rising trend in the initial period due to its high population density.

On 12 June 2020, when the government of Bangladesh identified risk zones inside the country, several districts of Dhaka and Chattogram divisions were designated as the red zone. After then, extra concerns were given to these locations by enhancing public awareness, expanding testing and treatment facilities, and prohibiting intercity mobility with nearby places. Therefore, these measures could be useful in reducing the incident rate. The districts of Barishal and Mymensingh divisions demonstrated a more gradual decline in incident rate (Sen's slope -0.3 for all districts). After the 12th week of the pandemic, these regions did not experience a rapid increase in the incident rate. Therefore, these regions responded favorably to the early control tactics deployed during the outbreak. Nonetheless, no substantial trend was anticipated in the districts of the Khulna division. Except for the Khulna district, other districts showed NTNO (No trend and no sudden change) pattern. A rapid change point has been detected in the 28th week of the first wave in the district of Khulna, which might be the result of the implementation of new measures in districts with a DTAC (Decreasing trend and abrupt change) pattern.

#### **4.2.2. During the second wave**

Since Bangladesh exhibits the NTNO pattern countrywide during the second wave, the ITAC (increasing trend and sudden change), NTAC, and NTNO patterns complement both the confirmed case and incident rate scenario (Figure 4.3). Figure 4.2 depicts how the second wave differed markedly from the first wave in terms of infection length, introduction of new viral strains, vaccination program availability, and so on. When weekly confirmed cases are examined, there are 15 districts with ITAC pattern, the majority of which are in the border region of Bangladesh (Figure 4.3). From the 11th to 15th week (Figure 4.6) of the second wave, there was a statistically significant increase of cases, as determined by the Pettit test results (11 May 2021 to 22 June 2021).

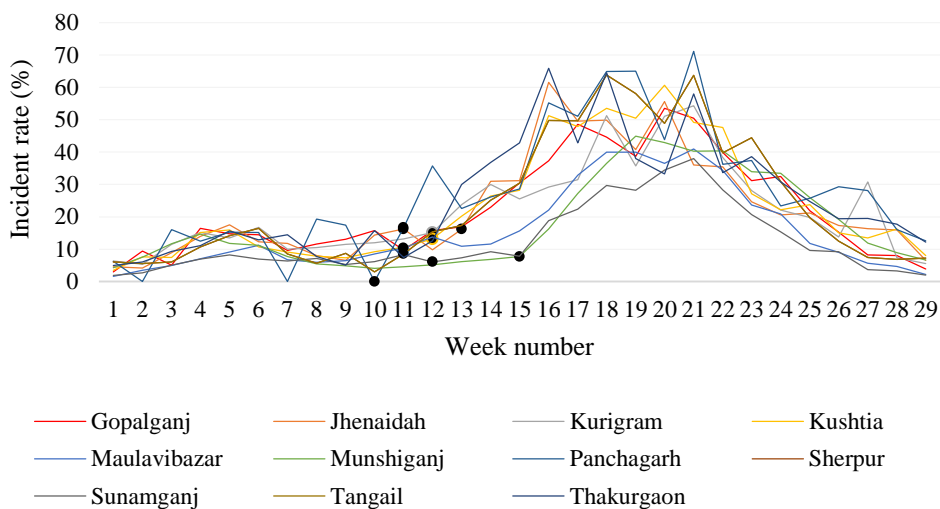


Figure 4.6: Trend of incident rate for districts showing ITAC pattern in the second wave

(Source: DGHS, 2022)

In terms of incident rate, Figure 4.6 depicts eight of 11 districts having ITAC pattern located close to the Bangladesh-India border (Figure 4.3). Since the middle of April 2021, the spread of COVID-19 increased in the Eastern and North-Eastern parts of India, which flank Bangladesh on all sides except the South. So Bangladesh's government again enforced a statewide lockdown, assuming that the situation would be as dangerous as in the neighboring countries. Additionally, all foreign entries were suspended. Figure 4.2 indicates that by the end of April 2021, the borders between Bangladesh and India were sealed except for trade and returnees on a limited scale. By the beginning of May 2021, the Indian Delta version of COVID-19 was found for the first time in Bangladesh. The reported one was the emergency returnee who arrived from India after taking medical treatment (Moona et al., 2021). Due to the application of border closing in a conditional manner, this variant started propagation in this country. The research indicates that the transmission power of the Delta variant is 1,260 times greater than the strain recorded in 2020 (Allen et al., 2022; Zhan et al., 2022). The consequences of this new variant might have caused a quick spike of the incident rate in the bordering areas of Bangladesh, despite the government taking some preventative steps.

In light of the virus' rapid spread, the government cut the price of the COVID-19 test. On 23 July 2021, a rigorous nationwide lockdown was implemented, and all factories and enterprises were ordered to close (Figure 4.2). This week, the infected districts with a notable upward trend were experiencing the highest incident rate peak (Figure 4.3). In contrast to the first wave, when Dhaka had the most infection, the leading regions in the second wave were the border districts of Bangladesh due to the geographical impact of the pandemic. As of the 22nd week of the second wave, the weekly incident rate in these places was beginning to decline. And the nationwide lockdown was lifted and industrial activity restarted. Finally, on 11 September 2021, all educational institutions reopened after the majority of control measures were withdrawn, as represented by the score of Stringency Indices (Appendix A). In addition, the country began its vaccination campaign seven months before the end of the second wave, and a portion of the population was vaccinated by this moment. This could help to limit the spread of the second wave.

However, the majority of NTAC districts were located in close proximity to ITAC districts. This might occur due to their proximity to the places where the significant increasing trend persisted. During the second wave, 35 districts of Bangladesh passed through the NTNO pattern, which indicates that the majority of districts in the nation exhibited neither a statistically significant trend nor a sudden change. Even Dhaka and Chattogram districts, which had the highest number of confirmed cases and the sharpest decline in incident rate during the first wave, were subjected to the NTNO pattern of incident rate. Since the majority of districts showed the NTNO pattern, this largely could contribute to form the NTNO pattern nationally.

#### **4.2.3. During the third wave**

Similar to the previous two waves, distinct patterns are visible across the districts during the third wave. While considering weekly confirmed cases, DTNO (11 districts) and NTNO (53 districts) patterns are identified. During the third wave, no sudden shift in the confirmed case occurred.

A statistically significant change point is observed in the weekly incident rate. DTAC (11 districts), DTNO (13 districts), and NTNO (40 districts) are detected as patterns based on the incident rate (Figure 4.3), despite the fact that this wave lasted for approximately 10 weeks. DTAC districts are mostly located in the central and eastern

regions of the country (Figure 4.3). Figure 4.7 demonstrates that nearly all districts with a DTAC pattern exhibited a sudden transition point in the 5th week (03 February 2022 to 09 February 2022) of the third wave. The incident rate began to fall approximately 14 days after the implementation of control measures. In this wave, mild interventions and no lockdown measures were implemented. Only the closure of educational institutions, the restriction of vehicle mobility, and the restriction of restaurant activities were employed as measures (Figure 4.2). The vaccination program has also been ongoing. Therefore, it can be claimed that the third wave wouldn't be as severe and has not been prolonged in Bangladesh due to a higher vaccination rate among the population and the restricted implementation of nonpharmaceutical interventions. In addition, no new strain of the virus has been found on this wave. This wave could likely be caused by the release of control measures (i.e. the reopening of educational institutions and the resumption of all activities) at the end of the second wave.

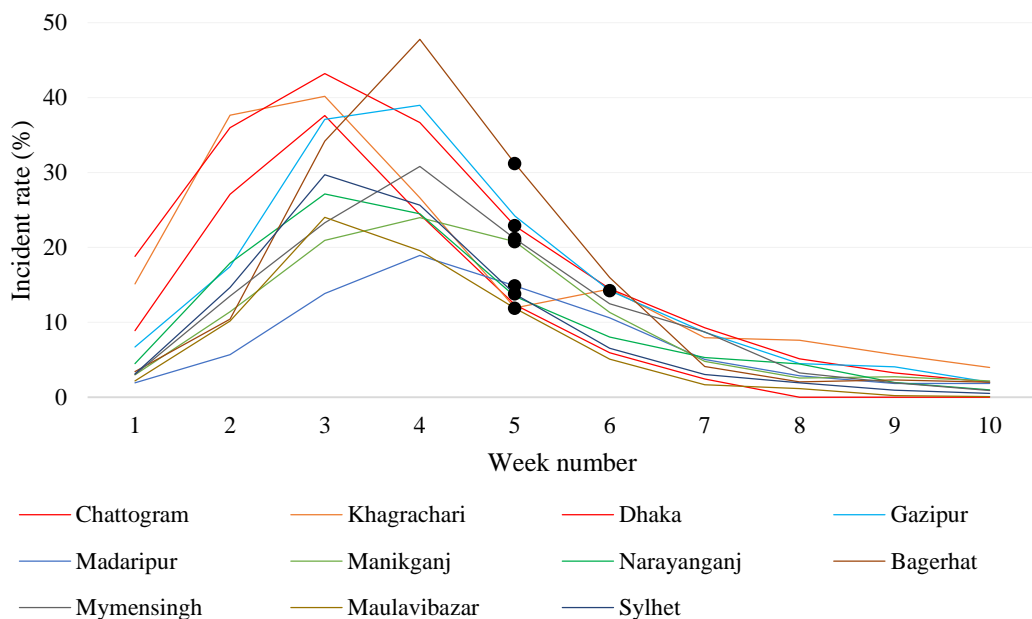


Figure 4.7: Trend of incident rate for districts showing DTAC pattern in the third wave  
(Source: DGHS, 2022)

This chapter examines the temporal pattern of COVID-19 in the three successive waves, both nationally and regionally considering aspatial countermeasures. Based on the discussions, it can be stated that exploration of pandemic wave scenarios at a regional scale is also necessary beside the national context. Several regions in the same wave respond with distinct patterns. The temporal patterns of waves are influenced by various aspatial strategies adopted to manage

the outbreak. Moreover, due to the distribution of the testing facilities and population concentration in Bangladesh, the incident rate is a more accurate indicator to reflect the actual situation.

From the first wave's experience, it is evident that when only nonpharmaceutical remedies have been implemented, it has taken a considerably longer period of time to suppress the outbreak. Due to their locational importance (i.e. higher concentration of population and activities), Dhaka and Chattogram regions are the most vulnerable during the waves. In the first wave, flexible measures have been mostly responsible for the increase of incident rate, but the introduction of new variants of COVID-19 and the limited connection with the most infected neighboring country have been primarily responsible for the rise in the second wave. This finding represents the regional effect of pandemic. The central and northwestern regions of the country have shown the same pattern of growth in the first and second waves of successive years, which may be the result of any spatial characteristic. The pandemic wave can be shortened by pharmaceutical and nonpharmaceutical interventions together, as evident by the second and third waves. The release of all control measures simultaneously poses a threat to the pandemic situation, which may be the primary cause of the emergence of the third wave in Bangladesh. Due to the application of countermeasures in a limited manner, the outbreak state finally has been brought under control in this wave.

## **Chapter 5 : Spatio-temporal Pattern of COVID-19 in Three Waves**

Firstly, the spatial pattern of COVID-19 is discussed in this chapter. The location of any significant spatial cluster is determined further using the local Moran's I technique. Assuming that the spatial pattern has shifted over the period of each wave, spatial autocorrelation techniques (Global and local Moran's I) are utilized for each incubation period of waves. Again, the identified clusters at each period may grow rapidly or slowly or their longevities may differ. These aspects cannot be shown by spatial autocorrelation. So, space-time scan statistics are used to determine the spatio-temporal cluster of cases and the total number of tests. Corresponding results are discussed in this chapter for each wave.

### **5.1. Spatio-temporal Pattern during First Wave**

By employing Global Moran's I, the spatial pattern of COVID-19 as a whole is identified. Each wave in the country persisted for an extended duration. At various points of a wave, it could be possible that dissimilar spatial form existed. Therefore, the spatial pattern of incident rate is examined for each incubation period of COVID-19. The incubation period refers to the length of time a virus can hide inside the body. After the end of the incubation period, the symptoms may appear, changing the total number of cases. To determine the spatial concentration of incident rate, 14 days incubation period is considered in this research for COVID-19 as Lie et al. (2020) stated.

Global Moran's I suggests that the COVID-19 incident rate clustered significantly during the first wave (Moran's I index = 0.43,  $p$ -value < 0.05). Table 5.1 illustrates the outcomes of spatial autocorrelation at each incubation period of the initial wave. At the beginning of the first wave, the incidences were distributed randomly around the space. Global Moran's I estimates that from 08 March 2020 to 13 June 2020 (the first to the seventh incubation period of the first wave), there was no statistically significant spatial autocorrelation of incident rate in Bangladesh ( $p$ -value > 0.05). After 13 June 2020, the clustering of incidents began to intensify, and the situation remained unchanged until

26 December 2020. Within this period, the I11 and I13 points displayed a stronger cluster (Table 5.1), as indicated by Moran's I index of 0.47 and 0.46, respectively.

Table 5.1: Spatial pattern of COVID-19 at each incubation period of the first wave

Incubation Period (I= Incubation Period)	Timeline (date)	Global Moran's I index (GMI)	P-value	Spatial pattern
I1	3/8/2020 - 3/21/2020	-0.05	0.72	Random
I2	3/22/2020 - 4/4/2020	-0.06	0.52	Random
I3	4/5/2020 - 4/18/2020	-0.01	0.95	Random
I4	4/19/2020 - 5/2/2020	-0.02	0.75	Random
I5	5/3/2020 - 5/16/2020	0.08	0.25	Random
I6	5/17/2020 - 5/30/2020	0.13	0.06	Random
I7	5/31/2020 - 6/13/2020	0.12	0.057	Random
I8	6/14/2020 - 6/27/2020	0.18	0.018	Cluster
I9	6/28/2020 - 7/11/2020	0.4	0.0001	Cluster
I10	7/12/2020 - 7/25/2020	0.34	0.0002	Cluster
I11	7/26/2020 - 8/8/2020	0.47	0	Cluster
I12	8/9/2020 - 8/22/2020	0.36	0.0001	Cluster
I13	8/23/2020 - 9/5/2020	0.46	0	Cluster
I14	9/6/2020 - 9/19/2020	0.39	0.0001	Cluster
I15	9/20/2020 - 10/3/2020	0.28	0.003	Cluster
I16	10/4/2020 - 10/17/2020	0.22	0.005	Cluster
I17	10/18/2020 - 10/31/2020	0.15	0.04	Cluster
I18	11/1/2020 - 11/14/2020	0.17	0.03	Cluster
I19	11/15/2020 - 11/28/2020	0.16	0.04	Cluster
I20	11/29/2020 - 12/12/2020	0.15	0.04	Cluster
I21	12/13/2020 - 12/26/2020	0.17	0.03	Cluster
I22	12/27/2020 - 1/9/2021	0.06	0.36	Random
I23	1/10/2021 - 1/18/2021	0.03	0.8	Random

All positive Moran's I statistics indicate that similar incident rate values formed the cluster. According to Figure 4.2, most of the control measures were been phased out one by one starting from June 2020. This period witnessed the resumption of international flights, the lifting of the nationwide lockdown, the opening of market areas and tourist sites, the movement of public vehicles, and the restart of inter-district transportation activities. This could have an impact on the formation of clustered spatial structures. However, following 26 December 2020, until the end of this wave, the distribution of incident rate had no geographical structure, despite the fact that the context of aspatial interventions remained uniform. Furthermore, associated spatial factors, which are discussed thoroughly in the next chapter, could have an effect.



According to the preceding discussion, COVID-19 incident rate followed a statistically significant clustered pattern structure during the pandemic's peak time; when the spread was lesser, the incidences were randomly distributed among the districts.

### **5.1.2. Spatial distribution of clusters and outliers**

Local Moran's I is calculated to investigate the location of clusters based on the results of Global Moran's I. The findings of the national context demonstrate that districts with identical incident rates formed the detected clusters. Nonetheless, it still remains unknown whether these values were lower or greater and functioned as coldspots or hotspots, respectively. This issue is examined using Local Moran's I.

Figure 5.1 highlights the locations of clusters and outliers when spatial patterns are found. Based on the outcome of Local Moran's I Index (LMI), four distinct patterns, namely High-High (HH) clusters, Low-Low (LL) clusters, High-Low (HL) outliers, and Low-High (LH) outliers, are identified for the nation. The early HH cluster of incident rate was located in the eastern portion of Bangladesh encompassing five districts (Habiganj, Brahmanbaria, Cumilla, Chandpur, and Lakshmipur) until 27 June 2020. Including the districts of Mymensingh and Sherpur, a cluster of LL performed as a cold spot. Bogura and Khulna are identified as HL outliers, symbolizing that these districts had a higher incident rate despite being surrounded by districts with a lower incident rate.

Immediately following this period, the HH cluster of the nation transferred to the South-Western region comprising Khulna and seven of its neighboring districts. During the preceding time period, only Khulna exhibited a higher incident rate, whereas its neighboring areas showed no discernible pattern. These regions also experienced an increase in incident rate over time, which might be a result of their proximity to a more infected area. Similarly, an LL cluster emerged in Mymensingh, Sherpur, Netrakona, and Kishoreganj, most likely as a result of a regional influence. By 25 July 2020, the situation of the country's active hotspot (HH) improved, and the number of districts within the hotspot decreased from eight to four. In contrast, two more districts (Gazipur and Narsingdi) added to the cold spot zone that made up the LL cluster.

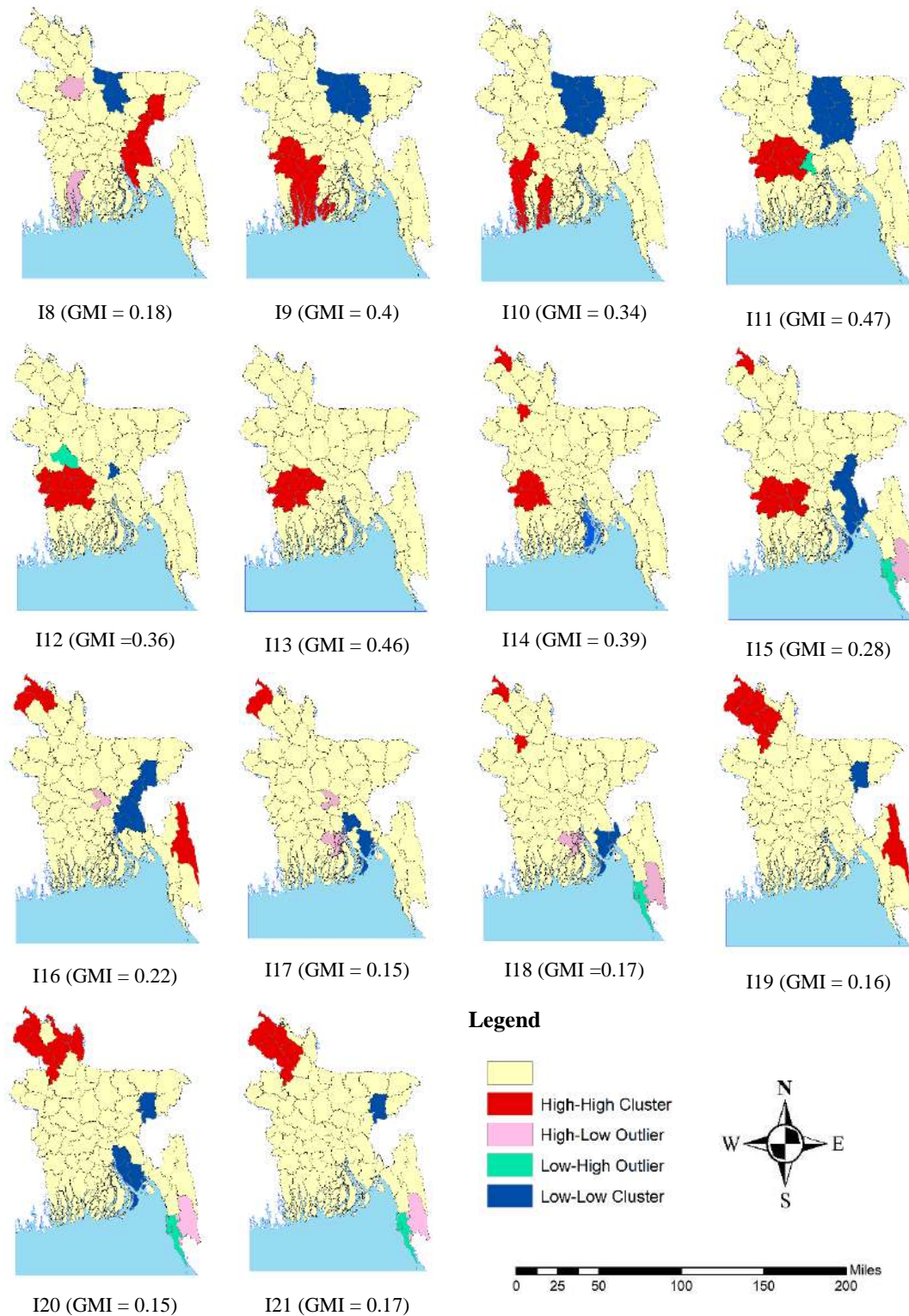


Figure 5.1: Location of clusters and outliers of incident rate during the first wave

After 25 July 2020, Brahmanbaria joined the coldspot zone by curbing its spread; however, a new hotspot consisting of seven districts arose in the Northern region of the

previous cluster on 3 October 2020 and persisted until 25 July 2020. In the Eastern area of the country where the first HH cluster was visible, a cluster of LL occurred at this time. This was likely owing to the implementation of potential control measures in the most infected locations, which reduced the severity of the outbreak. A HL outlier and LH outlier are found in Cox's Bazar and Bandarban, respectively. From August 2020 onward, all Bangladeshi tourism destinations would once again be accessible (Figure 4.2). Cox's Bazar contains the longest beach and is a popular tourist destination. Due to the reopening of the sites after a prolonged closure, more people might have visited the area, which might have an effect on the spread of the outbreak in this area.

From 4 October 2020, Dhaka and Barishal performed as HL outliers. The temporal analysis also reveals the rise in cases during this period. This might be the result of lifting the nationwide lockdown and resuming all activities. As a result of urbanization and improved community amenities, the majority of the population is concentrated in these core locations, which could increase the likelihood of an outbreak. On the other side, a HH cluster began to form in the country's Northern region and expanded actively until the end of the wave.

Based on the aforementioned facts, it can be claimed that large clusters (both HH and LL) of COVID-19 were strengthening with time by concentrating on the early detected low or high infected area. In some instances, the same place within the same wave acted as both a hotspot and a coldspot. In addition, a statistically significant HH cluster shifted from the South-Western to the North-Western side of the nation over time.

### **5.1.3. Space-time cluster of COVID-19 during the first wave**

The previous sections look into the spatial heterogeneity of incident rate at different times. Nonetheless, the risk zones might spontaneously and suddenly expand or shrink which is still unknown. Again the longevity of each cluster cannot be identified yet. The space-time scan statistic is used here to define high-risk areas by quantifying their risks. In this scenario, scan statistics are used both for confirmed cases and the number of tests, with the overlapping of them reflecting the successive risk of areas. The study period in the first wave is divided into three periods: (i) 08 March 2020 to 13 June 2020 (when the random distribution of incident rate appears in Global Moran's I result), (ii) 14 June 2020 to 26 December 2020 (when cluster patterns are found in Global Moran's

I result), and (iii) 27 December 2020 to 18 January 2021 (when the random distribution of incident rate appears in Global Moran's I result again).

Here, Period 1 and Period 3 are employed to obtain secondary clusters prior to and following the identification of spatial clusters, respectively. Figure 5.2 illustrates the location of space-time clusters of cases as risk zones, as well as the location of a higher number of tests during three periods.

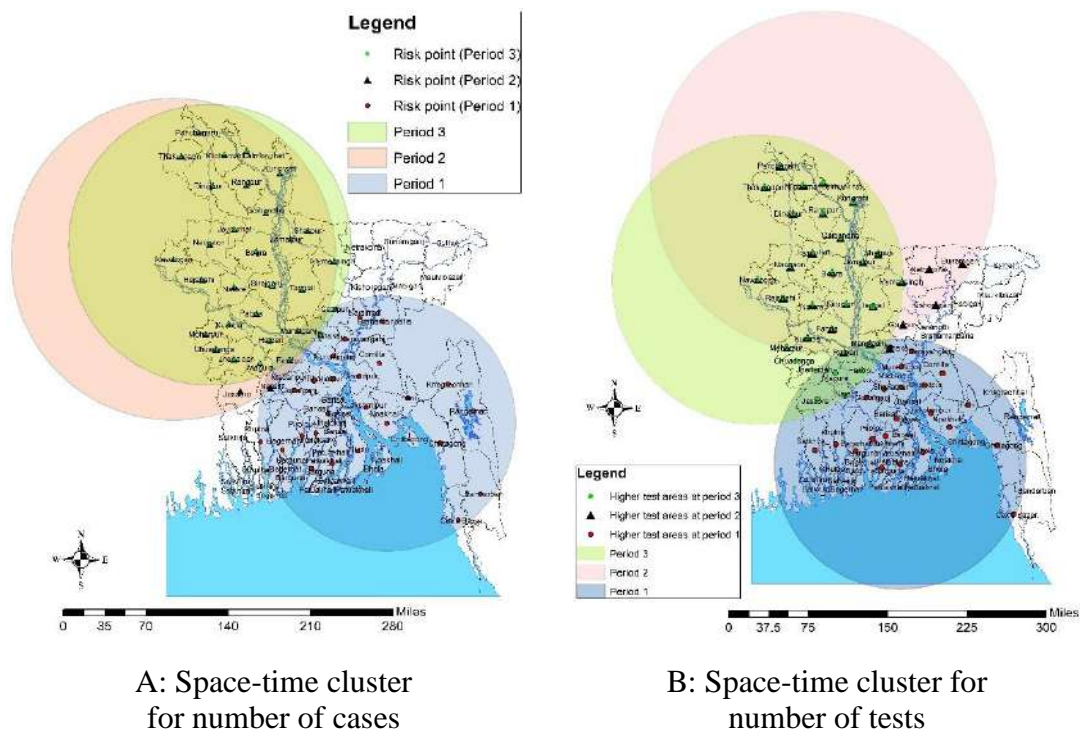


Figure 5.2: Space-time clusters of COVID-19 cases and tests in the first wave at the district level

Though no significant spatial clustering is found in Period 1 according to the result of Global Moran’s I test, until 11 June 2020 a primary fast-growing cluster with a radius of 175.43 km and a relative risk of 56.19 is observed in scan statistics (Table 5.2). This cluster comprised of thirty districts in Bangladesh's South-Eastern area. During this time, a greater number of COVID-19 tests were conducted in these regions (Figure 5.2). And this region leads a cluster of higher incident rate in the next period (Figure 5.1). Therefore, if this risky region could get special consideration and adequate countermeasures before, the later clusters of high incident rate could have been controlled.

During the second period, two clusters were formed over the course of 6.5 months, with the primary cluster of cases located in Dhaka and the secondary cluster including 30

districts in the country's North-Western region. The fast-growing cluster of Dhaka sustained till 04 July 2020. Even though the major cluster only existed in a single location, the population at risk was approximately sixteen times more than the secondary cluster. Dhaka probably contained a higher risk due to its high population density.

The result of local spatial autocorrelation indicates that the cluster of high incident rate was moving towards the North-Western portion of the country, which is supported by the outcome of scan statistics. A secondary risk zone emerged in the North-Western region on 17 July 2020 (RR = 7.59,  $p$ -value < 0.05) and persisted until 29 August 2020, including the same districts in Period 3. In Period 2, the districts within this secondary cluster had a 7.59-fold increased incidence of COVID-19 compared to non-cluster areas. During this time period, the number of tests was likewise elevated in this region and its surrounding locations (Figure 5.2). Due to the rapid spread of infections, the number of COVID-19 tests was likely increased in these locations and their surroundings to support the actual situation and take immediate actions. However, the risk was reduced by 2.93 times during Period 3, when the COVID-19 test was also diminished.

Table 5.2: Features of the detected space-time clusters of cases during the first wave

Cluster No	Observed	Expected	RR	LLR	Number of districts	Population at risk	Radius of cluster (in km)	Time frame
<b>Period 1: 08/03/2020 to 13/06/2020</b>								
1	11,865	269	56.19	34691.76	30	7,75,85,068	175.43	24/5/2020 to 11/06/2020
<b>Period 2: 14/06/2020 to 26/12/2020</b>								
1	89,327	13,536	8.56	102180.9	1	1,33,23,970	0	13/06/2020 to 04/07/2020
2	5,565	744	7.59	6410.9	30	6,73,74,203	221.08	17/07/2020 to 29/08/2020
<b>Period 3: 27/12/2020 to 18/1/2021</b>								
1	5,050	393	19.9	9180.8	1	1,33,23,970	0	29/12/2020 to 13/01/2021
2	702	248	2.93	283.92	29	6,72,83,153	192.64	04/01/2021 to 17/01/2021

Within the first wave, the cluster with the highest relative risk, RR = 56.19, was located in the South-Eastern region consisting of the districts of Dhaka, Chattogram, Barishal, and Khulna divisions. This cluster's districts were 56.19 times more susceptible to COVID-19 than the districts outside the cluster. Based on the above discussion, it can be reported that the number of COVID-19 tests varied depending on the severity of the

infection. Where the incidence of infection was the greatest, the number of tests was likewise increased. Throughout the wave period, the risky locations fluctuated. The identified risky region in scan statistics further acted as a highly infected area of the country. Dhaka was always the riskiest area during the initial wave. As a result of the application of rigorous control measures, the areas that initially posed a greater risk attained stability later. Additional new regions, particularly the districts of the Rajshahi and Rangpur divisions, presented a higher risk in subsequent periods of the first wave.

## 5.2. Spatio-temporal Pattern during the Second Wave

### 5.2.1. Spatial pattern at national context

The GMI result indicates that the second wave showed no statistically significant geographical pattern (Moran's I index = 0.14,  $p$ -value > 0.05). Nevertheless, as seen in Table 5.3, different patterns persisted at different incubation periods of the second wave.

Table 5.3: Spatial pattern of COVID-19 at each incubation period of the second wave

Incubation Period (I= Incubation Period)	Timeline (date)	Global Moran's I index (GMI)	$P$ -value	Spatial pattern
I1	3/10/2021 - 3/23/2021	0.16	0.03	Cluster
I2	3/24/2021 - 4/6/2021	0.08	0.26	Random
I3	4/7/2021 - 4/20/2021	-0.002	0.87	Random
I4	4/21/2021 - 5/4/2021	0.03	0.58	Random
I5	5/5/2021 - 5/18/2021	0.17	0.026	Cluster
I6	5/19/2021 - 6/1/2021	0.35	0.00001	Cluster
I7	6/2/2021 - 6/15/2021	0.45	0	Cluster
I8	6/16/2021 - 6/29/2021	0.46	0	Cluster
I9	6/30/2021 - 7/13/2021	0.18	0.016	Cluster
I10	7/14/2021 - 7/27/2021	0.042	0.49	Random
I11	7/28/2021 - 8/10/2021	0.067	0.32	Random
I12	8/11/2021 - 8/24/2021	0.066	0.33	Random
I13	8/25/2021 - 9/7/2021	0.085	0.23	Random
I14	9/8/2021 - 9/21/2021	0.15	0.035	Cluster
I15	9/22/2021 - 9/23/2021	0.27	0.0005	Cluster

According to Table 5.3, although the second wave began with a statistically significant cluster ( $p$ -value < 0.05), a random distribution of COVID-19 positive persisted around two months after the introduction of the wave. The cluster structure was then sustained

until 13 July 2021. Notably, the cluster was stronger in June 2021 (Table 5.3), as indicated by the higher GMI value. Once more, cluster formation began in early September of 2021 again. According to Figure 4.2, numerous novel Coronavirus strains were identified over these intervals, which could enhance the likelihood of clustering. In contrast to the first wave, the second wave had a fluctuating status of incident rate over its incubation period, which could explain why there was no noteworthy spatial pattern according to the result of Global Moran's I.

**5.2.2. Spatial distribution of clusters and outliers**

The spatial pattern at the local level is investigated further to identify the location of statistically significant clusters. Four types of clusters and outliers are depicted in Figure 5.3 for the second wave.

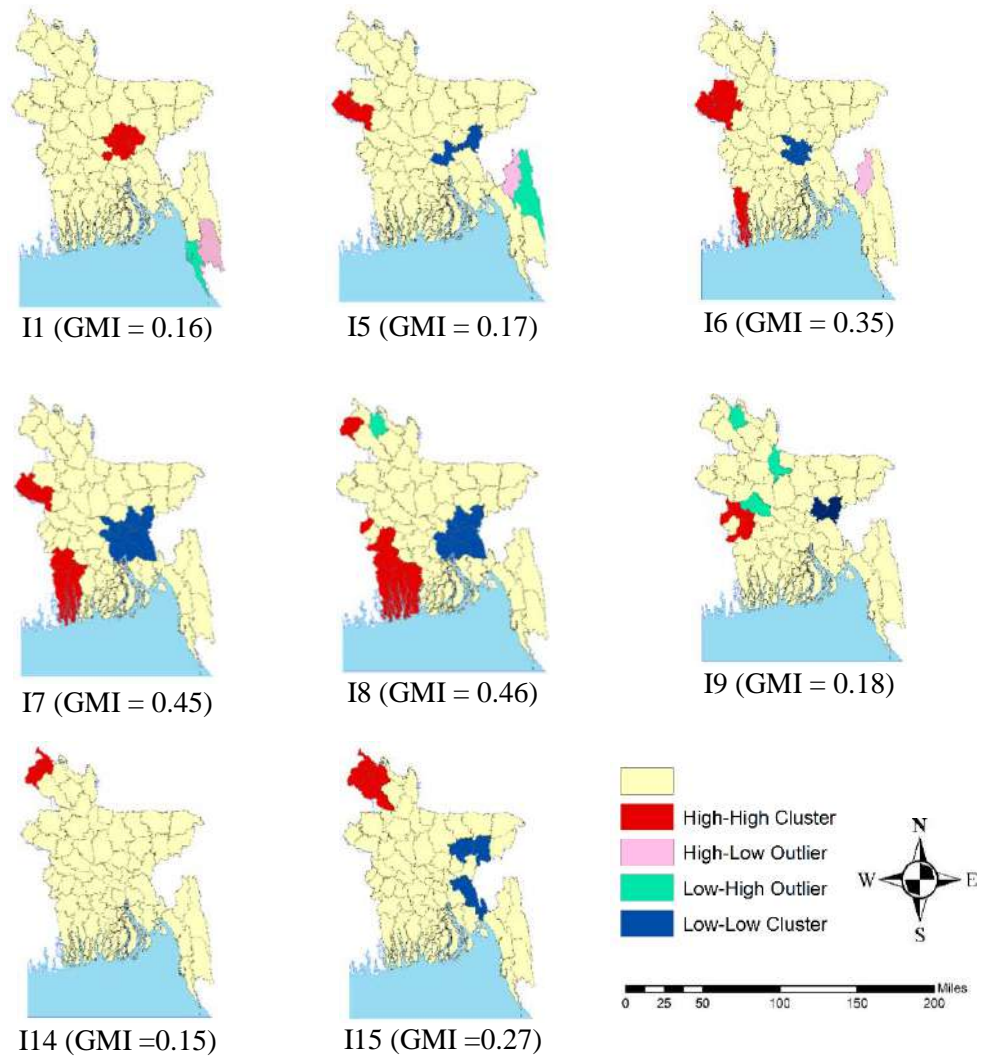


Figure 5.3: Location of clusters and outliers of incident rate during the second wave

Four districts formed a statistically significant HH cluster in the country's central area at the beginning of this wave (Dhaka, Gazipur, Narsingdi, Narayanganj). At this time, low and high combination outliers persisted in Bangladesh's hilly area. Until 18 May 2021, the highest incident rate was concentrated in the Western border region. Therefore, it is evident that although the same pattern was observed at different times, their locations were different. Chapainawabganj and Rajshahi were the most affected places later, as indicated by the temporal trend of incidence. The same region showed higher incidences in this time period of the year during the first wave. Probably any spatial attribute could contribute to this situation.

By 29 June 2021, another HH cluster extended to six districts within the Khulna region. In addition, a major LL cluster propagated to the East, including the core region. Similar to the initial wave, the HH cluster gradually moved towards the Northern portion of the country. Nonetheless, the bordering districts in the Western part of the nation always led the HH cluster during the second wave. After May 2021, the detection of an Indian variant could affect this result as this region is the main way of transport and communication with India. Although Figure 4.2 shows the border connection with India was restricted during this period at a limited scale, the growth of outbreak might occur rapidly due to the conditional entry through the border and the spreading nature of new strain.

### **5.2.3. Space-time cluster of COVID-19 during the second wave**

Based on the identified spatial pattern, the study period within the second wave is divided into four periods for space-time scanning: Period 1 (10 March 2021 to 04 May 2021), Period 2 (05 May 2021 to 13 July 2021), Period 3 (14 July 2021 to 07 September 2021), and Period 4 (07 September 2021 to 23 September 2021).

Figure 5.4 highlights the risk zones during the study periods including the space-time clusters of the number of COVID-19 test within the same time. In Period 1, two clusters are found; one was concentrated in Dhaka and the secondary cluster with a low relative risk ( $RR=2.5$ ,  $p$ -value  $<0.05$ ) configured with Chapainawabganj and Rajshahi districts. Same findings are also revealed from Local Moran's I. However the size of the secondary cluster is 47.77 km which was smaller than the last detected secondary cluster at the end of the first wave covering same geographic area (Radius = 192.64 km in Table 5.2). It is clear that this cluster was the continuation of the first wave though



the spatial expansion reduced significantly. The application of policy interventions (i.e. higher number of COVID-19 tests in this region at Figure 5.4) could be the reason for decreasing the risk. On the other hand, the primary cluster (Dhaka) of this period showed 20.72 times more risk compared to the areas outside the cluster (Table 5.4) with the highest population at risk. This fact indicates Dhaka needs special attention to control the pandemic outbreak.

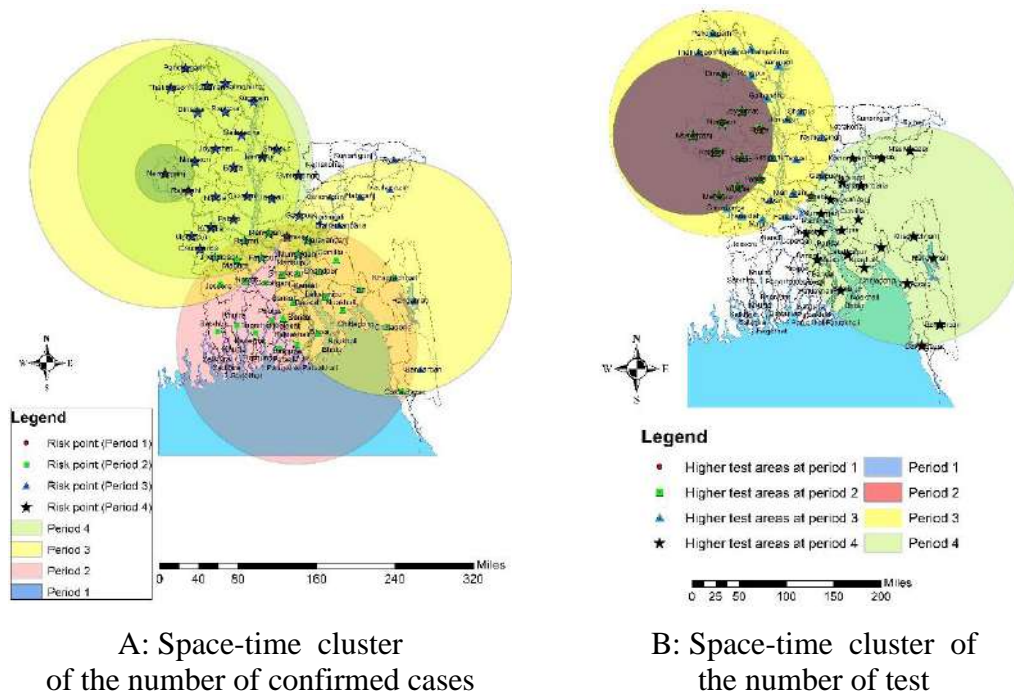


Figure 5.4: Space-time clusters of COVID-19 cases and test in the second wave

Till 02 July 2021, the main cluster appraised in the country encompassing the Central to Southern region with 30 districts. Some districts of Dhaka, Chattogram, Barishal and all districts of Khulna division were present there. The inner districts of this cluster showed 6.38 times more risk of COVID-19 infection than the outers.

It is noteworthy that Jashore district in the Khulna division contained Bangladesh's land port linking to India. Beginning in May of 2021, the Delta strain of COVID-19 severely affected India. This might also influence the neighboring districts of Bangladesh due to the conditional border connection, hence increasing the incident rate in this region. Spatial autocorrelation statistics also showed this Western region of Bangladesh experienced a higher cluster of incidences just immediately after this period. Therefore, considering the context of neighboring countries is also required for pandemic planning.

Table 5.4: Features of the detected space-time clusters of cases during the second wave

Cluster No	Observed	Expected	RR	LLR	Number of districts	Population at risk	Radius of cluster (in km)	Time frame
<b>Period 1 (10/03/2021 to 04/05/2021)</b>								
1	95,194	8,200	20.72	169180.1	1	1,33,23,970	0	18/03/2021 to 23/04/2021
2	722	289	2.5	228.68	2	46,93,620	47.77	11/04/2021 to 28/04/2021
<b>Period 2 (05/05/2021 to 13/07/2021)</b>								
1	127,885	31,141	6.38	103656.9	30	7,65,18,993	197.03	18/05/2021 to 23/06/2021
<b>Period 3 (14/07/2021 to 07/09/2021)</b>								
1	183,558	68,032	4.84	97153.12	26	7,68,69,953	194.79	26/07/2021 to 01/08/2021
2	16,218	7,453	2.24	3964.5	30	6,73,74,203	221.08	18/08/2021 to 02/09/2021
<b>Period 4 (10/9/2021 to 23/09/2021)</b>								
1	4729	342	19.18	8709.8	3	1,81,84,813	33.28	11/09/2021 to 18/09/2021
2	2104	1,267	1.76	254.2	29	6,72,83,153	135.18	13/09/2021 to 21/09/2021

During Period 3, two larger clusters with relatively limited risks ( $RR = 4.84$  and  $RR = 2.24$ , respectively) comprised of districts of the North-Western and South-Eastern regions occurred. Simultaneously, the number of tests increased in the North-Western region, but the situation in the South-Eastern region did not improve (Figure 5.4). This region had a large increase in testing immediately after this period. Though no statistically significant cluster is detected in this period (Table 5.3), two emerging risky clusters are found which finally formed the significant cluster of high incident rate in Period 4.

In the final period of the second wave, a cluster of three central districts (Dhaka, Narayanganj, and Munshiganj) with a radius of 33.28 kilometers was appraised. The number of tests was increased according to the situation. Moreover, until 21 September 2021, a relatively low-risk area persisted on the North-Western side which finally drove the situation towards control.

### 5.3. Spatio-temporal Pattern during Third Wave

#### 5.3.1. Spatial pattern in the national context

In the third wave, Global Moran's I demonstrates a statistically significant cluster of incident rate (Moran's I index = 0.36,  $p$ -value < 0.05). Table 5.5 displays the spatial pattern for the third wave's various incubation periods. The incident rates were strongly clustered throughout the time, and the positive value of GMI indicates that values conforming to these clusters were similar (Table 5.5). From 03 February 2022 to 16

February 2022, the cluster was more prominent as depicted by higher GMI. Nonetheless, the status of the clusters is investigated in the following part using the local spatial autocorrelation technique.

Table 5.5: Spatial pattern of COVID-19 at each incubation period of the third wave

Incubation Period (I= Incubation Period)	Timeline (date)	Global Moran's I index (GMI)	P-value	Spatial pattern
I1	1/6/2022 - 1/19/2022	0.17	0.025	Cluster
I2	1/20/2022 - 2/2/2022	0.28	0.0006	Cluster
I3	2/3/2022 - 2/16/2022	0.43	0	Cluster
I4	2/17/2022 - 3/2/2022	0.29	0.0003	Cluster
I5	3/3/2022 - 3/4/2022	0.16	0.029	Cluster

### 5.3.2. Spatial distribution of clusters and outliers

Local spatial autocorrelation is applied for every incubation period of the third wave, as they all exhibit a substantial cluster pattern. Figure 5.5 represents the position of clusters and outliers where HH, LL, HL, and LH patterns are all present.

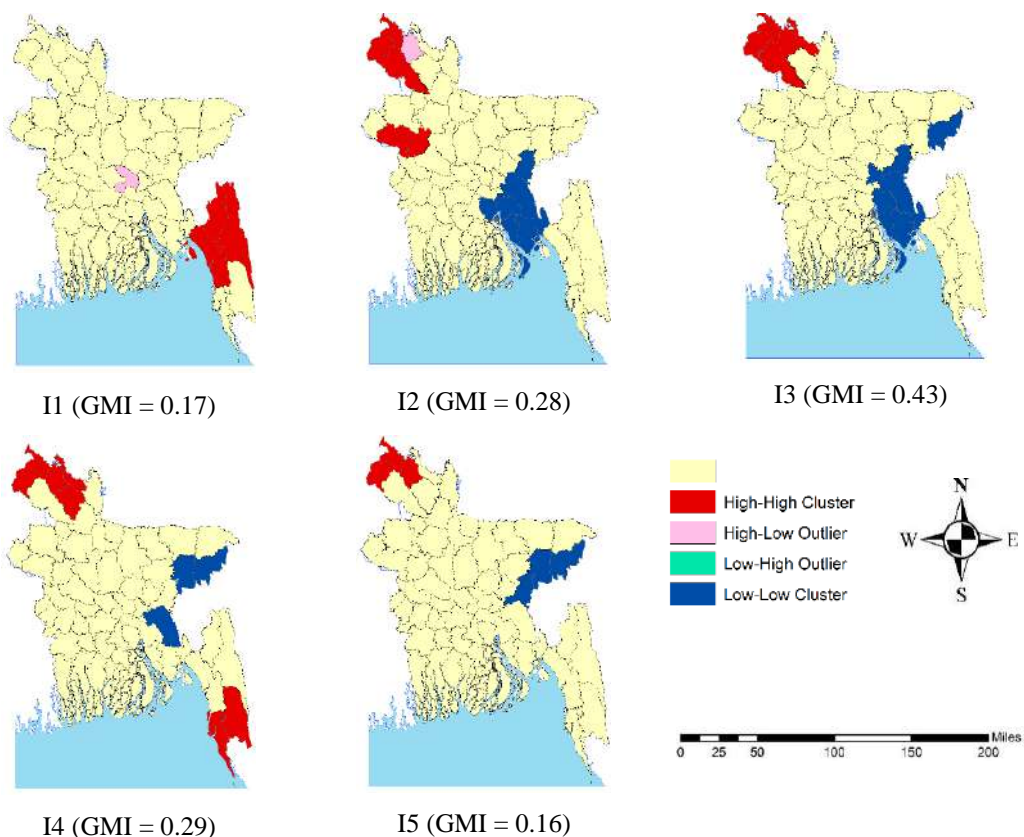


Figure 5.5: Location of clusters and outliers of incident rate during the third wave

Dhaka is identified as HL outlier during the first incubation period, indicating that the incident rate in Dhaka was much greater than in its nearby districts. In the Chattogram region consisting of Chattogram, Khagrachari, and Rangamati, there was a substantial HH cluster. After the second wave, the resumption of all activities might have contributed to the spread of these regions. Then HH and LL clusters were dominant in the North-Western and South-Eastern regions of the country, respectively. And these clusters remained active until the wave's termination. It is noteworthy that the coldspot zone (LL) began to spread in January 2021, when educational institutions closed and public transportation was restricted. Consequently, it may be claimed that control measures influenced both the spatial and temporal outbreaks.

### **5.3.3. Space-time cluster of COVID-19 during the third wave**

The result of spatial autocorrelation shows COVID-19 always follows a spatial cluster in the third wave. Figure 5.6 demonstrates the spatio-temporal cluster of cases in the third wave including the clusters of higher number of test.

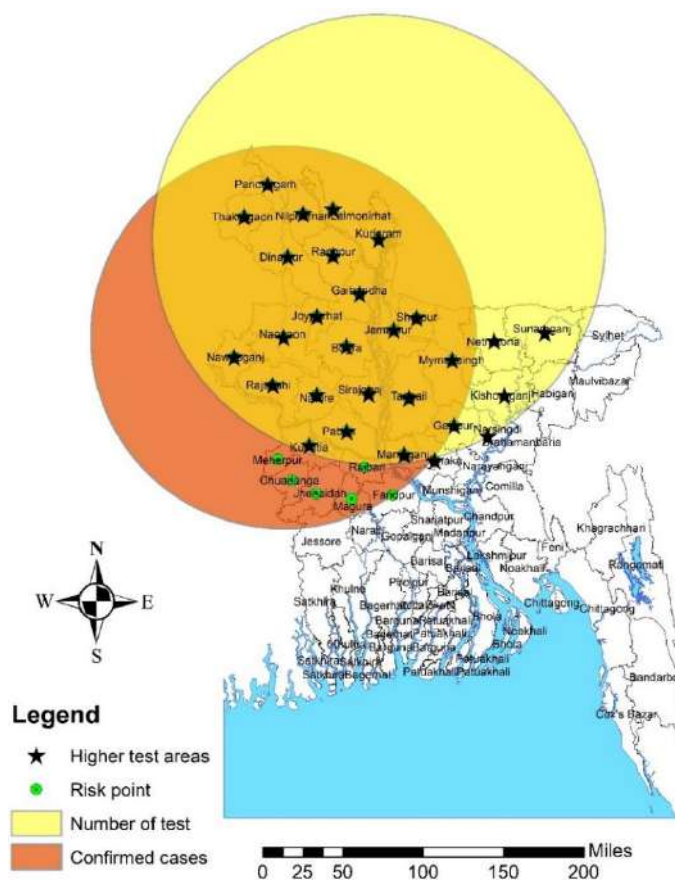


Figure 5.6: Space-time clusters of COVID-19 cases and test in the third wave

During the third wave, two active space-time clusters are discovered: a primary cluster in Dhaka and a secondary cluster including 29 districts in the country's Northern area (Figure 5.6). Dhaka was 18.36 times riskier than other regions (Table 5.6). Till 17 January 2022, Dhaka performed with the growing risk. Compared to Dhaka, the region of secondary cluster got riskier in the later period of the third wave. In response to the growing circumstances, COVID-19 testing increased in the majority of cluster districts and their adjacent regions, even if several districts in the Mymensingh and Sylhet divisions were in a depressed position.

Table 5.6: Features of the detected space-time clusters of cases during the third wave

Cluster	Observed	Expected	RR	LLR	Number of districts	Population at risk	Radius of cluster (in km)	Time frame
<b>Duration: 06/01/2022 to 04/03/2022</b>								
1	116,924	9,938	18.36	203286.9	1	1,33,23,970	0	08/01/2022 to 17/01/2022
2	16,735	2,281	7.7	19243.92	29	6,72,83,153	192.64	09/02/2022 to 27/02/2022

This chapter portrays the spatio-temporal pattern of COVID-19 incidents in Bangladesh considering three waves. Different types of spatial patterns were formed at different times within a wave. This chapter concludes that while COVID-19 incident rates were at their peaks, the incident rate retained its clustered form. The areas identified with higher risk according to the scan statistics performed as a highly infected area in the later period. The findings suggest undertaking timely and effective precautionary measures to tackle the pandemic. Throughout these waves, the center region, and the North-Western portions of the country were at greater risk. Due to the higher population density in Dhaka and its surroundings, the incidence of infection might escalate at certain times. Sharing a geographical border with India might influence the increase in cases in the border region due to conditional border connection after May 2021. After this moment, the cluster with the increased incident rate started to appear in the Western part of Bangladesh. Moreover, as a result of scan statistics, the number of tests in each location was always modified in accordance with the local situation. The number of COVID-19 test was increased in areas as well as in their surrounding regions where the incidences appeared to be higher. This could be applied as a response measure to combat the emerging epidemic.

## Chapter 6 : Influence of Spatial Attributes on COVID-19 Outbreak in Bangladesh

The influence of different spatial features on the incident rate of COVID-19 in three successive waves of Bangladesh is revealed in this chapter. The first section describes the variables that are investigated as spatial attributes. The later sections depict the impact of the associated spatial factors on the three consecutive waves, and the model results as well.

### 6.1. Variables Considered

COVID-19 incident rate is used as the dependent variable, and various spatial attributes are used as independent variables to determine the relationship between COVID-19 incident rate and spatial attributes. Table 6.1 shows the summary statistics for all the variables. This table illustrates that fifteen out of a hundred cases were found COVID-19 positive on average during the first wave, which is around 22 percent and 18 percent in the second and third waves, respectively. The highest incident rate was observed in the second wave, which was almost 1.5 times higher than that of the earlier one. Figure 6.1 depicts the distribution of the incident rate across the country in three waves. The incident rate varied from 4% to 25.2% from one district to another in the first wave, 8.9% to 40.4% in the second wave, and 8.6% to 35.8% in the third wave.

Table 6.1: Summary statistics of the considered variables

Variables	Name of the variables in the model	Mean	Std. Dev.	Min	Max
<b><u>Dependent Variables</u></b>					
Incident rate in the first wave	<i>1stInci</i>	15.0	5.0	4.0	25.2
Incident rate in the second wave	<i>2ndInci</i>	22.3	6.4	8.9	40.4
Incident rate in the third wave	<i>3rdInci</i>	17.8	6.7	8.6	35.8
<b><u>Independent Variables</u></b>					
<b>Demographic characteristics</b>					
Population in 2021 (Projected)	<i>Pop</i>	2489878	1928271	429606	13323970
Population density (per sq km)	<i>Popden</i>	1242	1166	96	9101
Urban population density (per sq km)	<i>urbpopden</i>	371	1060	30	8481
Female population	<i>Fempop</i>	1123961	827047	185003	5488440

Variables	Name of the variables in the model	Mean	Std. Dev.	Min	Max
Population above the age of 65years	<i>Pop65</i>	779396	544462	154790	3261509
Slum population in 2014	<i>popslum</i>	34876	25560	1143	737397
Literacy rate (%)	<i>Litrate</i>	72.0	6.8	59.0	88.6
<b>Healthcare facilities</b>					
Number of hospitals per thousand population	<i>hospital</i>	0.005	0.003	0.002	0.019
Number of doctors per thousand population	<i>doc</i>	0.126	0.000	0.126	0.127
Number of COVID-19 testing laboratories	<i>Covtest</i>	3.3	13.0	0	104.0
Number of treatment bed	<i>trtbed</i>	123.2	179.7	10.0	1228.0
Number of ICU bed	<i>ICUbed</i>	7.52	37.56	0	300.00
Percentage of population having hand wash facilities (%)	<i>handwash</i>	71.1	16.5	31.8	97.3
Number of people vaccinated during second wave	<i>vac2nd</i>	689466	688075	200010	5258506
Number of vaccination during third wave	<i>vac3rd</i>	1356674	1250164	186685	8452303
<b>Infrastructural facilities</b>					
Number of bus stations	<i>busstand</i>	34	30	5	130
Number of railway stations	<i>railstand</i>	8	8	0	40
Number of local markets	<i>locmarket</i>	136	93	7	514
Number of religious institutions	<i>relinsti</i>	4649	2279	989	11499
Trip length from the divisional epicenter of infection (km)	<i>trlen</i>	82.5	54.9	0	227
<b>Meteorological characteristics (in 2021)</b>					
Minimum temperature (°C)	<i>mintem</i>	10.6	2.6	5.8	21.8
Maximum temperature (°C)	<i>maxtem</i>	25.4	4.5	20.8	38.0
Rainfall (mm)	<i>rain</i>	2007.2	763.9	162.3	4637.0
Humidity (%)	<i>hum</i>	76.2	4.8	59.0	88.0
<b>Economic Characteristic (2016)</b>					
Poverty rate (%)	<i>povrate</i>	27.5	15.3	2.6	70.8
Monthly consumption (BDT)	<i>consum</i>	15420	9876	8858	25192

Table 6.1 displays descriptive statistics for all spatial attributes, assuming that these all had a possible effect on the incident rate. These variables are incorporated into regression models in order to determine relationships. According to Table 6.1, it is clear that the distributions of these spatial attributes are not uniform over the space. Such acute conditions might have an influence on the spread of COVID-19 which is determined by spatial modeling in the later sections.

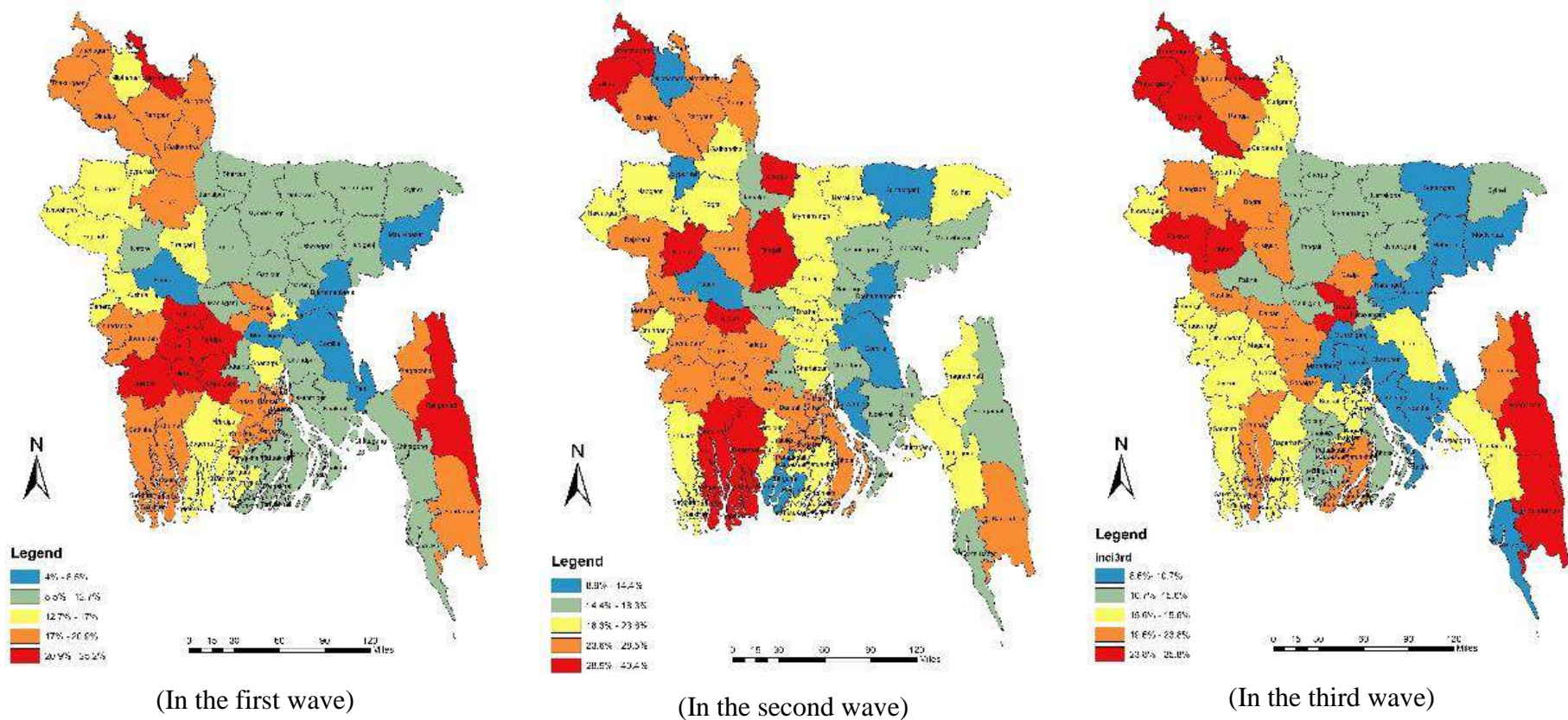


Figure 6.1: Spatial distribution of COVID-19 incident rate in three subsequent waves



## **6.2. Contribution of Spatial Attributes on the First Wave**

To identify the influential factors behind the spread of COVID-19 in the first wave, Ordinary Least Squares (OLS) and spatial regression models are used.

### **6.2.1. Results of the Ordinary Least Squares (OLS) and spatial regression models**

The estimated results of OLS, SLM and SEM models are presented in Table 6.2. Four independent variables, namely ‘population over the age of 65’, ‘number of ICU beds’, ‘poverty rate’, and ‘urban population density’ are found to be statistically significant. Here, population and number of doctors per thousand population appear to be correlated with first wave incident rate, but are discarded from the final model to avoid multicollinearity. Multicollinearity is absent in the developed OLS model because all *VIF* statistics are less than 5 and Tolerance (*T*) values are greater than 0.1. The Durbin-Watson statistic yields 2.3, indicating observational independence. The model's  $R^2$  value is 0.454, implying that the four independent variables can explain 45.4 percent of the variation in COVID-19 incident rates across Bangladesh during the first wave. The incident rate was statistically related to the number of ICU beds, poverty rate, and urban population density in a positive direction. On the other hand, the population over the age of 65 years had a significant negative relationship with the incident rate during the first wave.

However, after developing the OLS model, spatial autocorrelation and spatial heterogeneity in the residuals of the OLS model are examined to better understand the importance of spatial regression modeling. Moran's I diagnostics reveal statistically significant results ( $MI = 0.21$ ;  $p\text{-value} = 0.02$ ), suggesting that spatial autocorrelation exists in the model. As a result, the Spatial Lag Model (SLM) and Spatial Error Model (SEM) are developed to better understand the relationship between incident rate and spatial attributes while accounting for spatial autocorrelation. To assess spatial heterogeneity, the Breusch-Pagan (BP), Koenker-Bassett (KB), and White tests are used. The results of these tests are found to be statistically insignificant ( $p\text{-value} > 0.05$ ), stating that spatial heterogeneity is not present in the model (Appendix B). The relationship between the incident rate and the spatial characteristics remained consistent across districts. Therefore, no local spatial regression model (e.g., GWR) is developed,

and OLS, SLM, and SEM are found to be the better representation of the influence of spatial attributes on incident rate during the first wave.

Table 6.2 also displays the results of the SLM and SEM model. The  $R^2$  value of the SLM model is 0.62, which is greater than that of the OLS model. Furthermore, the *AIC* value is lower than that of the OLS model, indicating that the SEM model fits better than the OLS model. *Rho* also is found to be statistically significant ( $p$ -value < 0.05). Again, the  $R^2$  value in the SEM model is lower than the SLM model ( $R^2 = 0.576$ ) and the *AIC* is higher than the SLM model ( $AIC = 347$ ), indicating that the SLM model fits better than the SEM model. To figure out why the researcher looks at the findings of the OLS model's Lagrange Multiplier (LM)-lag and Lagrange Multiplier (LM)-error tests, found that the LM-lag result is statistically significant ( $p$ -value < 0.05) while the LM-error result is statistically insignificant ( $p$ -value > 0.05). As a consequence, SLM outperforms SEM in terms of model fit. In summary, it can be stated that significant spatial characteristics of neighboring areas influenced the COVID-19 incident rate of the concerned area during the first wave. And SLM model performs better than other models in representing the influence of spatial factors.

### **6.2.2. Findings from the developed models**

#### **Demographic factors:**

In all three models, urban population density and population over 65 years of age are found to be statistically significant demographic factors. There is a positive relationship between urban population density and incident rate in this study. According to the SLM model, if all other factors remain constant, an increase of one person per square kilometer in urban areas would result in a 0.0012 percent rise in COVID-19 incident rate during the first wave, other models exhibit almost similar impact. Furthermore, when the number of confirmed cases is taken into account as the dependent variable, urban population density is found to be statistically significant (Appendix B). These findings are also in line with previous researches, which have shown that an increase in urban population increases the risk of COVID-19 spread (Barak et al., 2021; Hamidi et al., 2020; Lee et al., 2021; M. H. Rahman et al., 2021).

Table 6.2: Results of the OLS and spatial regression models for the first wave

<i>OLS model</i>					<i>SLM model</i>				<i>SEM model</i>			
Attributes	Coefficient	Std. error	<i>t-</i> <i>statistic</i>	<i>p-value</i>	Coefficient	Std. error	<i>z-value</i>	<i>p-value</i>	Coefficient	Std. error	<i>z-value</i>	<i>p-value</i>
Rho					0.5338	0.1059	5.041	0.0000				
Lamda									0.5962	0.1139	5.231	0.0000
<i>Intercept</i>	81.677	12.922	6.321	.0000	53.148	11.319	4.696	0.0000*	56.898	11.977	4.751	0.00001*
<i>Pop65</i>	-12.693	2.146	-5.866	.0000*	-8.737	1.809	-4.831	0.0000*	-7.795	1.997	-3.902	0.0001*
<i>ICUbed</i>	.782	.207	3.782	.00003 *	0.633	0.1675	3.775	0.0001*	0.576	0.162	3.545	0.00039*
<i>povrate</i>	6.343	1.667	3.804	.00003 *	4.576	1.355	3.376	0.0007*	3.432	1.587	2.163	0.030*
<i>urbpopden</i>	.002	.001	2.668	.0001*	0.0012	0.0004	2.981	0.0028*	0.00117	0.000422	2.7877	0.00531*
<b>Model Statistics:</b> $F(5, 58) = 12.5$ , $P\text{-value} = 0.000$ ; $R^2 = 0.454$ ; $Adjusted R^2 = 0.42$ , $AIC = 356.305$ (*95% confidence level)					<b>Model Statistics:</b> $R^2 = 0.62$ ; $AIC = 340.593$ (*95% confidence level; ** 80% confidence level)				<b>Model Statistics:</b> $R^2 = 0.576$ ; $AIC = 346.921$ (*95% confidence level; ** 70% confidence level)			

Here, *Pop65* = Population above the age of 65years (*ln*); *ICUbed* = Number of ICU bed (*ln*); *povrate* = Poverty rate (*ln*); *urbpopden* = Urban population density

People are pulled to urban areas because of the improved community facilities, income prospects, and lifestyle, which is boosting urban population growth. When more individuals live in a given location and go out of their homes for work, the chances of human interaction grow. Given that humans are COVID-19's primary host, such a circumstance could increase the likelihood of viral propagation. As a result, densely populated urban regions including Dhaka, Chittagong, Khulna, Barishal, Rangpur, and some other districts saw higher incident rates than other districts. Therefore decrementing the population concentration in urban areas is necessary to combat future outbreaks. However, it is necessary to maintain the population concentration for running the urban economy. So, adequate control measures need to be promoted in urban areas with special consideration to tackle the pandemic outbreak.

The population over the age of 65 years shows a significant negative relationship with the incident rate. According to SLM model, a 1% increase in the number of people over the age of 65 years in an area could result in a 0.08 percent decline in the incident rate (Table 6.2). In the context of OLS and SEM models, it may cause 0.12 and 0.07 percent decrease in the incident rate respectively. All three models show almost identical results. COVID-19 incident rates are greater among the young generation and adults, according to the findings. This is likely owing to the fact that persons of this age are more interested in outside activities and communication, which increases the chances of interaction and, as a result, infection. People above the age of 65 years, on the other hand, are relatively less active and are usually retired from employment or activities. Presumably, they are not engaged in outside activities given the alarming outbreak of COVID-19. This fact could have minimized their risk of infection. Therefore, districts having a larger share of the younger population have got affected more during the first wave in Bangladesh. Almost similar findings have been revealed by Boehmer et al. (2020). Hutchins et al. (2020) has found that the older generation is more concerned with maintaining the COVID-19 mitigation measures and basic hygiene which may decrease their risk of getting infected. Literature have also shown that areas with the major share of older population in the demographic structure have experienced a higher death rate of COVID-19 due to lower immunity among the older groups (Guilmoto, 2020). Hence, in order to design a framework for pandemic mitigation measures, the age distribution of the population must be addressed.

### Healthcare facilities

The number of ICU beds in each district had a statistically significant relationship with the incident rate during the first wave in all three models. If all other factors remain constant, a 1% increase in ICU beds in a district would result in a 0.0063% rise in incident rate according to SLM model (Table 6.2). When confirmed cases are used as a dependent variable, the nearly same result is revealed (Appendix B).

For the COVID-19 patient with severe infection, the Intensive Care Unit (ICU) bed is usually recommended. So there could be a chance of infection from ICU if any mismanagement appears there. To deal with the impending epidemic, the Bangladesh government upgraded ICU facilities across the country, but it was not possible to increase ICU beds in an unlimited manner. Sometimes government increased the ICU facilities in the areas where the incident rate was continuing to rise. Thus the areas with higher infection got a higher number of ICU facilities. The incident rate still could not be controlled due to the deficiencies in demand and supply of beds (Anwar et al., 2020). To address this issue, reducing the demand for ICU beds can be a solution. If adequate non-therapeutic preventive measures can be enforced strictly at the onset of any pandemic, the pressure on ICU beds can be released by cutting out the propagation of the incident rate. An increase of initial medications, enhancing testing facilities and vaccination, adjusting the population and doctor ratio, creating awareness among people, and so on can help to mitigate the adverse situation. Moreover, according to the result of the Pearson correlation test, district-wise number of ICU beds and number of general treatment beds are statistically correlated ( $r = 0.81$ ;  $p\text{-value} < 0.05$ ). In the resource constraint situation, some treatment beds could be transformed into ICU beds temporarily as an immediate response to a pandemic like in other countries (Mari et al., 2020).

### Economic characteristics

As an economic determinant, the poverty rate is found statistically significant in the mentioned three models. It has a positive correlation with the incident rate. If all other circumstances remain constant, a 1% rise in the poverty rate would result in a 0.0457 percent increase in the incident rate. This result suggests that locations with poorer communities were infected more during the first wave.

In Bangladesh, a considerable share of the population lives from hands to mouth. They need to go outside everyday to earn their living. In the lockdown during the first wave, people needed to go to work to survive, which increased their chances of human contact and infection. Even when the Government of Bangladesh announced a special relief package for such social groups, the crisis persisted. Their awareness level of COVID-19 precautions was likewise insufficient, increasing the danger of transmission. According to Household Income and Expenditure Survey (HIES)-2016, the poverty rate is higher in the central region of Bangladesh. Chapter 5 shows that the incident rate was also higher in this region. This result is also consistent with Drefahl et al. (2020). Therefore, designing a pandemic management system should give special consideration to regions with higher poverty rates. But in Rahman et al. (2021), monthly consumption was also found as a significant factor behind the incident when it was considered in terms of population. People in the areas of higher consumption want to go out of home for their necessary goods which propagates their exposure to the virus. And where the population density is higher, their risk of infection also increases. That could be the reason to get such a relationship. However, the incident rate considering the number of tests could not contain any significant relationship with monthly consumption.

### **6.3. Contribution of Spatial Attributes on the Second Wave**

#### **6.3.1. Results of the OLS, SLM and SEM models**

Similar to the first wave, an OLS model is run for the second wave. Based on the results of OLS, SLM and SEM models are also developed. Table 6.3, shows the estimated results of the three models.

In the OLS model, only rainfall, the number of bus stations, and the distance from the divisional epicenter of infection are identified to be statistically significant. There is no multicollinearity in this OLS model because all *VIF* statistics are fewer than 5 and Tolerance (*T*) values are larger than 0.1. The Durbin-Watson statistic yields a value of 2.07, indicating the independence of observations. The  $R^2$  value of the model is 0.159, which suggests that these three independent variables could only account for 15.9% of the variation in the incident rate of COVID-19 across Bangladesh during the second wave. There could have been additional factors that influenced the change in incident rate during the second wave. As described in previous chapters, there could be a higher

influence of aspatial features (i.e. introduction of new strains on viral propagation, customized lockdown approach) on the incident rate of the second wave. Here, all independent variables except the number of bus stations had a significant negative relationship with the incident rate, implying that an increase in them would result in a drop in the incident rate.

Moran's I test and Breusch-Pagan (BP) test are performed to examine spatial autocorrelation and spatial heterogeneity in the residuals of the model. Both tests, however, exhibit statistically insignificant results ( $p\text{-value} > 0.05$ ). According to the statistics, the spatial features of the neighboring regions do not influence the incident rate of a given district, nor are they associated with one another. Consequently, SEM, SLM, and local models could not provide a better match scenario than the OLS model. After developing the SEM and SLM models, no significant changes in  $R^2$  and AIC values are identified; these are almost similar for all models (Table 6.3). The context is distinct from the first wave, in which nearby spatial characteristics have a substantial effect on the incident rate. Hence it can be stated that the scenario of the second wave was much different than the initial one.

### **6.3.2. Findings from the developed models**

#### **Meteorological characteristic**

Among meteorological attributes, rainfall demonstrated a statistically significant negative connection with incident rate. If all other factors remain static, a one percent increase in precipitation would result in a 0.108 percent decrease in the incident rate during the second wave according to the OLS model.

If there is an increase in precipitation, people might be unable to leave their homes, which would significantly raise the social distance between people. Long-lasting precipitation could well have decreased the likelihood of human interaction, hence decreasing the possibility of virus transmission. While the number of confirmed cases has been assigned as a dependent variable, rainfall revealed nearly same association (Appendix B). Additionally, some studies have demonstrated that places with higher precipitation had a decreased incidence of COVID-19 infection (Basray et al., 2021; Hassan et al., 2021). Thus, the districts like Sylhet, Sunamganj, Maulavibazar, and so on had relatively lower infections during the second wave. In contrast, the districts of Rangpur and Rajshahi divisions where precipitation is lower experienced higher

infection during the second wave. Hence in developing a proper pandemic management plan, the areas with lower precipitation should be emphasized more.

#### *Infrastructural facilities*

Again, the number of bus stations in each district is significantly correlated with the incident rate. Keeping all other variables unchanged, a one percent increase in the number of bus stations would increase the second wave incident rate by 0.057 percent in the OLS model. In this period, the lockdown was not as extensive as in the previous wave, and limited movement was permitted. The public transportations were also available with the application of social distancing measure. People in this country, however, have a propensity to be unwilling to maintain preventive measures (Rahman et al., 2021). This ultimately contributed to the escalation of the disease. Hence special containment measures need to be implemented in the areas with more transit stations and strict enforcement of them including adequate social awareness require to be ensured.

In addition to the number of bus stations, the relationship between travel distance from the divisional epicenter of spread and incident rate is proven to be statistically significant. If all other factors stay unchanged, an increase of one kilometer in travel distance could reduce the incident rate by 0.24 percent according to the OLS model. Therefore, nearby districts were infected more than distant ones, which ultimately contributed to the formation of the COVID-19 hotspot encircling the outbreak's divisional epicenter. This issue could be managed by limiting mobility from the epicenter to the surrounding areas. During the second wave, COVID-19 infection was localized in the country's north-western and south-western regions (Figure 6.1). If travel limits were implemented early on in the most affected district, the establishment of these hotspots might well be prevented. Therefore, after detecting the fast-growing infected area, the connection of it with other regions need to be closed in future. Public movement can also be restricted as a measure to prevent the emerging spread of future epidemics.



Table 6.3: Results of the OLS and spatial regression models for the second wave

<i>OLS model</i>					<i>SLM model</i>				<i>SEM model</i>			
Attributes	Coefficient	Std. error	<i>t</i> -statistic	<i>p</i> -value	Coefficient	Std. error	<i>z</i> -value	<i>p</i> -value	Coefficient	Std. error	<i>z</i> -value	<i>p</i> -value
Rho					0.1732	0.1550	1.117	0.2639				
Lamda									0.01386	0.18128	0.0764	0.93904
Intercept	63.50	12.54	5.06	0.00	55.5519	13.158	4.2218	0.0002 *	63.0612	12.2754	5.1372	0.00000*
<i>rain</i>	-10.83	3.69	-2.75	0.01*	-9.09566	3.5989	-2.5273	0.0114 *	-10.0484	3.61536	-2.7793	0.00545*
<i>busstand</i>	5.70	2.21	2.58	0.01*	5.252	2.129	-2.466	0.0136 *	5.62422	2.156	2.608	0.00909*
<i>trlen</i>	-0.242	0.491	-1.94	0.057**	-0.245	0.495	-1.95	0.056**	-0.252	0.54	-1.98	0.053**
<b>Model Statistics:</b> $F(2, 61) = 6.98$ , $P\text{-value} = 0.002$ ; $R^2 = 0.186$ ; $Adjusted R^2 = 0.159$ , $AIC = 410.345$ (*95% confidence level; ** 90% confidence level)					<b>Model Statistics:</b> $R^2 = 0.2$ ; $AIC = 410.1$ (* 95% confidence level; **80% confidence level)				<b>Model Statistics:</b> $R^2 = 0.186$ ; $AIC = 410.3$ (*95% confidence level; **75% confidence level)			

Here, *rain* = Rainfall (*ln*); *busstand* = Number of bus stations (*ln*); *trlen* = Trip length from the divisional epicenter of infection

Moreover, when the number of confirmed cases is examined instead of the incident rate, a statistically significant positive relationship has also been discovered between urban population density and maximum temperature (Appendix B). In Bangladesh, as in other nations, locations with greater temperatures suffered more cases (Raza et al., 2021). That might be the cause of the second wave's surge in infections in the North-Western regions (Rajshahi and Rangpur division) of Bangladesh. The number of vaccination is also considered to develop the models for understanding the effect of pharmaceutical measures. No significant relationship is revealed between vaccination and incident rate of the second wave. So public vaccination programs ultimately could not influence the spread of COVID-19 during the second wave. However, the models developed for the second wave demonstrate that spatial factors did not contribute more to the dissemination and spread of COVID-19 than those influenced during the first wave.

## **6.4. Contribution of Spatial Attributes on the Third Wave**

### **6.4.1. Results of the OLS, SLM and SEM models**

Table 6.4 displays the estimated results of the OLS, SLM and SEM models considering the incident rate of the third wave. Four of the independent factors are found to be statistically significant: the number of hospitals per thousand people, the minimum temperature, rainfall, and urban population density, where rainfall has a negative relationship with incident rate.

In the OLS model, multicollinearity is missing based on the results of *VIF* ( $VIF < 5$ ) and Tolerance ( $T > 0.1$ ). The Durbin-Watson statistic has a value of 1.9, indicating the independence of observations. The model's  $R^2$  score is 0.339, reflecting that these four independent variables could account for 33.9% of the variation in the incident rate of COVID-19 across Bangladesh during the third wave. By examining the OLS model's Moran's I findings, it is determined that spatial autocorrelation exists in the residuals during the third wave ( $MI = 0.35$ ;  $p\text{-value} = 0.000$ ).

Hence Spatial Lag Model (SLM) and Spatial Error Model (SEM) are introduced to obtain a better-fitting model than ordinary least squares (OLS). The spatial heterogeneity is thus evaluated using the Breusch-Pagan (BP), Koenker-Bassett (KB), and White tests. The results of these tests are statistically insignificant ( $p\text{-value} > 0.05$ ),

indicating that the model lacks geographical heterogeneity and has no need for local models. The  $R^2$  value of the developed SLM model is greater than that of the OLS model ( $R^2 = 0.56$ ), and the  $AIC$  value is lower, denoting that SLM provides a better match than OLS in this context.  $Rho$ 's value also demonstrates statistical significance ( $p\text{-value} < 0.05$ ). Consequently, the geographical characteristics of the nearby regions influence the incident rate of the third wave, which the SLM model could account for.

Again compared to SLM, the  $R^2$  value of the SEM model is markedly lower, and the  $AIC$  value is comparatively higher (Table 6.4). The results of the Lagrange Multiplier (LM)-lag and Lagrange Multiplier (LM)-error tests of OLS are compared, and it is discovered that the LM-lag statistic is indeed significant ( $p\text{-value} < 0.05$ ), while the LM-error statistic is insignificant ( $p\text{-value} > 0.05$ ). So to explain the scenario of the third wave, the SLM fit the data better than other models.

#### **6.4.2. Findings from the developed models**

##### **Demographic characteristic**

Among the demographic variables, urban population density demonstrates a significant positive relationship with incident rate similar to the first wave. According to all three models of the third wave, a one-person increase in the urban population per square kilometer would result in a 0.0016 percent growth in the incident rate (Table 6.4). Previous studies have also revealed this type of relationship (Barak et al., 2021; Hamidi et al., 2020; Lee et al., 2021; M. H. Rahman et al., 2021) and this is also same in the first wave (Table 6.1). This component may account for the identical dissemination patterns observed during the first and third wave. Hence proper adaptation measures should be designed for urban areas to mitigate the adverse impacts of pandemics.

##### **Meteorological factors**

Rainfall and minimum temperature show a significant relationship with incident rate as meteorological attributes, however, their directions are distinct. Due to less human interaction, the incident rate dropped with the increased rainfall, similar to the second wave. If all other factors remain constant, a 1% increase in rainfall would result in a 0.076 percent reduction in the incident rate during the third wave according to the SLM model (Table 6.4). Due to the influence of this factor, the Eastern region of Bangladesh could be less infected during the third wave. Hence seasonal and weather conditions should be considered in developing pandemic policies. The minimum temperature in

each district, on the other hand, reports a positive relationship in the third wave. With all other factors being equal, a 1% increase in temperature during the third wave would raise the incident rate by 0.21 percent (Table 6.4).

In the winter months of the year (December to February), Bangladesh experiences the lowest temperature. In addition, the third wave timeline is associated with this time period. As a result, this element is thus found to have an impact on the spread. Lower temperatures demotivate people to leave the house in the winter, reducing the chances of human interaction. People attempt to complete their outside activities when the temperature rises, which would contribute to an increase in incident rates. Furthermore, the country's North-Western parts are more susceptible to cold, and this region experiences a greater incident rate during the third wave. As a result, the minimum temperature, as well as the geographic location of this region, could raise the likelihood of spread and should be considered in developing containment strategies to control the outbreak.

#### *Healthcare facilities*

The number of hospitals per thousand population shows a significant relationship across all models as healthcare-related factors. It possesses a positive relationship. If all other factors stay constant, the increase in one hospital per thousand people increases the occurrence rate by 7.9% according to the SLM model, which is tremendous. So in the third wave, hospitals could act as a hub of infection. When people go to any hospital, their chance of getting exposed to the infected one gets higher. This situation could possibly be the outcome of improper management and a lack of public awareness. During the third wave, such a scenario might happen. During any pandemic, healthcare facilities generally serve to support minimizing the severity of infection. Again it could perform as the place of infection by facilitating the infected population. Thus higher number of hospitals could increase healthcare accessibility in terms of service delivery, likewise, mismanagement of them could be a curse during a pandemic. Therefore in addition to the establishment, hospital facility management must be ensured; otherwise, this could have the unintended consequence of worsening the pandemic outbreak.

Table 6.4: Results of the OLS and spatial regression models for the third wave

<i>OLS model</i>					<i>SLM model</i>				<i>SEM model</i>			
Attributes	Coefficient	Std. error	<i>t</i> - <i>statistic</i>	<i>p</i> - <i>value</i>	Coefficient	Std. error	<i>z</i> - <i>value</i>	<i>p</i> - <i>value</i>	Coefficient	Std. error	<i>z</i> - <i>value</i>	<i>p</i> - <i>value</i>
Rho					0.577622	0.1075	5.3710	0.0000				
Lamda									0.631662	0.107458	5.87825	0.0000
<i>Intercept</i>	78.2573	16.4167	4.766	0.00001*	48.6731	13.654	3.5647	0.00036*	48.5319	17.6602	2.7481	0.00599*
<i>hospital</i>	6.81	2.621	4.567	0.00003*	7.931	2.943	4.5540	0.00001*	6.9	2.76	4.13353	0.00004*
<i>mintem</i>	30.8995	7.75246	3.985	0.00019*	21.0282	6.21178	3.3852	0.00071*	17.6432	8.16818	2.15999	0.03077*
<i>rain</i>	-10.815	3.81237	-2.836	0.00624*	-7.64617	3.01024	-2.5400	0.01108*	-5.68024	0.000541	-1.60172	0.10922**
<i>urbpopden</i>	0.001643	0.00068	2.388	0.02016*	0.00166	0.000535	3.1079	0.00188*	0.0016343	0.000459	3.02016	0.00253*
<b>Model Statistics:</b> $F(4, 59) = 7.56$ , $P\text{-value} = 0.000$ ; $R^2 = 0.339$ ; $Adjusted R^2 = 0.294$ , $AIC = 407.346$ (*95% confidence level)					<b>Model Statistics:</b> $R^2 = 0.56$ ; $AIC = 388.405$ (* 95% confidence level)				<b>Model Statistics:</b> $R^2 = 0.55$ ; $AIC = 389.58$ (*95% confidence level; ** 80% confidence level)			

Here, *hospital*= Number of hospital per thousand population; *mintem* = Minimum temperature (*ln*); *rain* = Rainfall (*ln*); *urbpopden* = Urban population density

Based on the aforementioned findings, it can be concluded that a number of spatial factors influence the COVID-19 outbreak in Bangladesh, albeit these determinants are not the same in every wave. However, urban population density and the spatial distribution of hospitals per thousand population always influenced the waves to some extent. And more population always propagated the risk of COVID-19, indicating that population concentration of each area should be carefully emphasized in resource allocation to tackle the pandemic. Above all, the geographical factors must be considered when formulating pandemic management policies and spatial plans that integrate public health concerns.

## **Chapter 7 : Major Findings and Recommendations**

This chapter summarizes major findings from this research. Based on the findings, it shares some policy implications, which might be considered to develop an effective pandemic management framework for the country.

### **7.1. Spatio-temporal Analyses of Three COVID-19 Waves**

- *National context:* The incident rate of COVID-19 varied across the waves. Bangladesh experienced the highest incident rate during its second wave, whereas the first wave had the longest duration. During the first wave, there was no significant trend of infection in the country as a whole; nevertheless, on September 6, 2020, a sudden decline in cases occurred may be due to the implementation of long-term aspatial measures. The second wave, however, exhibited a uniform temporal pattern across the nation. On the other hand, a considerable lowering trend of COVID-19 has been observed during the third wave.
- *Effect of aspatial interventions:* During the first wave, only non-pharmaceutical countermeasures were implemented, whereas subsequent waves included both pharmaceutical and non-pharmaceutical countermeasures. In the initial wave of the pandemic, the Bangladesh government adopted many preventative steps. Initially, these approaches manifestly failed to control the pandemic. Identical findings were also presented by Shammi et al. (2021). However, current research indicates that the application of such non-pharmaceutical measures over the long term is somewhat effective in limiting the outbreak.

When both pharmaceutical and non-pharmaceutical measures were in action during the second and third waves, the situation appeared worst after May 2021 due to the arrival of new strains. Finally, the execution of some hard measures (e.g., banning the link with the most infected neighboring countries, locking down the entire nation, limiting the use of public transportation, and closing educational institutions) could bring a relatively better state.

- *Effect of the testing facilities:* Due to unequal distribution of COVID-19 testing facilities over the country, regions with a greater number of tests have a greater likelihood of cases and vice versa. In Bangladesh, the majority of facilities are located in the capital and district headquarters. As a result, these regions had the highest number of infected people, whereas the deprived regions had the lowest number as reported during the three waves. Consequently, the incident rate considering the number of people infected relative to the number of tests carried out is a better indicator for characterizing the pandemic scenario in Bangladesh.
- *Vulnerable regions:* Eastern region had a lower incident rate during pandemic waves than the Central and Western regions. Almost in every wave, Dhaka, the economic hub of the country, and its surroundings were the first to show a rising trend of spread. After analyzing the spatial factors, it is found that urban population density significantly propagated the incident rate. And population density is higher in Dhaka and its surrounding districts which could be the reason for a rapid outbreak in these areas. After Dhaka, a sudden spread has been observed in the Western region. According to the analysis, the Western region of the country shares the boundary with some Indian regions where the COVID-19 outbreak was relatively higher. The Bangladesh government closed the border connection as an emergency measure to control the outbreak. But border connection was permitted in a limited manner (i.e. emergency travel for medical treatment). This thing affected the later outbreak in Bangladesh, consequently neighboring districts with India experienced the shock of COVID-19 during the second wave.

Some meteorological factors, like temperature and rainfall, may also contribute to the COVID-19 spread in these areas. Geographically, the Western region experiences higher temperature and lower precipitation. Fu et al. (2021) showed dry environment boosts the immunity of the COVID-19 virus. The areas where higher temperature and lower precipitation prevail for a long time, the weather can experience dryness. This could probably be one of the reasons of the rapid spread in the Western region. However, Islam et al. (2021) showed absolute and relative humidity also influenced the transmission of COVID-19 in Bangladesh while the confirmed case was considered as a dependent variable. But this research shows no



such relationship while the incident rate is considered. And the findings are relevant to the COVID-19 scenario in the Western portion of the country. Therefore, special consideration should be given to the Central and Western regions of Bangladesh when formulating pandemic strategies with spatial considerations in mind.

- *Significantly responsive areas:* Prior studies of COVID-19 in Bangladesh have mostly focused on the spatial perspective based on the number of cases, while temporal aspects have been substantially overlooked (Islam et al., 2021; Mashrur et al., 2021). However, as this study demonstrates, merely a geographical perspective cannot adequately reflect the actual situation because the spread dynamics are also subject to temporal change. Earlier studies report a considerable surge of COVID-19 in Dhaka and Chattogram (Mashrur et al., 2021; M. H. Rahman et al., 2021). This study illustrates the same thing with changing circumstances over the period. After the initial detection of COVID-19, a rapid spike in incident rates occurred in Dhaka and Chattogram. As revealed from the spatial analyses, urban population density largely influenced the growth of the incident rate. Dhaka and Chattogram are the country's two largest hubs, containing the bulk of urban population. Most of the industrial areas, commercial places, community facilities, and transport facilities are concentrated in these areas and their surroundings. Due to better urban facilities and job opportunities, population density is also increasing there which increases the chance of human interaction. And more human interaction has a strong positive correlation with the pandemic spread. That is why when COVID-19 was detected first, Dhaka and Chattogram districts were affected more. After the declaration of lockdown and other control measures, the activities of all areas came to a standstill. Due to the application of such long-term measures, the outbreak situation started to improve. Dhaka and Chattogram, where the highest incidences happened, also started to respond. Closure of all activities in these areas could also minimize the incident rate with an abrupt decrementing trend. Therefore, it can be claimed that densely populated urbanized areas are more sensitive to pandemic spread as well as prevention measures. Such areas should be considered with careful attention in developing pandemic management policies.
- *Pandemic vulnerable period of the year:* During the first and second waves, the incident rate rose typically between May and July. Bangladesh observed the highest peak during both waves in this period. And nearly identical regions were affected

this time. During the second wave, the Western region of the country, particularly the districts of the Khulna and Rajshahi divisions, displayed an increase in incidences. During this period, the most alarming Delta variant of COVID-19 was identified in the Eastern region of India (Allen et al., 2022). This fact might have affected the neighboring regions of Bangladesh. Therefore, the location of the country on the globe is also an important factor that influences pandemic waves. This research also shows that aspatially flexible containment measures influenced the surge in the first and third waves, whereas the introduction of a new virus strain made the situation worse in the second wave.

- *Effects on tourist areas:* During the first and third waves, a statistically significant clustered spatial form was identified for the entire period. Different forms were apparent when the spatial pattern of the pandemic was analyzed for short periods such as the incubation period. Initial clusters of high incident rates were found in the central region, including Dhaka, and the clusters gradually shifted to the South-Western to North-Western portion of the country. Cox's Bazar and its nearby districts, which contain the majority of the country's tourist attractions, had the greatest incident rate from October to November 2020. According to the timeline of interventions reported, tourism places were reopened just before this period, which might have contributed to this spike.
- *Origin of clusters:* According to the scan statistics, the cluster of high incident rate areas was eventually formed by the areas which possessed the highest risk. Like during the first wave, the relative risk of Dhaka was higher in the initial phase. In the later phase of this wave, a cluster of higher infected areas was created concentrating on Dhaka. Although the frequency of tests in these locations was increased during this period as an immediate response, the outbreak could not be controlled much due to a lack of social awareness and flexible containment approaches. Therefore, if such an emerging risky area is discovered sooner, the outbreak can be prevented with the help of appropriate countermeasures.

## **7.2. Contribution of Spatial Characteristics on Incident Rate**

- *Spatial models:* Present research convincingly identifies that in all three waves, Spatial Lag Model (SLM) performs somewhat better than other models. This refers

to the fact that sometimes spatial characteristics of adjacent areas also have affected the incident rate of a given area. Hence, the local features like population concentration, meteorological characteristics, and distribution of emergency treatment facilities in the neighboring regions should also be considered during plan preparation of a particular area when public health issues are a matter of concern.

- *Highly influential spatial attributes:* Urban population density, rainfall, poverty rate, the number of elderly residents in an area, temperature, and travel distance from the nearby highly infected area could shape the distribution of incident rate. According to earlier studies, a few of these variables have also impacted pandemic occurrence (Islam et al., 2021). Rahman et al. (2021) showed monthly consumption pattern was also influential behind the spread while incident rate were considered in terms of population. But the incident rate with respect to the test has shown dissimilar findings. Only the poverty rate is found as an economic contributory variable during the first wave. It could be possible that the first wave experienced a long-term lockdown. Such conditions could affect the income level of the poor community. They needed to go out of home for living which increased their viral exposure. Thus areas with a higher poverty rate showed a bit higher incident rate. However, the influential spatial factors are not uniform across the waves. During the first and third waves, though spatial factors explain the scenario of spread, these are not so influential in the second wave.
- *Direction of spatial contributory factors in three waves:* Population over 65 years of age, number of ICU beds, poverty rate, and urban population density are identified as the first-wave contributors. Among these, the poverty rate, the urban population density, and the number of ICU beds have a positive correlation with the incident rate, indicating that a rise in a portion of these characteristics can increase the incident rate to some extent. The same holds true for the number of bus stations and the temperature for the second and third waves, respectively. In contrast, the incident rate is lower in places where the majority of residents are over 65 years old. During the second and third waves, incident rates are lower in regions with greater precipitation and lower temperature. Number of hospitals per thousand population contributed to the third wave. Whereas the incident rate increased in the places where the hospital density is higher during the third wave. This could possibly happen as hospital areas are potential locations to get interaction with the

infected people. The public movement was allowed during the third wave in a limited manner and no lockdown measure was implemented. Therefore people could go out without any restriction and hospitals were open to all which could affect the scenario of the third wave. You et al. (2020) showed the increment of hospital facilities reduced the incident rate by providing better healthcare access which is dissimilar from the findings. However, healthcare facilities could perform as a hub of viral transmission if any mismanagement appears during a pandemic. So the areas with higher hospital densities should get special consideration in pandemic management.

### **7.3. Recommendations**

- During the initial phase of a pandemic, it is important to identify the emerging danger zones; develop and implement preventive measures in the respective zones. In Bangladesh, strict lockdown, suspension of all activities, and restrictions on public mobility were marginally effective as control measures. In addition, the 3T approach (i.e., Test, Trace, and Treat) as mentioned in (Kim et al. (2020)) can be followed for high-risk zones. This method can aid in identifying cases and keeping them isolated for treatment. If such containment can be adopted at the onset, not only may the outbreak be controlled, but the pressure on hospital and ICU beds can also be reduced. According to the findings of spatial analyses, the areas with higher incident rate also had higher number of ICU beds due to the intervention of the government in upgrading the number of ICU beds. But it is not sustainable to supply the ICU beds in an unlimited manner. Therefore, the adoption of adequate measures like enforcement of non-pharmaceutical measures, enriching the initial treatment facilities, and raising health hygiene-related awareness among people could be an effective way to tackle the pandemic. Such countermeasures should be timely implemented in the emerging risk regions.
- In addition to a declaration, public awareness programs regarding pandemics and proper implementation of measures are also essential. Otherwise, the outbreak cannot be contained, as demonstrated by the first and second waves in Bangladesh. The study also reveals the step-by-step release of measures during the relaxation

period may be more effective than releasing all measures at once in flattening the trend of the outbreak.

- The pandemic management framework should be designed keeping the regional context in mind. Locational factors lead to a higher incidence of COVID-19 infection in the Western part of the country. Summer (April to August) is naturally the warmest season in this location, and this is when the first and second wave of cases exhibited the greatest increase. The analysis of meteorological features reveals, once more, that the incident rate is higher in regions with higher temperatures. Therefore, to formulate pandemic policies for Bangladesh, warmer regions particularly the Western portion should get special attention as the likelihood of spread is higher there. Delineating these areas as risk zone, restricting public movement within and outside of these areas during a pandemic, and enriching treatment facilities in these regions could be fruitful to mitigate the risk of a pandemic in those regions.
- Bangladesh has witnessed the biggest Covid peak from May to July, as evidenced by the first and second waves. This fact could be related to meteorological attributes like temperature. It is already found that warmer areas of the country experienced a higher incident rate. In a year, Bangladesh experiences its higher temperature from May to August as the effect of summer. This is why the overall incident rate could be higher at this time. Consequently, precautionary measures (i.e. raising pandemic awareness in this area, limiting public movement with warmer regions, and equipping healthcare facilities for this time period) should be devised considering this time frame.
- The international spread of the pandemic and the introduction of new strains must also be taken into account while formulating strategies to combat the outbreak. As Bangladesh is almost entirely surrounded by India, India's outbreak issue may also affect the country as evident in the second wave. After the introduction and rapid spread of the Delta variant in India, higher incidences have also happened in the neighboring regions of Bangladesh though the border was enclosed in a porous manner. Entry for medical treatment and emergency transportation was allowed. So when the virus appears to be more widespread in India, all border crossings must

be closed strictly with no entry and local connections to bordering districts must be curtailed.

- In districts, where urban population density is the highest, the pandemic spread is the maximum. Therefore, urban population density should be regulated to combat future epidemics. Dhaka should be considered especially in pandemic management due to its high population density. Bangladesh government already has developed some strategies to control unplanned urbanization in their 8<sup>th</sup> Five Year Plan and Perspective Plan 2021. The strategies include reducing the pressure on Dhaka through promoting balanced urbanization in secondary cities, changing the distribution of resource allocation, regulating land use within and outside urban areas, strengthening institutional capacities, and so on. Such initiatives could also be effective to minimize the risk of future outbreaks. When people get better opportunities and lifestyles in local areas, they might be less attracted to cities. Thus, the population of urban areas could be cut down which could ultimately minimize the chance of human interaction as well as viral transmission.
- Again, urban agglomeration is unavoidable as far as productivity and economic growth are concern. Thus, population concentration is increasing in urban areas. Due to agglomeration, both positive and negative externalities appear. Increment of productivity, improvement of quality of life, and employment generation are some of the positive externalities. These externalities are fruitful to boost the city's economy; so agglomeration can be promoted in this context (Mohanty et al., 2014). However, when cities become overburdened with population growth, negative externalities take place in different sectors (i.e. traffic congestion, emission, housing scarcity, health crisis) as literature states (Loibl et al., 2018; Vermeulen, 2017). As a consequence of agglomeration, the urban areas may go through the subversive effects of a pandemic. Therefore, urban policies should be designed in such a way that the negative externalities of agglomeration can be minimized. Urban agglomeration should be promoted to that extent when it can not be the reason of diseconomies. In order to tackle the pandemic scenario in urban areas, raising public awareness, maintaining proper hygiene practices, restricting public movement during rapid transmission, and so on could be adapted as measures.

- The cultural and political condition of the country can also contribute to manage the pandemic situation. To what extent the imposed pandemic interventions would be maintained sometimes depend on cultural context. Population of some areas may follow the pandemic rules properly; some may feel reluctant to maintain the interventions due to local perception and willingness to maintain the rules. How strictly local government deals with the emerging situation of pandemic also could influence the pandemic scenario. Therefore local cultural and political context also should be considered besides the demographic condition. Additionally, releasing population pressure from healthcare facilities and expansion of healthcare services might decrease the incidence of infection. Providing adequate treatment facilities in Bangladesh's impoverished districts can alleviate the pandemic's effects.
- According to the findings of spatial analyses, the poverty rate also had some impact on the dissemination of COVID-19 during the first wave. Greater incident rates were observed in regions with a higher poverty rate. If the population could be categorized according to their economic status, it could be possible to determine which segment of the poor was the most affected. But it could not be performed due to data paucity. However, this research indicates that Bangladesh's pandemic strategies should take into account the economic status of the districts, with a special emphasis on vulnerable impoverished communities.

## **Chapter 8 : Conclusion**

The world is currently experiencing a number of epidemic events, which are being exacerbated by a variety of important circumstances. With varying degrees of severity, these diseases can become pandemics, affecting entire continents in successive waves. The pandemic wave characteristics are also unstable in the emerging setting, based on what pandemic impacts fluctuate in the short and long run. Various local features like as demographic, social, economic, and environmental elements may shape the wave situation to some extent, but their performance cannot be anticipated at all times. To deal with the severity of pandemic waves, numerous pharmaceutical and non-pharmaceutical procedures are put in place. The same situation could play out in the ongoing COVID-19 pandemic. Bangladesh is one of the highly COVID-19 infected countries where three waves have been detected yet. The distribution of testing facilities is not also uniform over the districts of Bangladesh which should be taken into account to explore the country's pandemic scenario. To the best of the researcher's knowledge, no study has been carried out yet that compares both the spatial and temporal context of COVID-19 waves considering incident rate relative to the number of tests. The purpose of this study is to investigate the effect of geographical and aspatial factors on three successive COVID-19 waves in Bangladesh.

To conduct this research, the weekly incident rate of COVID-19 with respect to the number of test has been considered to know the spatio-temporal dynamics. Firstly temporal patterns of the pandemic waves have been explored both at national and local levels using nonparametric tests (i.e. Mann-Kendall test, Pettit test, and Sen's slope estimation). Taken policy initiatives also have been linked with the detected pattern so that the effects of the interventions could be understood. After identifying the temporal pattern, the spatial pattern of the incident rate has been investigated to know the risk regions of the country by applying spatial autocorrelation techniques. The temporal growth of the identified pattern also has been analyzed using space-time scan statistics. Finally, the geographical factors which could have influenced the spread of the pandemic have been determined using spatial regression modeling. Various



demographic, meteorological, infrastructural, economic, and healthcare facilities-related attributes have been taken into account as geographical factors.

The results have shown that the duration and temporal pattern of waves varied across the country. When the incident rate has been taken into account, most districts in Bangladesh exhibited a decreasing trend with an abrupt drop due to the application of non-pharmaceutical measures in the first wave. Although no major trend has been noticed during the second wave, the Western area of the country experienced an increase probably due to virus strain mutations. Bangladesh got the highest number of infections from May to July both in the first and second waves, and the majority of pandemic clusters emerged during this time. Any external factors that may have an impact should be investigated in future studies. However, long-term lockdown, activity closures, restrictions on public movement, reduced transit with other countries, closure of educational institutions, and other aspatial factors all had a consequence on the temporal patterns of the three waves.

During the first and third waves, some locational clusters of higher and lower incident rate have been detected in the country. The clusters were formed focusing on an adjacent area where the incident rate was higher or lower initially. Therefore if the highly infected areas could be identified and cordoned properly at an earlier period, the nationwide spread could be prevented. As a location, Dhaka was always the leader of waves and had the greatest incident rate. When the spatial aspects have been investigated, higher urban population density has been discovered to be a contributor to increase the infection both in the first and third waves. It is possible that because Dhaka has the highest urban population in the country, it was more infected with COVID-19. Moreover, the areas with higher hospital density experienced higher occurrences during the third wave. From this, it can be argued that when places were highly infected with cases, hospitals struggled to provide services, resulting in the spread of the disease. The dilemma is exacerbated by the relaxation of containment strategies and the introduction of new strains as revealed in the second wave.

In the initial phase of the outbreak, the heavily infected region experienced an increase in the number of diagnostic tests and intensive care unit (ICU) beds. Number of ICU beds also had a statistically positive relationship with incident rate during the first wave. Therefore increasing the number of ICU beds cannot be a remedy to control the

outbreak situation sustainably. Rather emphasis should be given to cut down the spread by applying different control strategies at the onset of a pandemic, equipping primary treatment facilities, allocating resources in public healthcare centers, and so on. As meteorological features, precipitation and temperature contributed in opposite directions during the second and third waves. Incident rates were lower in regions with abundant precipitation, while it was greater in regions where temperatures are very high. For such meteorological factors, the Eastern portion of the country could probably face lower infection over the waves. Besides Central and Western portions could experience a higher incident rate. Therefore local climatic scenarios should take into account while formulating pandemic policies.

During the initial surge, districts with a higher percentage of poverty demonstrated an increase in infection. But due to data paucity, it could not be possible to explore in this research which sections of the poor were more vulnerable. However, the study results indicate that the economic condition of the districts and consideration of impoverished communities should be emphasized in designing pandemic management activities. Above all, when formulating pandemic policies, urban population concentration, meteorological characteristics, the condition of healthcare facilities, and the economic situation of areas must be addressed as spatial considerations according to the experience of three successive COVID-19 waves in Bangladesh. The findings of this study would aid policymakers in the development of a pandemic management framework by identifying effective spatial and aspatial measures for outbreak containment.

## References

- Agrahari, A., Singh, P., Veer, A., Singh, A., Vidyarthi, A., & Khan, B. (2021). Prognosticating the effect on Unemployment rate in the post-pandemic India via Time-Series Forecasting and Least Squares Approximation. *Pattern Recognition Letters*, 152, 172-179.
- Ahmad, I., Tang, D., Wang, T., Wang, M., & Wagan, B. (2015). Precipitation trends over time using Mann-Kendall and spearman's rho tests in swat river basin, Pakistan. *Advances in Meteorology*, 2015.
- Ahmed, S. S. U., Ersbøll, A. K., Biswas, P. K., Christensen, J. P., & Toft, N. (2011). Spatio-Temporal Magnitude and Direction of Highly Pathogenic Avian Influenza (H5N1) Outbreaks in Bangladesh. *PLOS ONE*, 6(9), e24324. doi: 10.1371/journal.pone.0024324
- Allen, H., Vusirikala, A., Flannagan, J., Twohig, K. A., Zaidi, A., Chudasama, D., . . . Kall, M. (2022). Household transmission of COVID-19 cases associated with SARS-CoV-2 delta variant (B.1.617.2): national case-control study. *The Lancet Regional Health - Europe*, 12, 100252. doi: <https://doi.org/10.1016/j.lanepe.2021.100252>
- Andrade, L. A., Gomes, D. S., Góes, M. A. d. O., Souza, M. S. F. d., Teixeira, D. C. P., Ribeiro, C. J. N., . . . Santos, A. D. d. (2020). Surveillance of the first cases of COVID-19 in Sergipe using a prospective spatiotemporal analysis: the spatial dispersion and its public health implications. *Revista da Sociedade Brasileira de Medicina Tropical*, 53.
- Anwar, S., Nasrullah, M., & Hosen, M. J. (2020). COVID-19 and Bangladesh: Challenges and How to Address Them. *Frontiers in Public Health*, 8. doi: 10.3389/fpubh.2020.00154
- Auchincloss, A. H., Gebreab, S. Y., Mair, C., & Diez Roux, A. V. (2012). A review of spatial methods in epidemiology, 2000–2010. *Annual review of public health*, 33, 107-122.
- Baharom, M., Ahmad, N., Hod, R., Arsad, F. S., & Tangang, F. (2021). The Impact of Meteorological Factors on Communicable Disease Incidence and Its Projection: A Systematic Review. *International Journal of Environmental Research and Public Health*, 18(21), 11117.
- Bandaranayake, D., Jacobs, M., Baker, M., Hunt, D., Wood, T., Bissielo, A., . . . Huang, Q. S. (2011). The second wave of 2009 pandemic influenza A(H1N1) in New Zealand, January–October 2010. *Eurosurveillance*, 16(6), 19788. doi: [doi:https://doi.org/10.2807/ese.16.06.19788-en](https://doi.org/10.2807/ese.16.06.19788-en)
- Bank, W. (2020). *Global economic prospects, June 2020*: The World Bank.
- Barak, N., Sommer, U., & Mualam, N. (2021). Urban attributes and the spread of COVID-19: The effects of density, compliance and socio-political factors in Israel. *Science of The Total Environment*, 793, 148626. doi: <https://doi.org/10.1016/j.scitotenv.2021.148626>
- Basray, R., Malik, A., Waqar, W., Chaudhry, A., Wasif Malik, M., Ali Khan, M., . . . Ikram, A. (2021). Impact of environmental factors on COVID-19 cases and mortalities in major cities of Pakistan. *Journal of Biosafety and Biosecurity*, 3(1), 10-16. doi: <https://doi.org/10.1016/j.jobb.2021.02.001>

- Baveja, A., Kapoor, A., & Melamed, B. (2020). Stopping Covid-19: A pandemic-management service value chain approach. *Annals of Operations Research*, 289(2), 173-184. doi: 10.1007/s10479-020-03635-3
- BBS. (2015). Census of Slum Areas and Floating Population. Dhaka, Bangladesh.
- Bhaduri, E., Manoj, B., Wadud, Z., Goswami, A. K., & Choudhury, C. F. (2020). Modelling the effects of COVID-19 on travel mode choice behaviour in India. *Transportation Research Interdisciplinary Perspectives*, 8, 100273.
- Boehmer, T. K., DeVies, J., Caruso, E., van Santen, K. L., Tang, S., Black, C. L., . . . Gundlapalli, A. V. (2020). Changing Age Distribution of the COVID-19 Pandemic - United States, May-August 2020. *MMWR. Morbidity and mortality weekly report*, 69(39), 1404-1409. doi: 10.15585/mmwr.mm6939e1
- Bucsky, P. (2020). Modal share changes due to COVID-19: The case of Budapest. *Transportation Research Interdisciplinary Perspectives*, 8, 100141. doi: <https://doi.org/10.1016/j.trip.2020.100141>
- Carrel, M., Escamilla, V., Messina, J., Giebultowicz, S., Winston, J., Yunus, M., . . . Emch, M. (2011). Diarrheal disease risk in rural Bangladesh decreases as tubewell density increases: a zero-inflated and geographically weighted analysis. *International Journal of Health Geographics*, 10(1), 41. doi: 10.1186/1476-072X-10-41
- Chong, K. C., Zee, B. C. Y., & Wang, M. H. (2017). A statistical method utilizing information of imported cases to estimate the transmissibility for an influenza pandemic. *BMC Medical Research Methodology*, 17(1), 31. doi: 10.1186/s12874-017-0300-1
- Chowdhury, F. R., Nur, Z., Hassan, N., von Seidlein, L., & Dunachie, S. (2017). Pandemics, pathogenicity and changing molecular epidemiology of cholera in the era of global warming. *Annals of Clinical Microbiology and Antimicrobials*, 16(1), 1-6.
- Chowell, G., Erkoreka, A., Viboud, C., & Echeverri-Dávila, B. (2014). Spatial-temporal excess mortality patterns of the 1918–1919 influenza pandemic in Spain. *BMC Infectious Diseases*, 14(1), 371. doi: 10.1186/1471-2334-14-371
- Crichton, E. J., Elliott, S. J., Moineddin, R., Kanaroglou, P., & Upshur, R. (2007). A spatial analysis of the determinants of pneumonia and influenza hospitalizations in Ontario (1992–2001). *Social science & medicine*, 64(8), 1636-1650.
- Curseu, D., Popa, M., Sirbu, D., & Stoian, I. (2010). Potential Impact of Climate Change on Pandemic Influenza Risk. In I. Dincer, A. Hepbasli, A. Midilli & T. H. Karakoc (Eds.), *Global Warming: Engineering Solutions* (pp. 643-657). Boston, MA: Springer US.
- de Oliveira-Júnior, J. F., Gois, G., da Silva, E. B., Teodoro, P. E., Johann, J. A., & Junior, C. A. S. (2019). Non-Parametric tests and multivariate analysis applied to reported dengue cases in Brazil. *Environmental monitoring and assessment*, 191(7), 1-19.
- DGHS. (2022). Covid-19 Dashboard. from <https://dghs-dashboard.com/pages/covid19.php>
- Dinh, L., Chowell, G., & Rothenberg, R. (2018). Growth scaling for the early dynamics of HIV/AIDS epidemics in Brazil and the influence of socio-demographic factors. *Journal of theoretical biology*, 442, 79-86. doi: <https://doi.org/10.1016/j.jtbi.2017.12.030>
- Drefahl, S., Wallace, M., Mussino, E., Aradhya, S., Kolk, M., Brandén, M., . . . Andersson, G. (2020). A population-based cohort study of socio-demographic

- risk factors for COVID-19 deaths in Sweden. *Nature Communications*, 11(1), 5097. doi: 10.1038/s41467-020-18926-3
- Duerr, H. P., Brockmann, S. O., Piechotowski, I., Schwehm, M., & Eichner, M. (2007). Influenza pandemic intervention planning using InfluSim: pharmaceutical and non-pharmaceutical interventions. *BMC Infectious Diseases*, 7(1), 76. doi: 10.1186/1471-2334-7-76
- Dureab, F. A., Shibib, K., Al-Yousufi, R., & Jahn, A. (2018). Yemen: cholera outbreak and the ongoing armed conflict. *The Journal of Infection in Developing Countries*, 12(05), 397-403.
- Engelbrecht, F. A., & Scholes, R. J. (2021). Test for Covid-19 seasonality and the risk of second waves. *One Health*, 12, 100202. doi: <https://doi.org/10.1016/j.onehlt.2020.100202>
- Fotheringham, A. S., & Brunson, C. (1999). Local Forms of Spatial Analysis. *Geographical Analysis*, 31(4), 340-358. doi: <https://doi.org/10.1111/j.1538-4632.1999.tb00989.x>
- Fu, S., Wang, B., Zhou, J., Xu, X., Liu, J., Ma, Y., . . . Zhang, K. (2021). Meteorological factors, governmental responses and COVID-19: Evidence from four European countries. *Environmental Research*, 194, 110596. doi: <https://doi.org/10.1016/j.envres.2020.110596>
- Ganyani, T., Kremer, C., Chen, D., Torneri, A., Faes, C., Wallinga, J., & Hens, N. (2020). Estimating the generation interval for coronavirus disease (COVID-19) based on symptom onset data, March 2020. *Eurosurveillance*, 25(17), 2000257.
- Gayawan, E., Awe, O. O., Oseni, B. M., Uzochukwu, I. C., Adekunle, A., Samuel, G., . . . Adegboye, O. A. (2020). The spatio-temporal epidemic dynamics of COVID-19 outbreak in Africa. *Epidemiology and Infection*, 148, e212-e212. doi: 10.1017/S0950268820001983
- Ge, X.-Y., Li, J.-L., Yang, X.-L., Chmura, A. A., Zhu, G., Epstein, J. H., . . . Peng, C. (2013). Isolation and characterization of a bat SARS-like coronavirus that uses the ACE2 receptor. *Nature*, 503(7477), 535-538.
- Giuliani, D., Dickson, M. M., Espa, G., & Santi, F. (2020). Modelling and predicting the spatio-temporal spread of COVID-19 in Italy. *BMC Infectious Diseases*, 20(1), 700. doi: 10.1186/s12879-020-05415-7
- Goswami, K., Bharali, S., & Hazarika, J. (2020). Projections for COVID-19 pandemic in India and effect of temperature and humidity. *Diabetes & Metabolic Syndrome: Clinical Research & Reviews*, 14(5), 801-805. doi: <https://doi.org/10.1016/j.dsx.2020.05.045>
- Goto, K., Kumarendran, B., Mettananda, S., Gunasekara, D., Fujii, Y., & Kaneko, S. (2013). Analysis of Effects of Meteorological Factors on Dengue Incidence in Sri Lanka Using Time Series Data. *PLOS ONE*, 8(5), e63717. doi: 10.1371/journal.pone.0063717
- Graham, A., Atkinson, P. M., & Danson, F. (2004). Spatial analysis for epidemiology (Vol. 91, pp. 219-225): Elsevier.
- Graichen, H. (2021). What is the difference between the first and the second/third wave of Covid-19?—German perspective: Elsevier.
- Grennan, D. (2019). What is a Pandemic? *Jama*, 321(9), 910-910.
- Gross, B., Zheng, Z., Liu, S., Chen, X., Sela, A., Li, J., . . . Havlin, S. (2020). Spatio-temporal propagation of COVID-19 pandemics. *EPL (Europhysics Letters)*, 131(5), 58003.

- Guilmoto, C. Z. (2020). COVID-19 death rates by age and sex and the resulting mortality vulnerability of countries and regions in the world. *medRxiv*, 2020.2005.2017.20097410. doi: 10.1101/2020.05.17.20097410
- Hale, T., Angrist, N., Goldszmidt, R., Kira, B., Petherick, A., Phillips, T., . . . Tatlow, H. (2021). A global panel database of pandemic policies (Oxford COVID-19 Government Response Tracker). *Nature Human Behaviour*, 5(4), 529-538. doi: 10.1038/s41562-021-01079-8
- Hamidi, S., Sabouri, S., & Ewing, R. (2020). Does Density Aggravate the COVID-19 Pandemic? *Journal of the American Planning Association*, 86(4), 495-509. doi: 10.1080/01944363.2020.1777891
- Hassan, M. S., Bhuiyan, M. A. H., Tareq, F., Bodrud-Doza, M., Tanu, S. M., & Rabbani, K. A. (2021). Relationship between COVID-19 infection rates and air pollution, geo-meteorological, and social parameters. *Environmental monitoring and assessment*, 193(1), 29. doi: 10.1007/s10661-020-08810-4
- Hay, N., Onwuzurike, O., Roy, S., McNamara, P., McNamara, M., & McDonald, W. (2020). Impact of Traffic on Air Pollution in a Mid-Sized Urban City During Covid-19 Lockdowns. Available at SSRN 4068344.
- Henderson, D. A., Courtney, B., Inglesby, T. V., Toner, E., & Nuzzo, J. B. (2009). Public health and medical responses to the 1957-58 influenza pandemic. *Biosecurity and bioterrorism: biodefense strategy, practice, and science*, 7(3), 265-273.
- Hong, H. G., & Li, Y. (2020). Estimation of time-varying reproduction numbers underlying epidemiological processes: A new statistical tool for the COVID-19 pandemic. *PLOS ONE*, 15(7), e0236464. doi: 10.1371/journal.pone.0236464
- Huang, R., Liu, M., & Ding, Y. (2020). Spatial-temporal distribution of COVID-19 in China and its prediction: A data-driven modeling analysis. *The Journal of Infection in Developing Countries*, 14(03), 246-253.
- Hutchins, H. J., Wolff, B., Leeb, R., Ko, J. Y., Odom, E., Willey, J., . . . Bitsko, R. H. (2020). COVID-19 Mitigation Behaviors by Age Group - United States, April-June 2020. *MMWR. Morbidity and mortality weekly report*, 69(43), 1584-1590. doi: 10.15585/mmwr.mm6943e4
- Ibuka, Y., Chapman, G. B., Meyers, L. A., Li, M., & Galvani, A. P. (2010). The dynamics of risk perceptions and precautionary behavior in response to 2009 (H1N1) pandemic influenza. *BMC Infectious Diseases*, 10(1), 296. doi: 10.1186/1471-2334-10-296
- IEDCR. (2020). Disease Updates. Retrieved 16 April, 2021, from <https://iedcr.gov.bd/publication/articles>
- Islam, A. R. M. T., Hasanuzzaman, M., Shammi, M., Salam, R., Bodrud-Doza, M., Rahman, M. M., . . . Huq, S. (2021). Are meteorological factors enhancing COVID-19 transmission in Bangladesh? Novel findings from a compound Poisson generalized linear modeling approach. *Environmental Science and Pollution Research*, 28(9), 11245-11258. doi: 10.1007/s11356-020-11273-2
- Iyengar, K., Mabrouk, A., Jain, V. K., Venkatesan, A., & Vaishya, R. (2020). Learning opportunities from COVID-19 and future effects on health care system. *Diabetes & Metabolic Syndrome: Clinical Research & Reviews*, 14(5), 943-946. doi: <https://doi.org/10.1016/j.dsx.2020.06.036>
- Kato, H. (2021). Development of a Spatio-temporal Analysis Method to Support the Prevention of COVID-19 Infection: Space-Time Kernel Density Estimation Using GPS Location History Data *Urban Informatics and Future Cities* (pp. 51-67): Springer.

- Kim, S., & Castro, M. C. (2020). Spatiotemporal pattern of COVID-19 and government response in South Korea (as of May 31, 2020). *International Journal of Infectious Diseases*, 98, 328-333.
- Lafferty, K. D. (2009). The ecology of climate change and infectious diseases. *Ecology*, 90(4), 888-900.
- Lee, W., Kim, H., Choi, H. M., Heo, S., Fong, K. C., Yang, J., . . . Bell, M. L. (2021). Urban environments and COVID-19 in three Eastern states of the United States. *Science of The Total Environment*, 779, 146334. doi: <https://doi.org/10.1016/j.scitotenv.2021.146334>
- Lei, S., Jiang, F., Su, W., Chen, C., Chen, J., Mei, W., . . . Liu, D. (2020). Clinical characteristics and outcomes of patients undergoing surgeries during the incubation period of COVID-19 infection. *EclinicalMedicine*, 21, 100331.
- Lenzi, L., Wiens, A., Cavichiolo Grochocki, M. H., & Pontarolo, R. (2011). Study of the relationship between socio-demographic characteristics and new influenza A (H1N1). *The Brazilian Journal of Infectious Diseases*, 15(5), 457-461. doi: [https://doi.org/10.1016/S1413-8670\(11\)70227-6](https://doi.org/10.1016/S1413-8670(11)70227-6)
- Li, H., Li, H., Ding, Z., Hu, Z., Chen, F., Wang, K., . . . Shen, H. (2020). Spatial statistical analysis of coronavirus disease 2019 (Covid-19) in China. *Geospatial health*, 15(1).
- Lian, M., Warner, R. D., Alexander, J. L., & Dixon, K. R. (2007). Using geographic information systems and spatial and space-time scan statistics for a population-based risk analysis of the 2002 equine West Nile epidemic in six contiguous regions of Texas. *International Journal of Health Geographics*, 6(1), 42. doi: [10.1186/1476-072X-6-42](https://doi.org/10.1186/1476-072X-6-42)
- Liao, R.-J., Ji-Ke, C.-N., Zhang, T., Liao, Q., Li, L., Zhu, T.-Y., & Bian, S.-Y. (2020). Coronavirus disease 2019 epidemic in impoverished area: Liangshan Yi autonomous prefecture as an example. *Infectious Diseases of Poverty*, 9(1), 1-9.
- Loibl, W., Etminan, G., Gebetsroither-Geringer, E., Neumann, H.-M., & Sanchez-Guzman, S. (2018). Characteristics of urban agglomerations in different continents: History, patterns, dynamics, drivers and trends. *Urban agglomeration*, 29-63.
- Lopez, D., Gunasekaran, M., Murugan, B. S., Kaur, H., & Abbas, K. M. (2014). *Spatial big data analytics of influenza epidemic in Vellore, India*. Paper presented at the 2014 IEEE international conference on big data (Big Data).
- Mahmood, S., Hussain, T., Mahmood, F., Ahmad, M., Majeed, A., Beg, B. M., & Areej, S. (2020). Attitude, Perception, and Knowledge of COVID-19 Among General Public in Pakistan. *Frontiers in Public Health*, 8(861). doi: [10.3389/fpubh.2020.602434](https://doi.org/10.3389/fpubh.2020.602434)
- Maliszewski, P. J., & Wei, R. (2011). Ecological factors associated with pandemic influenza A (H1N1) hospitalization rates in California, USA: a geospatial analysis. *Geospatial health*, 6(1), 95-105.
- Mamelund, S.-E. (2018). 1918 pandemic morbidity: The first wave hits the poor, the second wave hits the rich. *Influenza and Other Respiratory Viruses*, 12(3), 307-313. doi: <https://doi.org/10.1111/irv.12541>
- Mandal, S., Mandal, M. D., & Pal, N. K. (2011). Cholera: a great global concern. *Asian Pacific Journal of Tropical Medicine*, 4(7), 573-580. doi: [https://doi.org/10.1016/S1995-7645\(11\)60149-1](https://doi.org/10.1016/S1995-7645(11)60149-1)
- Mann, H. B. (1945). Nonparametric tests against trend. *Econometrica: Journal of the econometric society*, 245-259.

- Marco Arieli, H.-V., Maytee, C.-A., & Carlos, C.-C.
- Mari, G. M., Crippa, J., Casciaro, F., & Maggioni, D. (2020). A 10-step guide to convert a surgical unit into a COVID-19 unit during the COVID-19 pandemic. *International journal of surgery (London, England)*, 78, 113-114. doi: 10.1016/j.ijssu.2020.04.052
- Martini, M., Gazzaniga, V., Bragazzi, N. L., & Barberis, I. (2019). The Spanish Influenza Pandemic: a lesson from history 100 years after 1918. *Journal of preventive medicine and hygiene*, 60(1), E64-E67. doi: 10.15167/2421-4248/jpmh2019.60.1.1205
- Mashrur, F. R., Roy, A. D., Chhoan, A. P., Sarker, S., Saha, A., Hasan, S. M. N., & Saha, S. (2021). Impact of demographic, environmental, socioeconomic, and government intervention on the spreading of COVID-19. *Clinical Epidemiology and Global Health*, 12. doi: 10.1016/j.cegh.2021.100811
- Masrur, A., Yu, M., Luo, W., & Dewan, A. (2020). Space-Time Patterns, Change, and Propagation of COVID-19 Risk Relative to the Intervention Scenarios in Bangladesh. *International Journal of Environmental Research and Public Health*, 17(16), 5911.
- Meliker, J. R., & Sloan, C. D. (2011). Spatio-temporal epidemiology: Principles and opportunities. *Spatial and spatio-temporal epidemiology*, 2(1), 1-9.
- Middleton, J., Lopes, H., Michelson, K., & Reid, J. (2020). Planning for a second wave pandemic of COVID-19 and planning for winter. *International Journal of Public Health*, 65(9), 1525-1527. doi: 10.1007/s00038-020-01455-7
- Miller, H. J. (2004). Tobler's first law and spatial analysis. *Annals of the association of American geographers*, 94(2), 284-289.
- MoF. (2020). Socio-economic indicators of Bangladesh. Retrieved July, 2021, from [https://mof.portal.gov.bd/sites/default/files/files/mof.portal.gov.bd/page/f2d8fab\\_b29c1\\_423a\\_9d37\\_cdb500260002/6.%20Socio-Economic%20Indicators](https://mof.portal.gov.bd/sites/default/files/files/mof.portal.gov.bd/page/f2d8fab_b29c1_423a_9d37_cdb500260002/6.%20Socio-Economic%20Indicators).
- Mohanty, P. K., & Mishra, A. K. (2014). Cities and Agglomeration Externalities: Lessons for Urban Public Policy in Asian Countries. *Environment and Urbanization ASIA*, 5(2), 235-251. doi: 10.1177/0975425315577171
- Moon, A. A., Daria, S., Asaduzzaman, M., & Islam, M. R. (2021). Bangladesh reported delta variant of coronavirus among its citizen: Actionable items to tackle the potential massive third wave. *Infect Prev Pract*, 3(3), 100159. doi: 10.1016/j.infpip.2021.100159
- Mottaleb, K. A., Mainuddin, M., & Sonobe, T. (2020). COVID-19 induced economic loss and ensuring food security for vulnerable groups: Policy implications from Bangladesh. *PLOS ONE*, 15(10), e0240709. doi: 10.1371/journal.pone.0240709
- Murray, C. J., Lopez, A. D., Chin, B., Feehan, D., & Hill, K. H. (2006). Estimation of potential global pandemic influenza mortality on the basis of vital registry data from the 1918–20 pandemic: a quantitative analysis. *The Lancet*, 368(9554), 2211-2218.
- Mwaba, J., Debes, A. K., Shea, P., Mukonka, V., Chewe, O., Chisenga, C., . . . Ali, M. (2020). Identification of cholera hotspots in Zambia: A spatiotemporal analysis of cholera data from 2008 to 2017. *PLOS Neglected Tropical Diseases*, 14(4), e0008227. doi: 10.1371/journal.pntd.0008227
- Nieto-Chaupis, H. (2021). *Identifying Second Wave and New Variants of Covid-19 from Shannon Entropy in Global Pandemic Data*. Paper presented at the 2021 Fifth World Conference on Smart Trends in Systems Security and Sustainability (WorldS4).



- Oliveira Júnior, J. F. d., Gois, G. d., Silva, E. B. d., Silva Junior, C. A., & Teodoro, P. E. (2018). Non-parametric tests applied to reported cases of dengue in the southeast region of Brazil. *Biosci. j.(Online)*, 1010-1016.
- Ozili, P. K. (2020). COVID-19 pandemic and economic crisis: the Nigerian experience and structural causes. *Journal of Economic and Administrative Sciences, ahead-of-print(ahead-of-print)*. doi: 10.1108/JEAS-05-2020-0074
- Pal, S. C., Chowdhuri, I., Saha, A., Ghosh, M., Roy, P., Das, B., . . . Shit, M. (2022). COVID-19 strict lockdown impact on urban air quality and atmospheric temperature in four megacities of India. *Geoscience Frontiers*, 101368. doi: <https://doi.org/10.1016/j.gsf.2022.101368>
- Parimala, M., & Lopez, D. (2016). Spatio-temporal modelling of frequent human mobility pattern to analyse the dynamics of epidemic disease. *International Journal of Intelligent Engineering and Systems*, 9(4), 167-178.
- Patrinley, J. R., Berkowitz, S. T., Zakria, D., Totten, D. J., Kurtulus, M., & Drolet, B. C. (2020). Lessons from Operations Management to Combat the COVID-19 Pandemic. *Journal of Medical Systems*, 44(7), 129. doi: 10.1007/s10916-020-01595-6
- Pokhrel, S., & Chhetri, R. (2021). A Literature Review on Impact of COVID-19 Pandemic on Teaching and Learning. *Higher Education for the Future*, 8(1), 133-141. doi: 10.1177/2347631120983481
- Prentice, M. B., & Rahalison, L. (2007). Plague. *The Lancet*, 369(9568), 1196-1207.
- Qiu, W., Rutherford, S., Mao, A., & Chu, C. (2017). The pandemic and its impacts. *Health, culture and society*, 9, 1-11.
- Rababah, A., Al-Haddad, L., Sial, M. S., Chunmei, Z., & Cherian, J. (2020). Analyzing the effects of COVID-19 pandemic on the financial performance of Chinese listed companies. *Journal of Public Affairs*, 20(4), e2440.
- Rahman, M. H., Zafri, N. M., Ashik, F. R., Waliullah, M., & Khan, A. (2021). Identification of risk factors contributing to COVID-19 incidence rates in Bangladesh: A GIS-based spatial modeling approach. *Heliyon*, 7(2), e06260. doi: <https://doi.org/10.1016/j.heliyon.2021.e06260>
- Rahman, M. M., Khan, S. J., Sakib, M. S., Halim, M. A., Rahman, F., Rahman, M. M., . . . Yeasmin, M. T. M. (2021). COVID-19 responses among general people of Bangladesh: Status and individual view toward COVID-19 during lockdown period. *Cogent Psychology*, 8(1), 1860186. doi: 10.1080/23311908.2020.1860186
- Raza, A., Khan, M. T. I., Ali, Q., Hussain, T., & Narjis, S. (2021). Association between meteorological indicators and COVID-19 pandemic in Pakistan. *Environmental Science and Pollution Research*, 28(30), 40378-40393. doi: 10.1007/s11356-020-11203-2
- Sannigrahi, S., Pilla, F., Basu, B., Basu, A. S., & Molter, A. (2020). Examining the association between socio-demographic composition and COVID-19 fatalities in the European region using spatial regression approach. *Sustainable Cities and Society*, 62, 102418. doi: <https://doi.org/10.1016/j.scs.2020.102418>
- Sarkodie, S. A., & Owusu, P. A. (2020). Impact of meteorological factors on COVID-19 pandemic: Evidence from top 20 countries with confirmed cases. *Environmental Research*, 191, 110101. doi: <https://doi.org/10.1016/j.envres.2020.110101>
- Scarpone, C., Brinkmann, S. T., Große, T., Sonnenwald, D., Fuchs, M., & Walker, B. B. (2020). A multimethod approach for county-scale geospatial analysis of emerging infectious diseases: a cross-sectional case study of COVID-19

- incidence in Germany. *International Journal of Health Geographics*, 19(1), 1-17.
- Shaik, M. E., Hossain, Q. S., & Rony, G. M. F. F. (2021). Impact of COVID-19 on Public Transportation and Road Safety in Bangladesh. *SN Computer Science*, 2(6), 453. doi: 10.1007/s42979-021-00849-5
- Shammi, M., Bodrud-Doza, M., Islam, A. R. M. T., & Rahman, M. M. (2021). Strategic assessment of COVID-19 pandemic in Bangladesh: comparative lockdown scenario analysis, public perception, and management for sustainability. *Environment, development and sustainability*, 23(4), 6148-6191. doi: 10.1007/s10668-020-00867-y
- Shamshiripour, A., Rahimi, E., Shabanpour, R., & Mohammadian, A. K. (2020). How is COVID-19 reshaping activity-travel behavior? Evidence from a comprehensive survey in Chicago. *Transportation Research Interdisciplinary Perspectives*, 7, 100216.
- Sharifi, A., & Khavarian-Garmsir, A. R. (2020). The COVID-19 pandemic: Impacts on cities and major lessons for urban planning, design, and management. *Science of The Total Environment*, 749, 142391. doi: <https://doi.org/10.1016/j.scitotenv.2020.142391>
- Shi, W., Tong, C., Zhang, A., Wang, B., Shi, Z., Yao, Y., & Jia, P. (2021). An extended Weight Kernel Density Estimation model forecasts COVID-19 onset risk and identifies spatiotemporal variations of lockdown effects in China. *Communications biology*, 4(1), 1-10.
- Siam, Z. S., Arifuzzaman, M., Ahmed, M. S., Khan, F. A., Rashid, M. H., & Islam, M. S. (2021). Dynamics of COVID-19 transmission in Dhaka and Chittagong: Two business hubs of Bangladesh. *Clinical Epidemiology and Global Health*, 10, 100684. doi: <https://doi.org/10.1016/j.cegh.2020.100684>
- Siljander, M., Uusitalo, R., Pellikka, P., Isosomppi, S., & Vapalahti, O. (2022). Spatiotemporal clustering patterns and sociodemographic determinants of COVID-19 (SARS-CoV-2) infections in Helsinki, Finland. *Spatial and spatio-temporal epidemiology*, 41, 100493. doi: <https://doi.org/10.1016/j.sste.2022.100493>
- Simonsen, L., Clarke, M. J., Schonberger, L. B., Arden, N. H., Cox, N. J., & Fukuda, K. (1998). Pandemic versus epidemic influenza mortality: a pattern of changing age distribution. *Journal of infectious diseases*, 178(1), 53-60.
- Tang, W., Liao, H., Marley, G., Wang, Z., Cheng, W., Wu, D., & Yu, R. (2020). The changing patterns of coronavirus disease 2019 (COVID-19) in China: A tempogeographic analysis of the severe acute respiratory syndrome coronavirus 2 epidemic. *Clinical infectious diseases*, 71(15), 818-824.
- Vermeulen, W. (2017). Agglomeration externalities and urban growth controls. *Journal of Economic Geography*, 17(1), 59-94.
- Viasus, D., Cordero, E., Rodríguez-Baño, J., Oteo, J., Fernández-Navarro, A., Ortega, L., . . . Payeras, A. (2012). Changes in epidemiology, clinical features and severity of influenza A (H1N1) 2009 pneumonia in the first post-pandemic influenza season. *Clinical Microbiology and Infection*, 18(3), E55-E62.
- WHO. (2020). Disease outbreaks. Retrieved 10 May, 2021, from <https://www.who.int/emergencies/diseases/en/>
- Wilson, J. M., Brediger, W., Albright, T. P., & Smith-Gagen, J. (2016). Reanalysis of the anthrax epidemic in Rhodesia, 1978–1984. *PeerJ*, 4, e2686.
- Workie, E., Mackolil, J., Nyika, J., & Ramadas, S. (2020). Deciphering the impact of COVID-19 pandemic on food security, agriculture, and livelihoods: A review

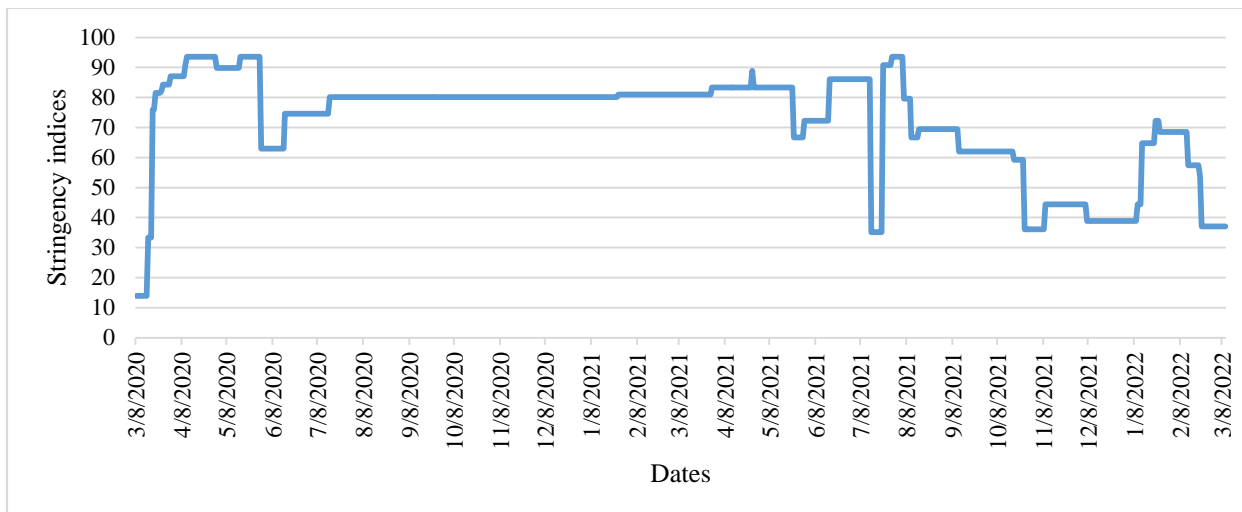
- of the evidence from developing countries. *Current Research in Environmental Sustainability*, 2, 100014. doi: <https://doi.org/10.1016/j.crsust.2020.100014>
- worldometer. (2022). COVID-19 CORONAVIRUS PANDEMIC.
- Xu, H., Yan, C., Fu, Q., Xiao, K., Yu, Y., Han, D., . . . Cheng, J. (2020). Possible environmental effects on the spread of COVID-19 in China. *Science of The Total Environment*, 731, 139211. doi: <https://doi.org/10.1016/j.scitotenv.2020.139211>
- Yang, W., Deng, M., Li, C., & Huang, J. (2020). Spatio-Temporal Patterns of the 2019-nCoV Epidemic at the County Level in Hubei Province, China. *International Journal of Environmental Research and Public Health*, 17(7), 2563.
- Yip, T. L., Huang, Y., & Liang, C. (2021). Built environment and the metropolitan pandemic: Analysis of the COVID-19 spread in Hong Kong. *Building and environment*, 188, 107471.
- You, H., Wu, X., & Guo, X. (2020). Distribution of COVID-19 Morbidity Rate in Association with Social and Economic Factors in Wuhan, China: Implications for Urban Development. *International Journal of Environmental Research and Public Health*, 17(10), 3417.
- Zafri, N. M., Afroj, S., Ali, M. A., Hasan, M. M. U., & Rahman, M. H. (2021). Effectiveness of containment strategies and local cognition to control vehicular traffic volume in Dhaka, Bangladesh during COVID-19 pandemic: Use of Google Map based real-time traffic data. *PLOS ONE*, 16(5), e0252228. doi: [10.1371/journal.pone.0252228](https://doi.org/10.1371/journal.pone.0252228)
- Zafri, N. M., Afroj, S., Nafi, I. M., & Hasan, M. M. U. (2021). A content analysis of newspaper coverage of COVID-19 pandemic for developing a pandemic management framework. *Heliyon*, 7(3), e06544. doi: <https://doi.org/10.1016/j.heliyon.2021.e06544>
- Zhan, Y., Yin, H., & Yin, J.-Y. (2022). B.1.617.2 (Delta) Variant of SARS-CoV-2: features, transmission and potential strategies. *International journal of biological sciences*, 18(5), 1844-1851. doi: [10.7150/ijbs.66881](https://doi.org/10.7150/ijbs.66881)
- Zhang, N., Shang, J., Li, C., Zhou, K., & Du, L. (2020). An overview of Middle East respiratory syndrome coronavirus vaccines in preclinical studies. *Expert review of vaccines*, 19(9), 817-829.
- Zheng, L., Ren, H.-Y., Shi, R.-H., & Lu, L. (2019). Spatiotemporal characteristics and primary influencing factors of typical dengue fever epidemics in China. *Infectious Diseases of Poverty*, 8(1), 24. doi: [10.1186/s40249-019-0533-9](https://doi.org/10.1186/s40249-019-0533-9)
- Zietz, B. P., & Dunkelberg, H. (2004). The history of the plague and the research on the causative agent *Yersinia pestis*. *International journal of hygiene and environmental health*, 207(2), 165-178.

## Appendix A

### List of experts to define the pandemic waves

Name	Designation
Dr. Ahmad Raihan Sharif	Medical Officer, Institute of Epidemiology, Disease Control & Research (IEDCR)
Dr. Md. Ariful Islam	Medical Officer, Directorate General of Health Service (DGHS)

### National Stringency Indices of Bangladesh



## Appendix B

### Results of spatial heterogeneity tests

	Breusch-Pagan (BP)		Koenker-Bassett (KB)		White tests	
	Stat	p-value	Stat	p-value	Stat	p-value
<b>First wave</b>	2.6505	0.75368	2.3494	0.79898	14.9132	0.78135
<b>Second wave</b>	2.0589	0.35720	1.8049	0.40557	9.9132	0.58135
<b>Third wave</b>	5.1776	0.26955	3.0640	0.54718	11.8347	0.61957

### Results of OLS model considering confirmed cases of the first wave

Variables	Unstandardized Coefficients		Standardized Coefficients	t	Sig.
	B	Std. Error	Beta		
(Constant)	3122.143	1514.529		2.061	.044
No of COVID-19 COVID-19 lab	803.635	160.867	.427	4.996	.000
No of ICU bed	252.828	41.416	.389	6.105	.000
Urban population density	.003	.001	.188	4.061	.000
Maximum temp	-125.977	58.591	-.023	-2.150	.036

### Results of OLS model considering confirmed cases of the second wave

Variables	Unstandardized Coefficients		Standardized Coefficients	t	Sig.
	B	Std. Error	Beta		
(Constant)	3847.338	1262.428		3.048	.003
Maximum temperature	922.719	308.527	.304	2.991	.004
Urban population density	.013	.002	.535	8.578	.000
Rainfall	-94.462	31.769	-.037	-2.973	.004
No of ICU bed	183.158	74.856	.175	2.447	.017
No of busstand	44.502	20.627	.034	2.157	.035

**Results of OLS model considering confirmed cases of the third wave**

Variables	Unstandardized Coefficients		Standardized Coefficients	t	Sig.
	B	Std. Error	Beta		
(Constant)	-1541.427	600.809		-2.566	.013
No of COVID-19 COVID-19 lab	666.316	104.136	.491	6.399	.000
Urban population density	.003	.000	.295	6.547	.000
No of ICU bed	104.253	26.060	.222	4.001	.000
Rainfall	-35.384	11.199	-.031	-3.160	.003